Fetal cardiovascular dysfunction in intrauterine growth restriction as a predictive marker of perinatal outcome and cardiovascular disease in childhood

Mónica Cristina Cruz Lemini

CLÍNIC BARCELONA Hospital Universitari

UNIVERSITAT DE BARCELONA

IDIBAPS Institut D'Investigacions Biomèdiques August Pi i Sunyer

PhD THESIS

Departament d'Obstetrícia i Ginecologia, Pediatria, Radiologia i Anatomía

Programa Doctorat Medicina RD 1393/2007

FETAL CARDIOVASCULAR DYSFUNCTION IN INTRAUTERINE GROWTH RESTRICTION AS A PREDICTIVE MARKER OF PERINATAL OUTCOME AND CARDIOVASCULAR DISEASE IN CHILDHOOD

Submitted by

Mónica Cristina Cruz Lemini

To obtain the degree of "Doctor in Medicine"

and the International Doctor Mention

SEPTEMBER, 2013

Directors:

Professor Eduard Gratacós Solsona
Head of the Fetal and Perinatal Medicine Research Group
Department of Maternal-Fetal Medicine
Hospital Clínic, University of Barcelona, Spain

Professor Fátima Crispi Brillas
Fetal and Perinatal Medicine Research Group
Department of Maternal-Fetal Medicine
Hospital Clínic, University of Barcelona, Spain

fetal i+D FETAL MEDICINE RESEARCH CENTER

TESIS DOCTORAL

Departament d'Obstetrícia i Ginecologia, Pediatria, Radiologia i Anatomía.

Programa Doctorat Medicina RD 1393/2007

DISFUNCIÓN CARDIOVASCULAR FETAL EN RESTRICCIÓN DEL CRECIMIENTO INTRAUTERINO COMO MARCADOR PREDICTIVO DE RESULTADO PERINATAL Y ENFERMEDAD CARDIOVASCULAR EN LA NIÑEZ

Presentada por

Mónica Cristina Cruz Lemini

Para obtener el grado de "Doctor en Medicina"

con Mención de Doctor Internacional

SEPTIEMBRE, 2013

Directores:

Profesor Eduard Gratacós Solsona
Jefe del Grupo de Investigación en Medicina Fetal y Perinatal
Departamento de Medicina Materno-Fetal
Hospital Clínic, Universidad de Barcelona, España

Profesora Fátima Crispi Brillas
Grupo de Investigación en Medicina Fetal y Perinatal
Departamento de Medicina Materno-Fetal
Hospital Clínic, Universidad de Barcelona, España

ACKNOWLEDGEMENTS

I would like express my gratitude to all the people who have helped me through the completion of this thesis and to only some of whom it is possible to give particular mention here.

To my directors Eduard Gratacós and Fátima Crispi. They are two amazing individuals, both personally and professionally, that lead by example, and I am very grateful to both for everything they have taught me during the past 4 years. It is because of the opportunity they granted me by their acceptance in this wonderful group, and to take on this ambitious project, that I am here today.

To all the people whose patience and teachings allowed me to develop the skills for this project, particularly Olga Gómez and Francesc Figueras. They introduced me to the world of fetal echocardiography and IUGR, taught me most of what I know on both subjects, and I am also proud to call them both friends.

To the people from the Fetal and Perinatal Medicine Group, Department of Fetal Medicine at Hospital Clínic, and my fellow companions. They have been friends and family throughout this experience and I couldn't have done it without them.

Finally, to my family for their constant support from far away. Knowing they were with me at all times made this journey a lot easier.

Thank you.

Acknowledgements for financial support:
I wish to thank the Mexican National Council for Science and Technology (CONACyT), in Mexico City, for its financial support.

"The most exciting phrase to hear in science, the one that heralds the most discoveries, is not "Eureka!", but 'That's funny..."

— Isaac Asimov —

Barcelona, September 11th, 2013.

Professor Eduard Gratacós Solsona
Professor in Obstetrics and Gynecology
Head of the Fetal and Perinatal Medicine Research Group
Hospital Clínic, University of Barcelona, Spain

Professor Fátima Crispi Brillas
Cardiovascular Research Line Coordinator
Fetal and Perinatal Medicine Research Group
Hospital Clínic, University of Barcelona, Spain

We declare that **Mónica Cristina Cruz Lemini** has performed under our supervision the studies presented in the thesis **"Fetal cardiovascular dysfunction in intrauterine growth restriction as a predictive marker of perinatal outcome and cardiovascular disease in childhood"**.

This thesis has been structured following the normative for PhD thesis as a compendium of publications, to obtain the degree of **International Doctor in Medicine** and the mentioned studies are ready to be presented to a Tribunal.

Eduard Gratacós Solsona
Thesis Director

Fátima Crispi Brillas
Thesis Director

PRESENTATION

The present thesis has been structured following the normative for PhD thesis, as a compendium of publications, to obtain the degree of International Doctor in Medicine. It was approved by the *Comisión de Doctorado de la Facultad de Medicina* on the 17th June, 2011. Projects included in this thesis belong to the same research line, leading to four articles published or submitted for publication in international journals:

1. Cruz-Lemini M, Crispi F, Valenzuela-Alcaraz B, Figueras F, Sitges M, Gómez O, Bijnens B, Gratacós E. Value of annular M-mode displacement *vs* tissue Doppler velocities to assess cardiac function in intrauterine growth restriction. Ultrasound Obstet Gynecol. 2013;42(2):175-81.
   Status: published. *Journal Impact Factor*: 3.557, quartile 1st.

2. Crispi F, Sepulveda-Swatson E, Cruz-Lemini M, Rojas-Benavente J, Garcia-Posada R, Dominguez JM, Sitges M, Bijnens B, Gratacós E. Feasibility and reproducibility of a standard protocol for 2D speckle tracking and tissue Doppler-based strain and strain rate analysis of the fetal heart. Fetal Diagn Ther. 2012;32(1-2):96-108.
   Status: published. *Journal Impact Factor*: 1.902, quartile 3rd.

3. Cruz-Lemini M, Crispi F, Van Mieghem T, Pedraza D, Cruz-Martínez R, Acosta-Rojas R, Figueras F, Parra-Cordero M, Deprest J, Gratacós E. Risk of perinatal death in early-onset intrauterine growth restriction according to gestational age and cardiovascular Doppler indices: a multicenter study. Fetal Diagn Ther. 2012;32(1-2):116-22.
   Status: published. *Journal Impact Factor*: 1.902, quartile 3rd.

4. Cruz-Lemini M, Crispi F, Valenzuela-Alcaraz B, Figueras F, Gómez O, Sitges M, Bijnens B, Gratacós E. A fetal cardiovascular score to predict infant hypertension and arterial remodeling in intrauterine growth restriction. Am J Obstet Gynecol 2013.
   Status: submitted. *Journal Impact Factor*: 3.877, quartile 1st.

TABLE OF CONTENTS

1. INTRODUCTION

1. INTRODUCTION

1.1 Cardiovascular disease and fetal programming

Cardiovascular disease remains the main cause of mortality in developed countries, causing 38% of all deaths in North America and being the most common cause of death in European men under 65 years of age and the second most common cause in women[1]. There is also an increasing prevalence in developing countries, associated to the rising incidence of obesity and diabetes in the Western world[2]. Research has demonstrated that there is a long subclinical phase that may include decades before the presence of clinical symptoms; indeed, short-term calculation of cardiovascular risk is defined as 10-year risk estimates with current models being developed to account for risk factors present since birth[3].

The "developmental origins of disease" hypothesis proposed by Barker stipulated that low birth weight was associated with the presence of cardiovascular disease in the adult[4]. It was based on observations of a large cohort affected by nutritional disorders, because of the social and economic situation at the time of birth, and proposed a novel idea that *in utero* programming of disease could occur. Now, more than three decades later, this concept known as "fetal programming", is one of the most important approaches to prevention of disease in the adult. Adverse conditions throughout pregnancy have been associated with neurodevelopmental delay, psychiatric disorders such as schizophrenia or autism, metabolic syndrome and cardiovascular disease[5]. Barker's initial studies showed an association of birth weight, not gestational age at birth, with important cardiovascular outcomes such as stroke, myocardial infarction or cardiovascular dysfunction[4]. This has created a new line of research to try and identify the group of fetuses at risk for this adverse programming, in an effort to look for interventions that may lower their risk of developing these diseases in adulthood.

The relationship between birth weight and cardiovascular disease was one of the first described, thus it would make sense to target the group at risk for low birth weight prenatally in order to identify those susceptible to monitoring and postnatal interventions. This group is prenatally known as fetuses with *intrauterine growth restriction (IUGR)*.

1.2 Intrauterine growth restriction and placental insufficiency

The concept of "normal" birth weight or "adequate" fetal growth has changed throughout the years[6]. It is generally accepted that IUGR fetuses are those below the 10th percentile of estimated fetal weight, or below the 5th centile of abdominal circumference, who have no other abnormalities (chromosomal, structural, infectious or other diseases)[7-9].

Intrauterine growth restriction (IUGR) due to placental insufficiency[10] is a leading cause for perinatal death and long-term cardiovascular[4] and neurodevelopmental adverse outcomes[11, 12]. The evaluation of the fetus in recent years has advanced importantly, and the incorporation of Doppler ultrasound to routine screening has led to changes in the definition and management of pregnancies with IUGR fetuses[13]. Doppler ultrasound has also allowed to demonstrate placental dysfunction as the leading cause of diminished growth and further classify the severity of growth restriction[14]. Placental function evaluation by umbilical artery (UmbA) Doppler velocimetry is the clinical standard for evaluating IUGR[15] and there is evidence that its use in these pregnancies improves a number of obstetric care outcomes and reduces perinatal deaths[7]. Most studies evaluate IUGR using the pulsatility index (PI) of the UmbA and presence of its end-diastolic flow. However, in late-gestation cases, most events of adverse outcome attributable to IUGR occur in fetuses with normal UmbA Doppler[16], thus other vascular territories have been proposed. Gestational age at birth and birth weight centile are also considered two of the most important standard perinatal criteria currently used to define severity in IUGR, with perinatal and neurodevelopmental outcomes being worse in younger and smaller babies[10, 17-20].

In view of this, clinical presentation of IUGR has been divided into two main classifications based on gestational age at diagnosis and UmbA Doppler patterns[21, 22]. *Early-onset IUGR fetuses* (before 34 weeks' gestation) typically present with a pattern of Doppler abnormalities that deteriorate quickly, progressively and which culminate in premature delivery of the fetus in order to preserve its life[10, 14, 23-25]. In contrast, *late-onset IUGR fetuses* rarely present UmbA abnormalities, are usually delivered near or at term, and are sometimes referred to as *small-for-gestational-age (SGA) fetuses*, considered by some as "constitutionally small" babies[6, 20]. However, adverse outcomes are not exclusive to premature and severe IUGR. Recent evidence suggests that a proportion of these late-onset SGA fetuses represent true forms of IUGR, with a mild degree of placental insufficiency (not reflected by UmbA Doppler) and poorer perinatal[26] and long-term results,

including suboptimal neurobehaviour[11, 12, 16], cortical development[27] and postnatal cardiovascular risk[28]. Although few studies have evaluated cardiac function in late-onset IUGR fetuses, recent data suggest that these fetuses might also show features of cardiac dysfunction[29-31]; therefore, sensitive Doppler and cardiovascular parameters could be useful to identify the subgroup of small fetuses at higher perinatal and long-term risk. For this purpose, other vessels in the fetal circulation have been incorporated in the evaluation of the IUGR fetus. The uterine arteries (UtA) PI, middle cerebral artery (MCA) PI, cerebroplacental ratio, ductus venosus (DV) and aortic isthmus (AoI) have all been reported to assess fetal circulation in IUGR[31-33]. These vessels aid in describing changes which are progressive, show deterioration of fetal wellbeing and have been associated to prenatal cardiac dysfunction and worse perinatal outcomes[10, 11, 21, 34-36]. However, these parameters are peripheral vessels that work as surrogates of cardiac function in the fetus, and few studies have explored the prenatal heart's physiology and adaptation to IUGR with echocardiographic parameters.

1.3 Heart physiology and adaptation to intrauterine growth restriction

The heart is a central organ in the fetal adaptive response to a variety of insults during prenatal life. Consequently, assessment of fetal cardiac function may be helpful in the diagnosis or monitoring of several fetal conditions[34, 37, 38]. The three prenatal shunts – DV, ductus arteriosus, and foramen ovale – are essential distributional arrangements, making the fetal circulation a flexible and adaptive system for intrauterine life[39]. The hemodynamic properties and functional ranges of these shunts are important determinants of the development of the fetal heart and circulation during the second and third trimesters. Understanding the particularities of fetal circulation is essential for adequate comprehension of fetal cardiac function changes in normal and pathological conditions. We also now know that the heart's myocardial fibre distribution is not homogeneous and that there is a twisting motion that occurs during the cardiac cycle with the apex rotating counter-clockwise and the base rotating clockwise during ejection[40]. This twisting motion has brought new questions and new techniques for its evaluation, in order to obtain information on cardiac motion as a whole[41].

In the initial stages of an insult, the heart usually manages to adapt and there is a long subclinical period of cardiac dysfunction before end-stage heart failure[34, 42]. During this period of cardiac adaptation, changes in cardiac function, as well as in the heart's shape and size, can be measured. IUGR illustrates how cardiac dysfunction in the fetus is largely subclinical and requires sensitive methods for its identification[34]. Recent studies using myocardial imaging techniques have demonstrated that systolic annular peak velocities are decreased from the very early stages of IUGR, long before atrial flow in the DV becomes abnormal[43, 44]. Additionally, fetuses with early IUGR show signs of impaired relaxation (diastolic dysfunction) from early stages of deterioration[34]. This decrease in longitudinal motion and impaired relaxation may be a fetal adaptive mechanism to the chronic hypoxia and volume/pressure overload of placental insufficiency. These mechanisms, which are the heart's attempt to adapt to an insult, constitute a process known as cardiac remodeling[45].

Postnatal persistence of cardiovascular remodeling has recently been demonstrated in a cohort of 5-year-old children who suffered early or late IUGR[28]. IUGR children showed changes in cardiac shape (more globular morphology), subclinical cardiac dysfunction (increased heart rate and reduced stroke volume and myocardial peak velocities), and vascular remodeling (increased blood pressure and carotid intima media thickness). These findings suggest that IUGR induces primary cardiac changes, which could explain the increased predisposition to cardiovascular disease in adult life[46]. The question then arises, whether these changes could be detected by fetal echocardiography, and would allow us to identify those fetuses with higher cardiovascular risk. This would require a complete fetal echocardiographic function evaluation and follow up into childhood.

1.4 Fetal cardiovascular function assessment

Fetal echocardiography has various limitations with regards to echocardiography in children or adults. The fetus is a complex patient, ever moving, with different positions in regards to the maternal abdomen. This, associated to maternal factors such as abdominal wall thickness, influences greatly on the quality and evaluation of cardiovascular function[42]. Most measurements currently used in echocardiography are angle-dependent; thus they rely on an adequate positioning of the transducer to obtain them. An additional challenge is that fetal cardiac dysfunction is essentially subclinical[34, 37, 38]. Fetuses rarely go into cardiac

failure and when they do, the outcome is generally dire, with very few exceptions[34, 47, 48]. Results of a cardiac examination in most fetuses with clinical relevance will be completely normal by child or adult cardiology standards. Thus, classical indexes used to determine the existence of cardiac failure in postnatal life are of little use in fetuses. Fortunately, adult cardiology has substantially developed in the last few years and a variety of new methods able to identify extremely subtle changes in cardiac function[49]. Implementation of these technologies in the fetus is far from straightforward, but these advances have already shown highly promising results[50-52].

Traditionally, echocardiographic evaluation in the fetus is based mainly on conventional pulsed Doppler waveforms, M-mode and 2D imaging. Recently, assessment of direct myocardial motion and deformation has been proposed using tissue Doppler imaging (TDI) and 2D speckle tracking imaging[49, 53-57] (Table 1). Blood flow assessment is a common approach to evaluate fetal cardiac function[54, 58]. Conventional Doppler allows blood outflow (systole) and inflow (diastole) in the heart, as well as time events, to be evaluated.

Doppler measurement of flow through the outflow tracts reflects *systolic* function. This measurement can be multiplied by the area of the outflow tracts to calculate the *stroke volume* (the amount of blood ejected per heart beat)[59] and the *cardiac output* (volume per minute), which in fetuses should normally be expressed as the *cardiac index* (cardiac output adjusted by fetal weight)[58, 59]. Cardiac output is a classical parameter to assess cardiac function but only becomes abnormal in the very late stages of deterioration when the heart fails to adapt and insufficient blood is ejected to meet organ requirements[58].

The main Doppler indices used to evaluate *diastolic* function are the early (E) and late (A) diastolic filling velocities, E/A ratios and precordial veins. Doppler allows evaluation of the blood flow filling the ventricle, which typically has a biphasic pattern reflecting E and A. Calculation of the *E/A ratio* essentially reflects ventricular relaxation but this parameter is of little use in fetal life as it is strongly affected by respiratory and corporal movements, and a high fetal heart rate usually leads to temporarily fused E/A waves[42, 60]. Diastolic function can also be indirectly evaluated with Doppler assessment of the precordial veins, which reflect pressure changes in the right atrium and indirectly provide information on diastolic function of the right heart[42, 60]. The DV is the most commonly used vein in fetal medicine as

it is known to reflect impaired relaxation and has been used in clinical practice as an early marker of disease[10].

Pulsed Doppler is usually applied to assess blood flow but can also be used to calculate *time periods*[58]. Of great interest are the isovolumetric contraction and relaxation times, defined as the time elapsed from the start of contraction/relaxation and the closure/opening of the outflow valve, respectively. These periods, particularly the *isovolumetric relaxation time* (IRT), become abnormal in the very early stages of dysfunction, reflecting an increase in the time required to properly relax the myocardium. Time events can be displayed individually or as a composite parameter, such as the *myocardial performance index* (MPI), which takes several systolic and diastolic time events into account[61]. The MPI is considered a marker of global cardiac function and it has been shown to be a highly sensitive parameter of dysfunction[25, 31].

M-mode techniques are traditionally used in a transverse 4-chamber view to measure the difference in end-systolic and end-diastolic ventricular diameters, calculating the shortening and ejection fractions by applying Teicholz's formula[62]. *Ejection fraction* is defined as the percentage of blood ejected in each heart cycle and, although it is considered an essential parameter for characterization of heart failure in adulthood[63], it is usually altered only in the late stages of fetal deterioration, as it mainly reflects radial function[60]. M-mode can be also applied in the long axis of the heart to evaluate *tricuspid and mitral annular-plane systolic excursions* (TAPSE/MAPSE), which have been proposed as sensitive markers of cardiac dysfunction as they reflect global longitudinal function[50, 64].

Tissue Doppler imaging (TDI) is a technique that evaluates *myocardial velocities* within the ventricular walls; particularly ventricular motion in the long-axis, from the apex to the base[65]. While conventional echocardiographic techniques are based on blood flow, TDI uses frequency shifts in ultrasound waves to calculate myocardial velocity, which is characterized by a lower velocity and higher amplitude[59, 65]. This technique has been widely used in the adult patient to diagnose diastolic heart failure, and has also been described as applicable to fetuses[66]. It can be applied online to evaluate annular or myocardial velocities, and offline TDI analysis also allows deformation parameters (*strain* and *strain rate*) to be calculated. Peak velocities evaluated at the mitral or tricuspid annulus reflect global systolic (S') or diastolic (E' and A') myocardial motion and have been shown to be early and

sensitive markers of cardiac dysfunction[43]. Peak systolic strain and strain rate assessed at each myocardial segment provide information on myocardial deformation and interaction with neighboring segments. The main limitation TDI has in the fetus is that it is completely angle-dependant, thus the acquisition of the image provides only information on the heart's long-axis function.

Recent reports have described the use of non-Doppler technology for evaluation of cardiac function in the adult. 2D speckle tracking techniques allow myocardial deformation to be quantified by using frame-by-frame tracking of bright myocardial areas (speckles)[49]. *2D speckle tracking* requires post-processing and off-line analysis of 2D images, allowing for myocardial strain and strain rate to be calculated. Despite its potential advantages, this is a recent technique that still requires validation for use in the fetal heart[57, 67].

Table 1. Parameters for evaluation of fetal cardiac function.

Parameter	Definition	Technique
Systolic function		
Blood volume estimation		
Ejection fraction	Percentage of blood volume ejected from the ventricle within a heart beat	2D (Simpson), M-mode, 2D speckle tracking
Cardiac output	Blood volume pumped by the ventricle per minute	2D, conventional Doppler
Myocardial motion		
Longitudinal annular displacement	Distance of longitudinal movement of the atrioventricular valve annulus	M-mode, 2D speckle tracking
Systolic annular peak velocity (S')	Movement speed of the atrioventricular valve annulus during systole	Spectral or color TDI
Myocardial deformation		
Strain	Amount of deformation (percentage of change in length of myocardial segment)	Color TDI or 2D speckle tracking
Strain rate	Speed of deformation (change of strain over time)	Color TDI or 2D speckle tracking
Diastolic function		
Precordial veins blood flow (DV and others)	Blood pattern in precordial veins during atrial contraction, which indirectly reflects cardiac compliance	Conventional Doppler
E/A ratio	Ratio between early (E) and late (A) ventricular filling velocities	Conventional Doppler
Diastolic annular peak velocities (E' and A')	Movement speed of the atrioventricular valve annulus during early and late diastole	Spectral or color TDI
E/E' ratio	Transmitral-to-mitral annular diastolic velocity ratio	Conventional Doppler and spectral TDI
Isovolumetric relaxation time	Time between closure of the airtic valve and opening of the mitral valve	Conventional Doppler or spectral/color TDI
Global cardiac function		
Myocardial performance index	Ratio between isovolumetric times (contraction plus relaxation) and ejection time	Conventional Doppler or spectral/color TDI

TDI, tissue Doppler imaging; DV, ductus venosus.

1.5 Infant cardiovascular function assessment

The neonate, child and adult have the distinct advantage over the fetus that cardiac evaluation can be performed directly over the heart. This is accomplished with a series of acquisition planes that are different from the fetal planes; distinctly the short axis views of the left ventricle are commonly used and the right ventricle is not routinely scanned[68, 69]. The standard views of a 2D echocardiogram are defined by the American Society of Echocardiography[68]. The imaging planes are identified by transducer location (apical, parasternal) and by the plane of examination relative to the heart (4-chamber, long-axis, and short-axis). In addition, imaging planes may be described as anatomic planes (sagittal, parasagittal, transverse, or coronal). Measurements involved are slightly different, because other structures can be evaluated in these populations; for example, strain measurements are much more applicable because all planes can be obtained at different levels of the heart with accuracy. This allows a more precise evaluation of twist motion in the ventricles. TDI is more precise because of the feasibility that exists to acquire an apical 4-chamber view. Thus, in these patients information can be obtained of long-axis and short-axis function of the heart and measurements of strain and torsion can be obtained for both ventricles. This allows a better understanding of cardiac function postnatally and provides a better assessment of cardiac dysfunction[70].

There are other measurements directly related to cardiovascular function and disease which cannot be measured in the fetus, such as blood pressure measurement. Current clinical guidelines contemplate screening for hypertension in children, in order to provide strategies for promoting cardiovascular health that can be integrated into comprehensive pediatric care[71]. Hypertension (blood pressure above the 95th centile) in the child has been associated with substantial long-term health risks and considered an indication for lifestyle modifications[72]. Guidelines for the pediatric population suggest blood pressure monitoring from 3 years of age onward, and provide normal reference values and standardisation of the technique for the pediatric population[72, 73].

Another measurement that has been studied recently as a risk factor for cardiovascular disease is the measurement of vascular intima-media thickness. Imaging of arteries to identify and quantify the presence of subclinical vascular disease has been suggested to further refine cardiovascular disease risk assessment. As a screening test, imaging must be safe, be sensitive, be affordable, and lead to interventions that can

favorably alter the natural history of cardiovascular disease. Measurement of carotid intima-media thickness with B-mode ultrasound is a non-invasive, sensitive, and reproducible technique for identifying and quantifying atherosclerotic burden and cardiovascular risk in adults[74]. It is a well-validated research tool that has been translated increasingly into clinical practice. Aortic intima-media thickness (aIMT) measurement may allow detection of cardiovascular risk at an earlier age in children[75, 76] and previous studies have shown thicker aIMT in IUGR newborns[77]. aIMT values greater than or equal to the 75th percentile are considered high and indicative of increased risk[74].

1.6 Relevance and justification of the research study

Most risk factors leading to cardiovascular disease are already present in childhood and the importance of early identification of pediatric cardiovascular risk factors is now well recognized. Hypertension in the child has been associated with substantial long-term health risks and considered an indication for lifestyle modifications[72]. Current clinical guidelines contemplate screening for hypertension in children over 3 years of age, in order to provide strategies for promoting cardiovascular health, that can be integrated into comprehensive pediatric care[71]. Interventions in the IUGR group could go from blood pressure monitoring before 3 years of age, recommending lack of exposure to other risk factors (secondary smoking, obesity), surveillance of catch-up growth or administration of hypotensors[71, 78] and specially, promoting exercise and physical activity. A recent randomized trial in a large cohort of children suggest that the inverse association of fetal growth with arterial wall thickness in childhood can be prevented by dietary ω-3 fatty acid supplementation over the first 5 years of life[79]. IUGR is not listed among those conditions presumed to increase cardiovascular risk, in current guidelines[71-73]. Considering IUGR affects 5-10% of all newborns, the findings of this study would affect thousands of children per year. Currently, there are no prenatal parameters described that may aid in selecting those fetuses with later hypertension and arterial remodeling that may benefit for early screening in infancy and other preventive measures or interventions.

Both fetal and child cardiovascular evaluations have proven to be reliable techniques for describing changes in IUGR; cardiovascular dysfunction has been found subclinically and may have implications for cardiovascular risk in future life. The main aim of this work was to evaluate cardiovascular function parameters in IUGR fetuses as predictors of perinatal and postnatal cardiovascular outcome. In order to do this, we looked to validate

the reproducibility of measurements and techniques not previously described in IUGR fetuses (*studies 1 and 2*), to evaluate whether fetal cardiovascular parameters could help us predict perinatal outcome (*study 3*) and finally to assess the value of fetal echocardiography for prediction of postnatal cardiovascular risk factors, specifically hypertension and arterial remodeling (*study 4*).

2. HYPOTHESES

2. HYPOTHESES

2.1 MAIN HYPOTHESIS:

Fetal echocardiography predicts postnatal cardiovascular outcome in IUGR.

2.2 SPECIFIC HYPOTHESES:

1. IUGR fetuses have abnormalities in cardiovascular function in comparison with normally grown fetuses as measured by echocardiography.
2. Fetal echocardiography is useful to predict perinatal outcome in IUGR cases.
3. Fetal echocardiography is useful to predict cardiovascular outcome and the presence of risk factors associated with future cardiovascular events in IUGR children, specifically hypertension, subclinical cardiovascular dysfunction and increased aortic intima-media thickness.

3. OBJECTIVES

3. OBJECTIVES

3.1 MAIN OBJECTIVE:

To evaluate fetal cardiovascular parameters in IUGR as predictors of perinatal and postnatal cardiovascular outcome in childhood.

3.2 SPECIFIC OBJECTIVES:

1. To evaluate reproducibility of measurements not previously described in fetuses that will be performed during fetal cardiac evaluations, mainly longitudinal axis motion by M-mode and TDI/2D strain-derived parameters.
2. To compare fetal echocardiography including comprehensive morphometric and functional assessment in IUGR and normally grown fetuses, in order to evaluate the presence of differences among groups.
3. To evaluate whether fetal echocardiography in IUGR fetuses can predict perinatal outcome.
4. To evaluate whether fetal echocardiography in IUGR fetuses can predict cardiovascular outcome and the presence of risk factors associated with future cardiovascular events in infants at six months of age, specifically hypertension, subclinical cardiovascular dysfunction and increased aortic intima-media thickness.

4. METHODS

4. METHODS

4.1 STUDY DESIGN

Between April 2010 and September 2012, a cohort was created of consecutive cases of IUGR singleton fetuses, at the Department of Maternal-Fetal Medicine, Hospital Clinic, Barcelona, Spain. IUGR was defined as an estimated fetal weight and confirmed birth weight below the 10th centile according to local reference curves[80]. Early-onset IUGR was defined as cases that died or were delivered before 34 weeks of gestation; late-onset IUGR were those cases delivered beyond 34 weeks. Exclusion criteria were structural or chromosomal abnormalities, evidence of fetal infection or pregnancies achieved by assisted reproduction technologies. Additionally, for study 3 (multicenter study), cases were included from the University Hospital of Gasthuisberg Leuven (Belgium) and Hospital Clínico of Santiago (Chile). A reference cohort of fetuses with normal estimated fetal weight and birth weight (between 10th–90th percentiles) were randomly sampled from pregnancies at our institution and selected as control group.

4.2 STUDY VARIABLES

4.2.1 Baseline variables

Maternal and paternal age, height, body mass index, ethnicity, smoking, socioeconomic status and medical history, parity and last menstrual period corrected by first trimester crown-rump length were recorded upon the fetal examination. Estimated fetal weight was calculated according to the method of Hadlock et al; both estimated fetal weight and birth weight centile were calculated using local reference curves[81].

Prenatal Doppler ultrasound was performed using a Siemens Sonoline Antares (Siemens Medical Systems, Malvern, PA, USA) ultrasound machine equipped with a 2-6 MHz linear curved-array transducer and a phased-array 2-10 MHz transducer for tissue Doppler. Recordings were performed in the absence of fetal movements and voluntary maternal suspended breathing. Pulsed Doppler parameters were performed automatically from three or more consecutive waveforms, with the angle of insonation as close to 0° as possible. A high pass wall filter of 70 Hz was used to record low flow velocities and avoid artifacts. All studies were performed upon diagnosis of IUGR and weekly till delivery, with the last ultrasound examination within 72 hrs before birth.

Conventional fetoplacental Doppler evaluation: uterine arteries, umbilical artery, middle cerebral artery, ductus venosus and aortic isthmus (*Figure 1*).

- ***Uterine artery (UtA)*** PI was obtained by placing the probe on the lower quadrant of the abdomen, angled medially, with color Doppler imaging used to identify the apparent crossover of the UtA with the external iliac artery; measurement was obtained 1 cm distal to the crossover point[82]. The PI of the left and right arteries was measured, and the mean PI was calculated.
- ***Umbilical artery (UA)*** pulsatility index (PI) was measured from a free-floating cord loop. Normal UA was considered as a PI below the 95th percentile[83]. Presence, absence (AEDV) or reversal (REDV) of the end-diastolic velocity was also recorded.
- ***Middle cerebral artery (MCA)*** PI was obtained in a transversal view of the fetal head, at the level of its origin from the circle of Willis. The ***cerebroplacental ratio (CPR)*** was calculated dividing the middle cerebral artery PI by the umbilical artery PI. Both parameters were considered abnormal if below the 5th percentile, and indicative of cerebral blood flow redistribution[32, 83].
- ***Ductus venosus (DV)*** PI was measured in a mid-sagittal or a transverse section of the fetal abdomen, positioning the Doppler gate at the isthmic portion. Normal DV was considered as a PI below the 95th percentile[84]. Presence (PAV), absence/reversal (RAV) of the 'a' wave was also recorded.
- ***Aortic isthmus (AoI)*** PI was measured either in a sagittal view of the fetal thorax with clear visualization of the aortic arch, placing the gate a few millimetres beyond the origin of the left subclavian artery; or in a cross-sectional view of the fetal thorax, at the three vessels and trachea view, placing the gate just before the convergence of the AoI and the arterial duct[85, 86]. Normal AoI was considered as a PI below the 95th percentile[85]. The ***isthmus flow index (IFI)*** was calculated dividing (systolic+diastolic)/systolic velocity-time integrals (VTI); it was considered abnormal below the 5th percentile[87] (*Figure 2*).

Figure 1. Conventional fetoplacental Doppler evaluation.

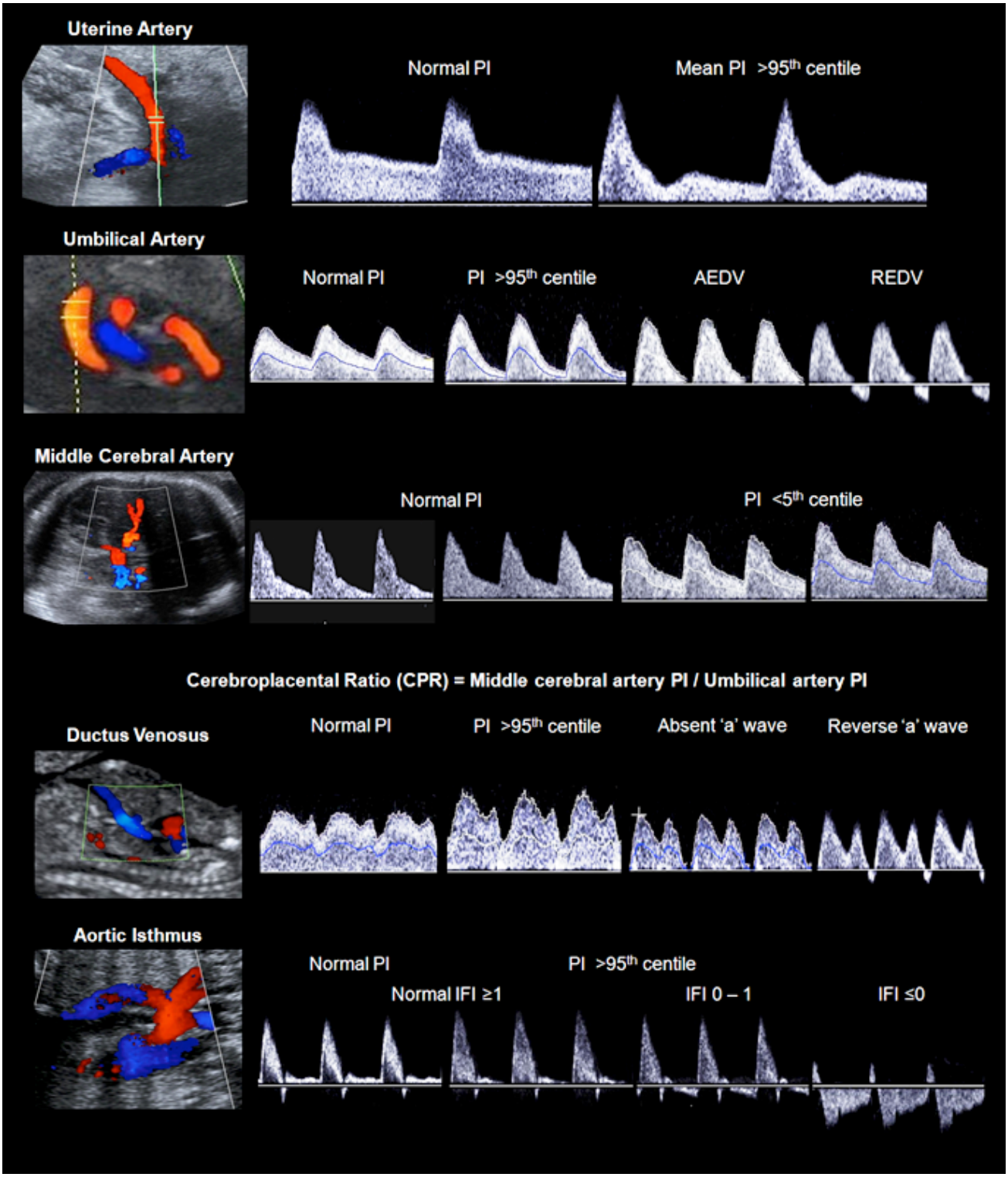

PI, pulsatility index; AEDV, absent end-diastolic velocity; REDV, reversed end-diastolic velocity; IFI, isthmus flow index.

Figure 2. Aortic isthmus flow index (IFI).

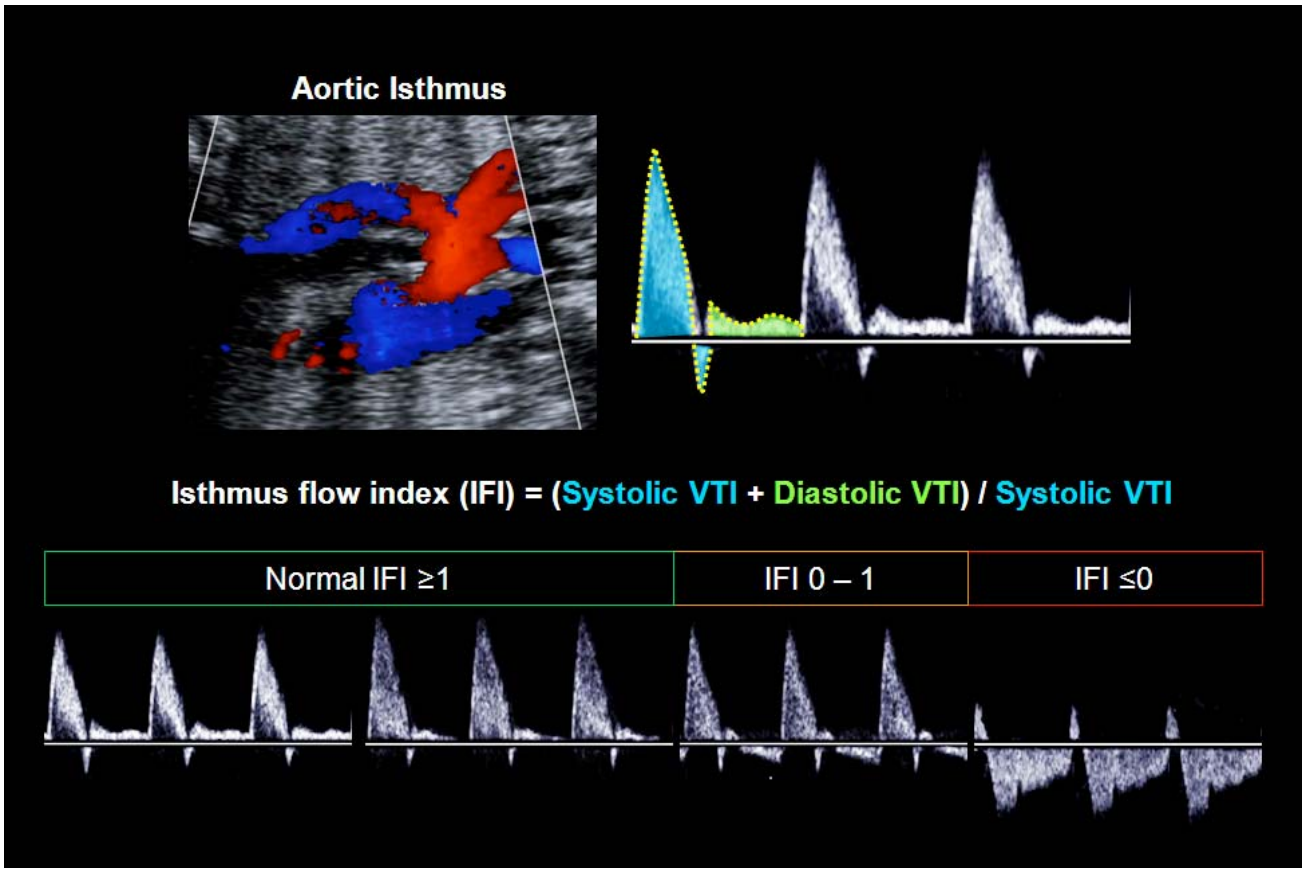

VTI, velocity-time integral.

4.2.2 Fetal echocardiography

A complete two-dimensional echocardiographic examination was performed initially to assess structural heart integrity using a Siemens Sonoline Antares machine (Siemens Medical Systems, Malvern, PA, USA). Cardiovascular evaluation, both morphometric and functional, was performed using a curved-array 2-6 MHz transducer, with the exception of tissue Doppler measurements that required a phased-array 2-10 MHz transducer.

Cardiovascular morphometric parameters: cardiothoracic ratio, atrial areas, cardiac and ventricular sphericity indexes and wall thicknesses (*Figure 3*).

- The ***cardiothoracic ratio (CTR)*** was measured in a cross-sectional view of the fetal thorax, at the level of the four-chamber view of the heart, by the ellipse method[88].
- Left and right ***atrial areas*** were measured on 2D images from an apical four-chamber view at end-ventricular systole (maximum point of atrial distension)[89]. Left and right ***atrium/heart ratios*** were calculated as atrial area/heart area.

- Cardiac, left and right ventricular ***sphericity indexes (SI)*** were measured on 2D images from an apical four-chamber view at end-diastole; they were calculated as base-to-apex length/mid-transverse diameter of the heart, left and right ventricles respectively [90, 91].
- Ventricular end-diastolic ***septal and free wall thicknesses*** were measured by M-mode from a transverse four-chamber view and adjusted by the transverse cardiac diameter[92].

Figure 3. Fetal cardiovascular morphometric parameters.

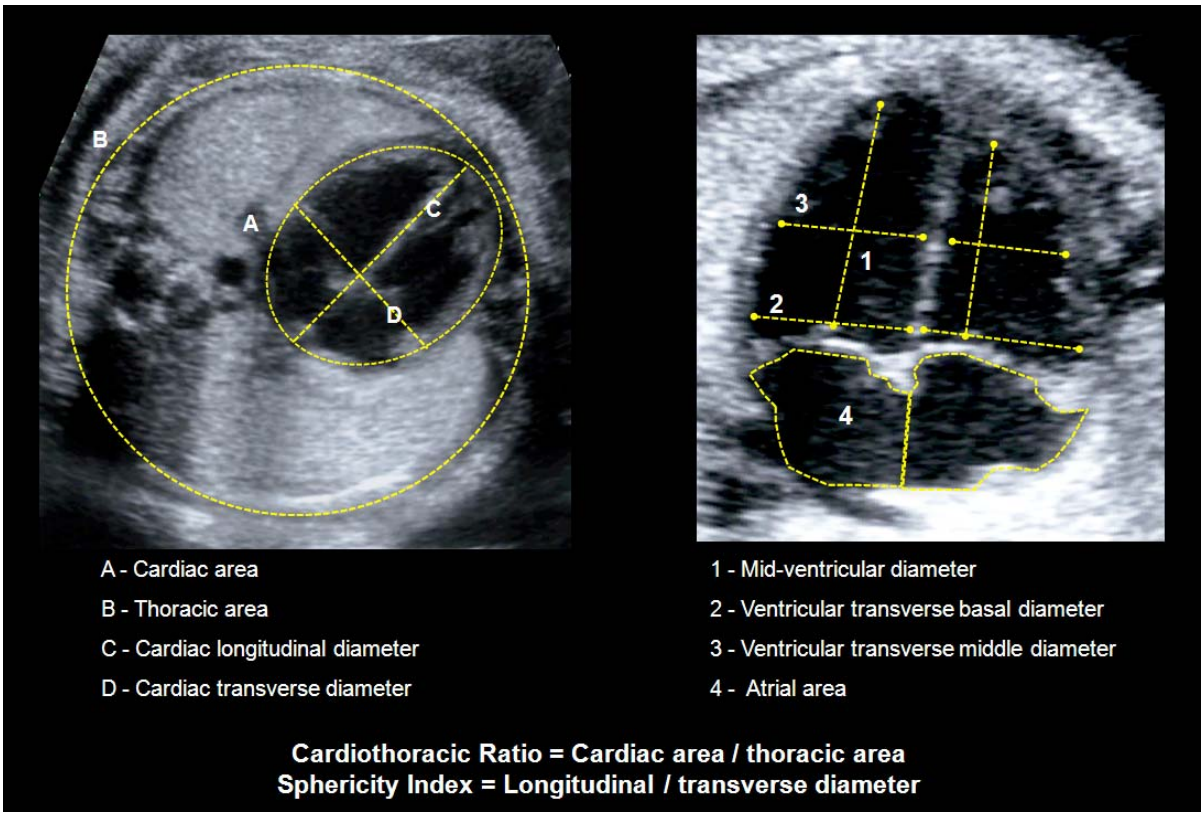

Systolic function parameters: stroke volume, cardiac output, combined cardiac output, cardiac index, shortening and ejection fractions, mitral/tricuspid/septum annular plane systolic excursion (MAPSE/TAPSE/SAPSE) and systolic annular peak velocities (S').

- Left and right ***stroke volumes (SV)*** were calculated as π/4*(aortic or pulmonary valve diameter)^2*(aortic or pulmonary artery systolic flow velocity-time integral). Diameters of the aortic and pulmonary valves were measured in frozen real-time images during systole by the leading-edge-to-edge method[93]. Aortic systolic flow was obtained in an apical or basal 5-chamber view of the heart, and the pulmonary artery systolic flow was obtained in a right ventricle outflow tract view; both at angles as close to 0º as possible. Velocity-time integrals were calculated by manual trace of the spectral Doppler area [58] (*Figure 4*).
- Left and right ***cardiac outputs (CO)*** were calculated as left or right SV*fetal heart rate[42].
- ***Combined cardiac output (CCO)*** was obtained by the addition of right and left CO.
- ***Cardiac index (CI)*** was obtained by the formula CCO/estimated fetal weight, and expressed in mL/min/Kg[94].
- ***Fetal heart rate (FHR)*** was calculated in the spectral Doppler image of the aortic flow.
- Left and right ***shortening fraction (SF)*** and ***ejection fraction (EF)*** were obtained from a transverse four-chamber view by M-mode, by measurement of the end-systolic (ESD) and end- diastolic (EDD) diameters, applying Teicholz's formula[95] (*Figure 5*).
- ***Mitral, septal and tricuspid annular plane systolic excursion (MAPSE, SAPSE** and **TAPSE)*** were measured real time in an apical or basal four-chamber view, by placing the cursor at a right angle to the atrioventricular junction, marked by the valve rings at the mitral or tricuspid valve. Maximum amplitude of motion was taken as the extent of displacement between end-systole and end-diastole, measured in millimeters[50] (*Figure 6*).
- ***Myocardial systolic annular peak velocity (S')*** by tissue Doppler imaging (TDI) was obtained using a 2–10-MHz phased-array transducer, with frame rate above 100 fps. In a four-chamber-view, sample volume was placed in the basal part of the left ventricular wall (mitral annulus), interventricular septum and right ventricular wall (tricuspid annulus)[96] (*Figure 6*).

Figure 4. Measurement and calculation of fetal stroke volumes, cardiac outputs, cardiac index and heart rate.

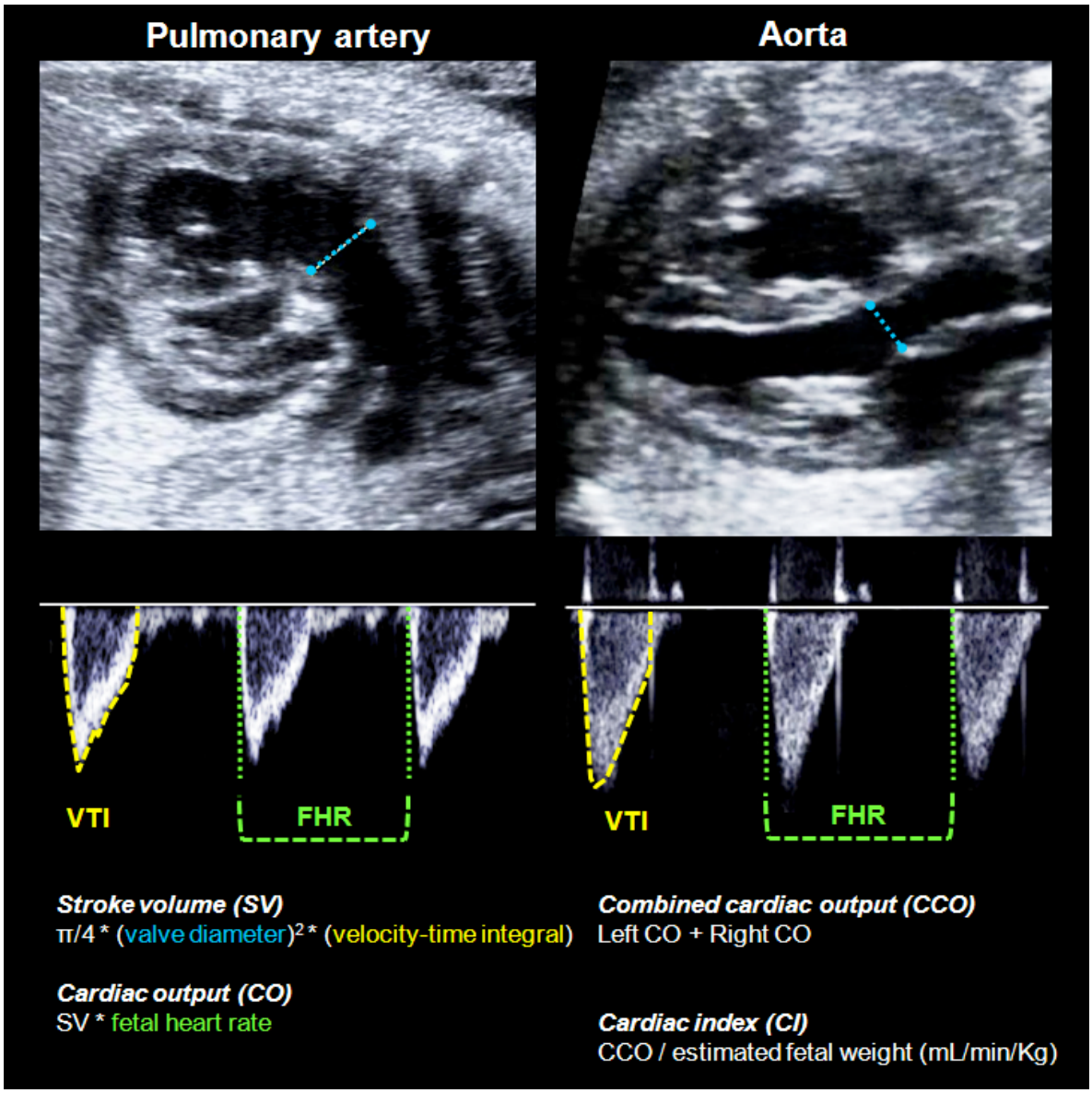

Figure 5. Measurement and calculation of fetal shortening fraction, ejection fraction and ventricular wall thicknesses.

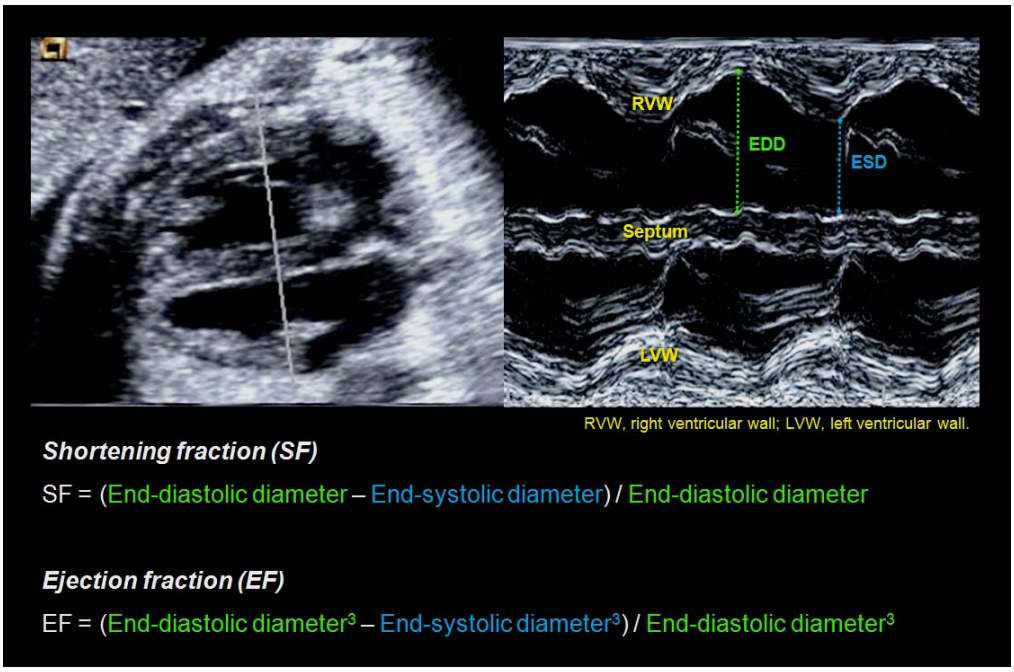

RVW, right ventricular wall; EDD, end-diastolic diameter; ESD, end-systolic diameter; LVW, left ventricular wall.

Figure 6. Measurement of longitudinal-axis motion in the right fetal heart by tissue Doppler and M-mode.

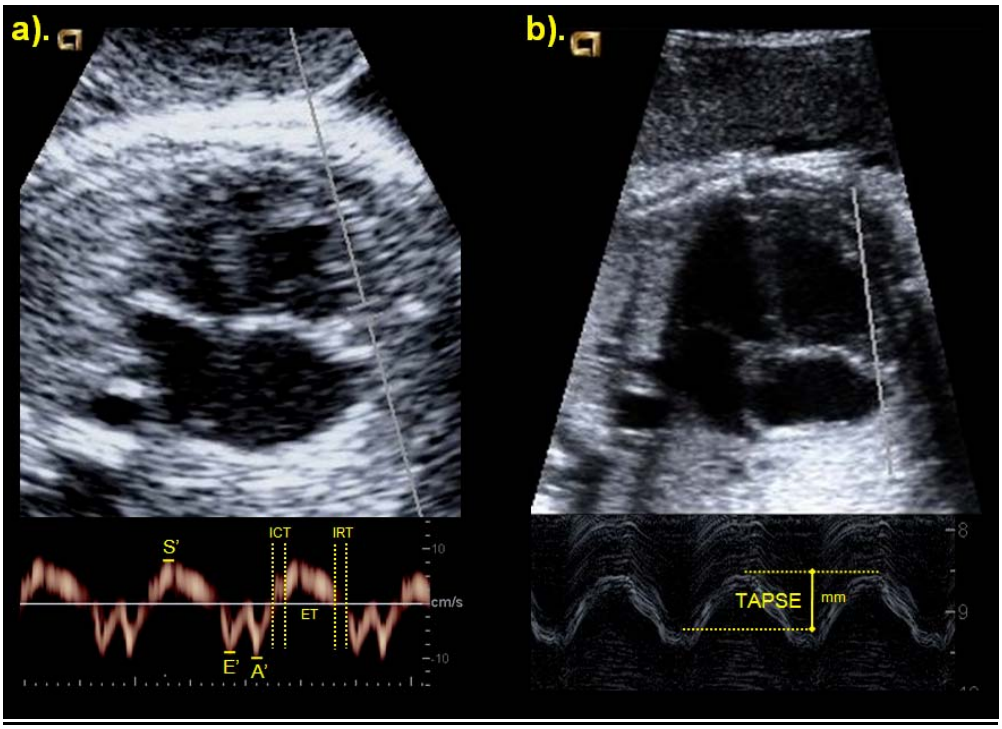

a) Tissue Doppler annular peak velocities for early diastole (E'), atrial contraction (A') and systole (S') in centimeters per second. Components for the myocardial performance index (MPI') are also shown.

b) M-mode TAPSE (tricuspid annular plane systolic excursion) in millimeters.

Diastolic function parameters: peak early and late transvalvular filling velocities, E/A ratio, E deceleration time, A wave duration time, early-diastolic and atrial contraction annular peak velocities, E/E' ratio, E'/A' ratio, myocardial performance index by TDI.

- ***Peak early (E)*** and ***late (A) transvalvular filling velocities*** were obtained from a basal or apical four-chamber view, placing the pulsed Doppler sample volume just below the valve leaflets[58, 86] (*Figure 7*).

- ***E to A ratio (E/A)*** was calculated for both left and right sides of the heart.

- ***E deceleration time (Edec)*** was measured as the time from the maximum mitral/tricuspid velocity to the baseline[97].

- ***A wave duration time (Adur)*** was measured from the beginning to the end of atrial contraction/A wave[97].

- ***Myocardial early-diastole (E') and atrial contraction (A') annular peak velocities*** by tissue Doppler imaging (TDI) were obtained using a 2–10-MHz phased-array transducer, with frame rate above 100 fps. In a four-chamber-view, sample volume was placed in the basal part of the left ventricular wall (mitral annulus), interventricular septum and right ventricular wall (tricuspid annulus)[96].

- ***E to E' ratio (E/E')*** was calculated for the left and right sides of the heart[96].

- ***E' to A' ratio (E'/A')*** was calculated for the interventricular septum, mitral and tricuspid annuli[96].

Global function parameters: myocardial performance index by pulsed and tissue Doppler.

- ***Myocardial performance index (MPI)*** was measured in a cross-sectional view of the fetal thorax, in an apical projection, at the level of the four-chamber view of the heart. The Doppler sample volume was placed to include both the lateral wall of the ascending aorta and the mitral valve where the clicks corresponding to the opening and closing of the two valves can be clearly visualized. Spectral Doppler images were obtained using a sample volume of 3-4mm, gain level of 60, high Doppler sweep velocity, and with the E/A waveforms displayed as positive flows. The isovolumetric contraction time (ICT), isovolumetric relaxation time (IRT) and ejection time (ET) were calculated using the beginning of the mitral and aortic valve clicks as landmarks and the MPI was calculated as follows: (ICT+IRT)/ET[61]. Abnormal MPI was defined as above the 95th centile[98, 99] (*Figure 8*).

- ***Myocardial performance index by TDI (MPI')***, was obtained using a 2–10-MHz phased-array transducer, with frame rate above 100 fps. In a four-chamber-view, sample volume was placed in the basal part of the left ventricular wall (mitral annulus), interventricular septum and right ventricular wall (tricuspid annulus) [96]. The following time-periods were calculated: isovolumetric contraction time (ICT'), ejection time (ET') and isovolumetric relaxation time (IRT'). Finally, left, right and septal MPI' were calculated as (ICT' + IRT')/ET'[96].

Figure 7. Measurement of fetal peak early (E) and late (A) transvalvular filling velocities and time periods.

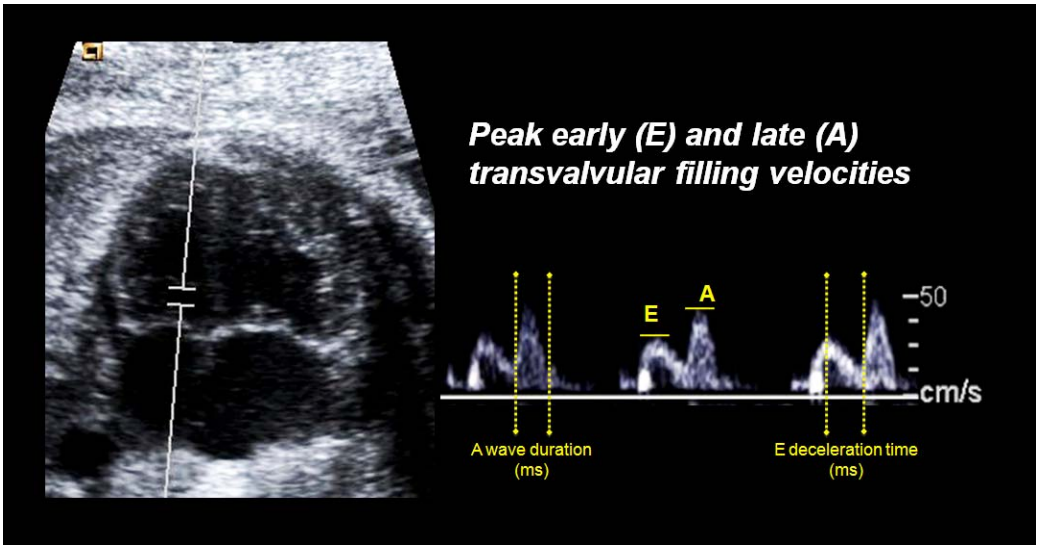

Figure 8. Measurement and calculation of the fetal left myocardial performance index (MPI).

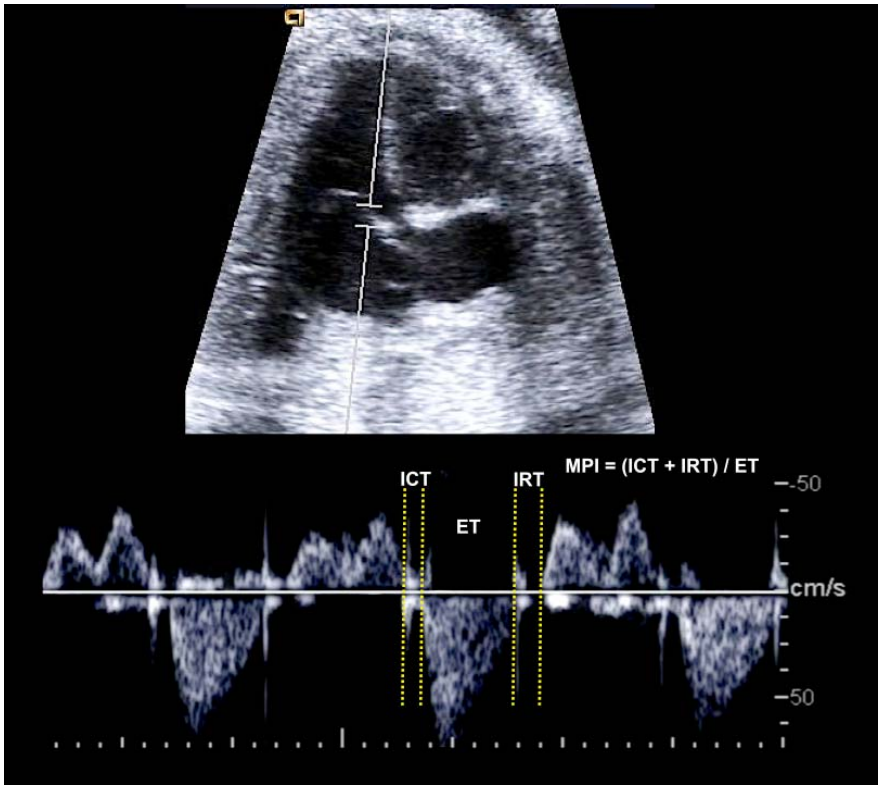

ICT, isovolumetric contraction time; IRT, isovolumetric relaxation time; ET, ejection time.

Myocardial deformation: strain and strain-rate by tissue Doppler and 2D speckle tracking analysis.

For offline deformation analysis, all patients underwent an ultrasonographic examination using a Vivid Q (General Electric Healthcare, Horten, Norway) ultrasound system. A phased array sector probe of 1.4-2.5 MHz was used to obtain an apical or basal four chamber view with the septum or free wall aligned parallel to the Doppler beam (<10º without further angle correction) in 2D for subsequent analysis. Three additional color TDI video-clips were obtained from septum, and left and right free wall (*Figure 9*). If needed, a sector tilt was used to make sure that the angle between the probe and myocardial motion was below 15º. No angle correction was applied off-line. While recording the loop, the 2D scan area and the TDI color box were kept as small as possible to obtain the highest frame rate. The color gain was adjusted to avoid aliasing. Scans were performed in the absence of maternal and fetal breathing or movements. Caution was taken to achieve >150 frames per second (fps) for TDI and >70 fps for 2D strain. The frame rate/heart rate ratio was calculated for each technique. For each acquisition, 7.5 seconds of non-compressed data were stored in cine-loop format and analyzed offline using commercially available software (GE EchoPAC PC 108.1.x, General Electric Healthcare). The cine-loops were reviewed and only those with at least 5 consecutive measurable cardiac cycles were considered valid for the study.

Figure 9. 2D and TDI clips of the fetal heart for subsequent deformation analysis.

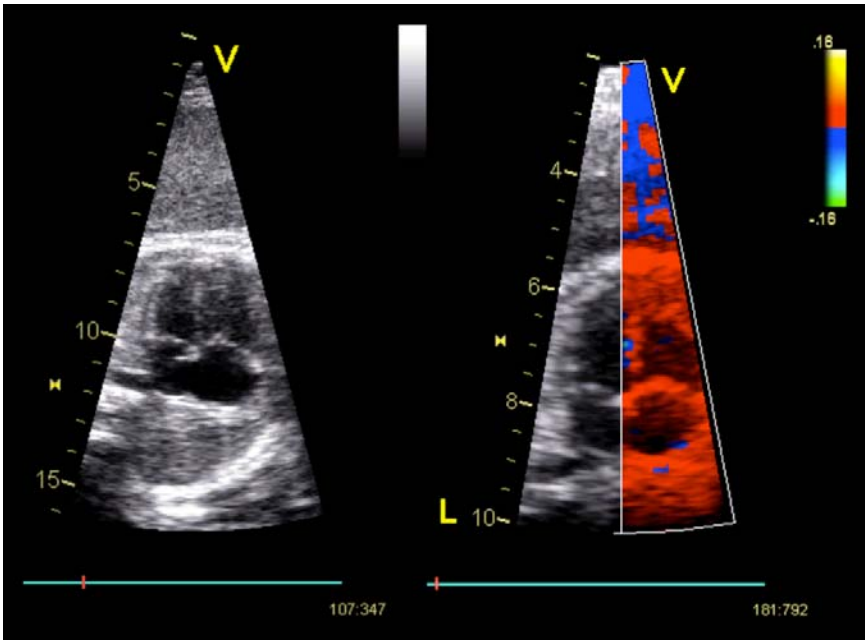

❖ ***TDI offline analysis*** of 10–13 cardiac cycles from 5–10 tissue Doppler sequences was performed following a standardized protocol as described below:

Aortic valve closure and opening were manually marked on the spectral aortic flow (*Figure 10*). Mitral valve closure, corresponding to the electrocardiogram (EKG) R wave, was manually indicated on the clip in order to use it for timing events during the cardiac cycle in the absence of real EKG. Gain and velocity lowering were used in order to improve the visualization of mitral valve movement.

Figure 10. Manual indication of mitral valve (MV) closure corresponding to the EKG R wave in the 2D cine loop.

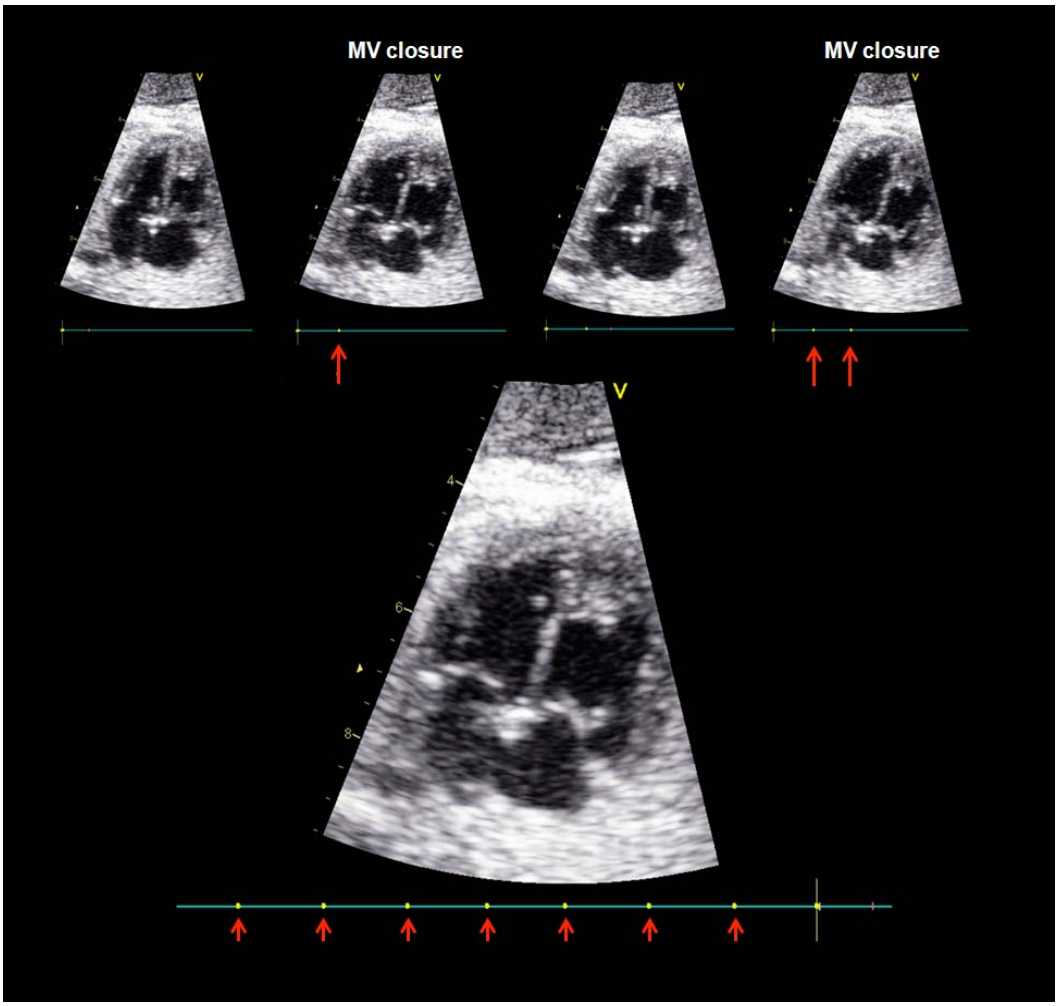

- ***Longitudinal peak systolic strain and strain rate by TDI*** were calculated offline and averaged over 5 consecutive heart cycles by placing a 2 x 3 mm sample area at the basal part of the septum, left and right ventricular free walls on the color TDI clip. Strain length was standardized at the minimum size (2 mm). No angle correction was applied. Caution was taken that the sample area and strain length were within the myocardium in all phases of the cycle by reviewing, and correcting where needed, region placement frame by frame all along the analyzed cardiac cycles. Linear drift compensation was applied to the deformation curves and only cycles with low drift compensation (<20%) were accepted as valid. Peak systolic strain and strain rate measurement were performed and averaged over 5 consecutive homogeneous cycles with low linear drift compensation. The time spent in the whole analysis including dummy EKG indication and deformation analysis in three areas (basal left and right free walls and septum) was recorded for each fetus (*Figure 11*).

- ***2D-Strain analysis*** of 10–13 cardiac cycles from 2D grayscale cineloops was performed following a standardized protocol as described below:

  Aortic valve closure and opening were manually marked on the spectral aortic flow. Mitral valve closure, corresponding to the EKG R wave, was manually indicated in the 2D cine loop as described above (*Figure 10*).

  Separately, both left and right ventricles' endocardial borders were manually traced on one arbitrary frozen frame that provided the best resolution of the endocardial border. The tracing started and ended at the mitral or tricuspid valve plane, respectively, without involvement of papillary muscles. The outer border was adjusted to approximate the epicardial border, and tracing width was kept at the minimum size (6 mm) in all cases (*Figure 12*). Next, the software automatically detected the motion of the delineated myocardium in the subsequent frames. Visual control of tracking quality was performed and, if required, optimized by adjusting the region of interest or manually correcting the contour to ensure adequate automatic tracking. The software then provided a profile of longitudinal peak strain and strain rate for each segment together with the global deformation. Spatial and temporal smoothing were kept at 0% to visually assess the strain and strain rate curve quality and then fixed at 50% to obtain the peak systolic strain and strain values at the basal left and right septal and free wall segments as well as globally (*Figure 13*).

Figure 11. Fetal tissue Doppler-derived strain (a) and strain rate (b) waveforms from basal lateral free wall of the right ventricle.

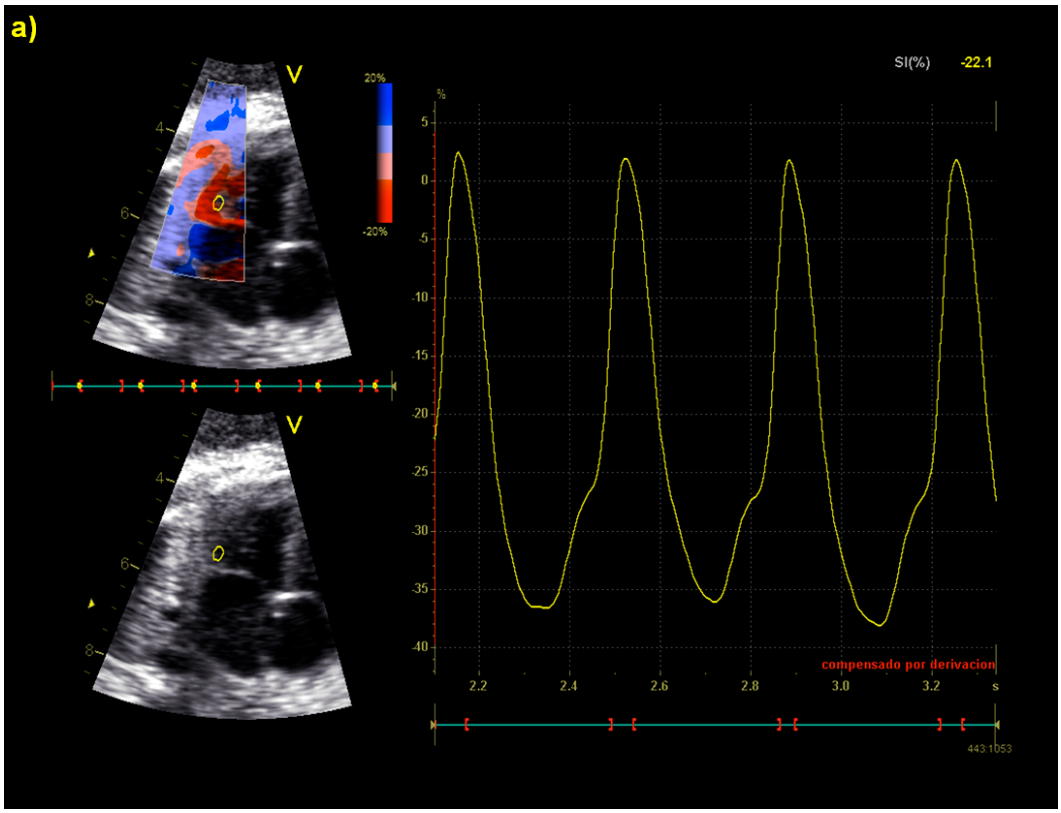

Figure 12. Left ventricle endocardial border, with manual delineation; 2D clip.

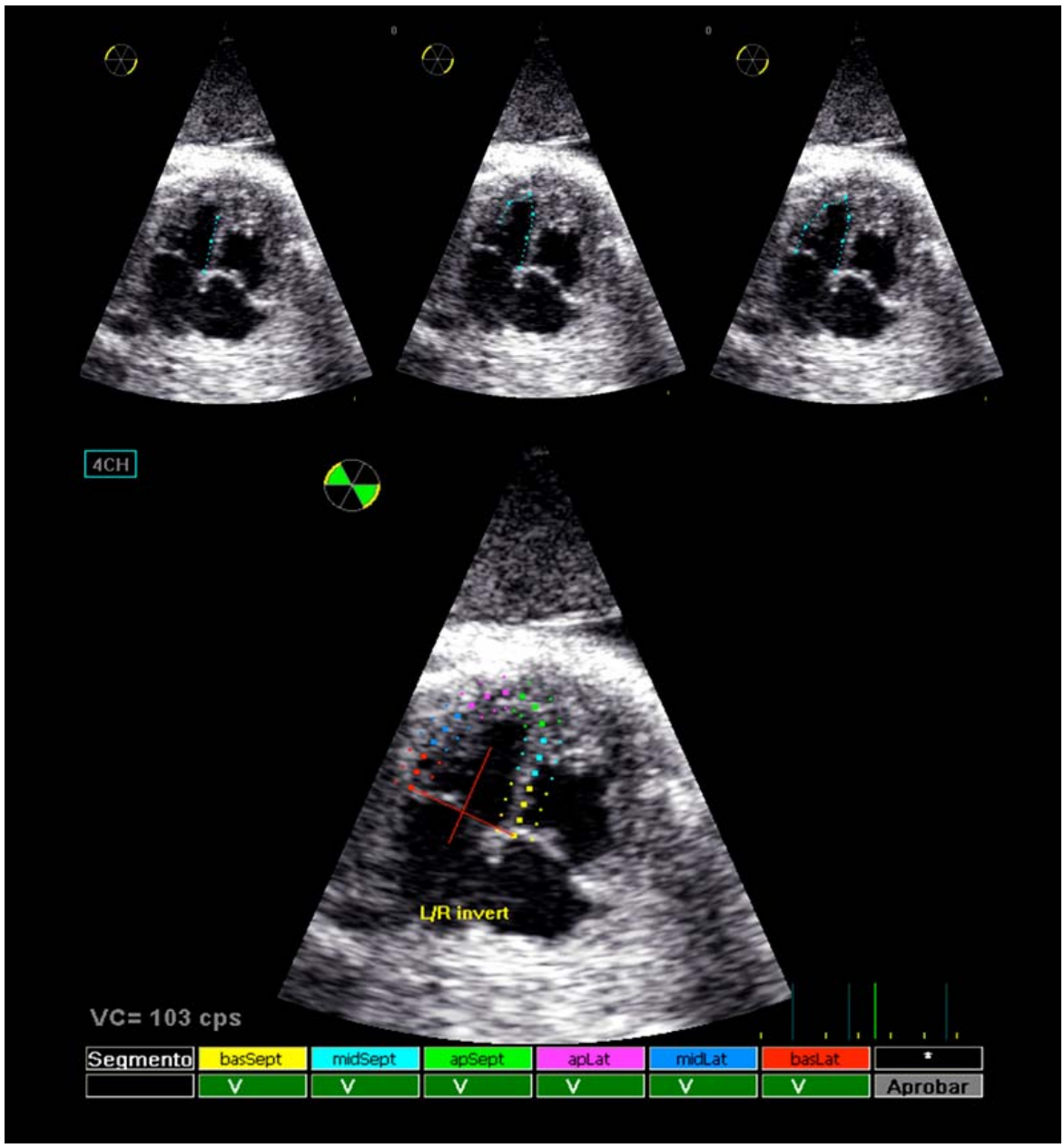

Figure 13. Fetal 2D speckle tracking derived strain (**a**) and strain rate (**b**) waveforms of the left ventricle.

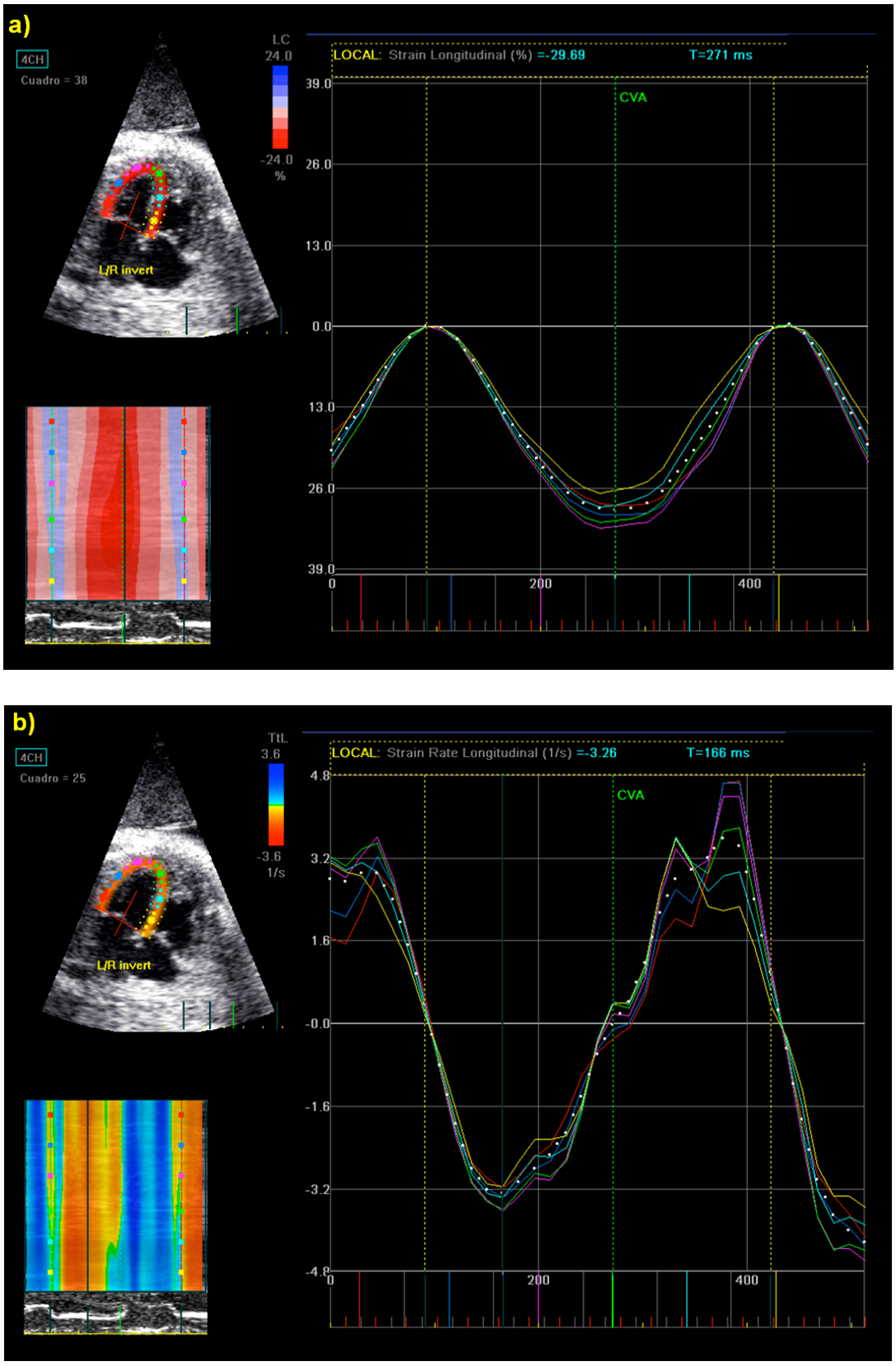

TABLE 2. SUMMARY OF FETAL CARDIOVASCULAR EVALUATION

Plane	Measurements
Apical/basal 4 chamber view	
• 2D • Pulsed Doppler • Pulsed TDI • M-Mode • Color TDI clip	✓ Cardiothoracic ratio, atrial areas, sphericity indexes. ✓ Peak early (E) and late (A) transvalvular filling velocities. ✓ Myocardial peak velocities and MPI' in mitral, septal and tricuspid annuli. ✓ Mitral, septal and tricuspid annular plane systolic excursion. ✓ Offline analysis of myocardial peak velocities, strain, strain-rate and MPI' in mitral, septal and tricuspid annuli.
Apical/basal 5 chamber view	
• 2D • Pulsed Doppler	✓ Aortic valve diameter. ✓ Aortic systolic flow, fetal heart rate and myocardial performance index.
Transverse 4 chamber view	
• M-Mode	✓ Shortening and ejection fractions. ✓ Ventricular end-diastolic septal and free wall thicknesses.
Right ventricle outflow tract view	
• 2D • Pulsed Doppler	✓ Pulmonary valve diameter. ✓ Pulmonary artery systolic flow.
3-vessel and trachea view	
• Pulsed Doppler	✓ Aortic isthmus pulsatility index and isthmus flow index.
Thoraco-abdominal mid-sagittal view	
• Pulsed Doppler	✓ Ductus venosus pulsatility index.
Abdominal aorta sagittal view	
• 2D	✓ Aortic intima-media thickness.

4.2.3 Perinatal outcome parameters

Perinatal: preeclampsia, prenatal exposure to glucocorticoids, gestational age at delivery, mode of delivery, labor induction, presence of fetal distress, perinatal mortality and pregnancy complications.
Neonatal: gender, birth weight, birth weight centile, 5 minute Apgar score, arterial and venous umbilical cord pH, days in neonatal intensive care unit, neonatal morbidity and neonatal mortality.

4.2.4 Infant anthropometric data

All examinations were carried out al 5-7 months corrected age by first-trimester crown-rump length[100]. Anthropometric data included the infant's height, weight, and calculation of body mass index and body surface area at the time of the examination, with centiles and z-scores calculated according to local reference values[101].

4.2.5 Infant vascular evaluation

Vascular parameters: blood pressure, aortic IMT.

- ***Systolic and diastolic blood pressures (BP)*** were obtained at the beginning of the medical evaluation by a trained physician from the brachial artery using a validated ambulatory automated Omron 5 Series device, while the infant was resting. Blood pressure centiles were calculated according to published reference values[72].
- ***Aortic intima-media thickness (aIMT)*** was measured using Vivid Q (General Electric Healthcare, Horten, Norway), with a 12L-RS linear-array 6.0-13.0 MHz transducer. Infants were studied when resting quietly or asleep. aIMT measurement involved obtaining longitudinal clips of the far wall of the proximal abdominal aorta in the upper abdomen[76, 77]. aIMT measurements were performed offline according to a standardized protocol based on a trace method with the assistance of a commercially available software (GE EchoPAC PC 108.1.x, General Electric Healthcare). To obtain aIMT, three end-diastolic frames were selected across a length of 10 mm and analyzed for mean and maximum aIMT, and the average reading from these three frames was calculated.

Figure 14. Aortic intima-media thickness measurement in a 6 month-old infant.

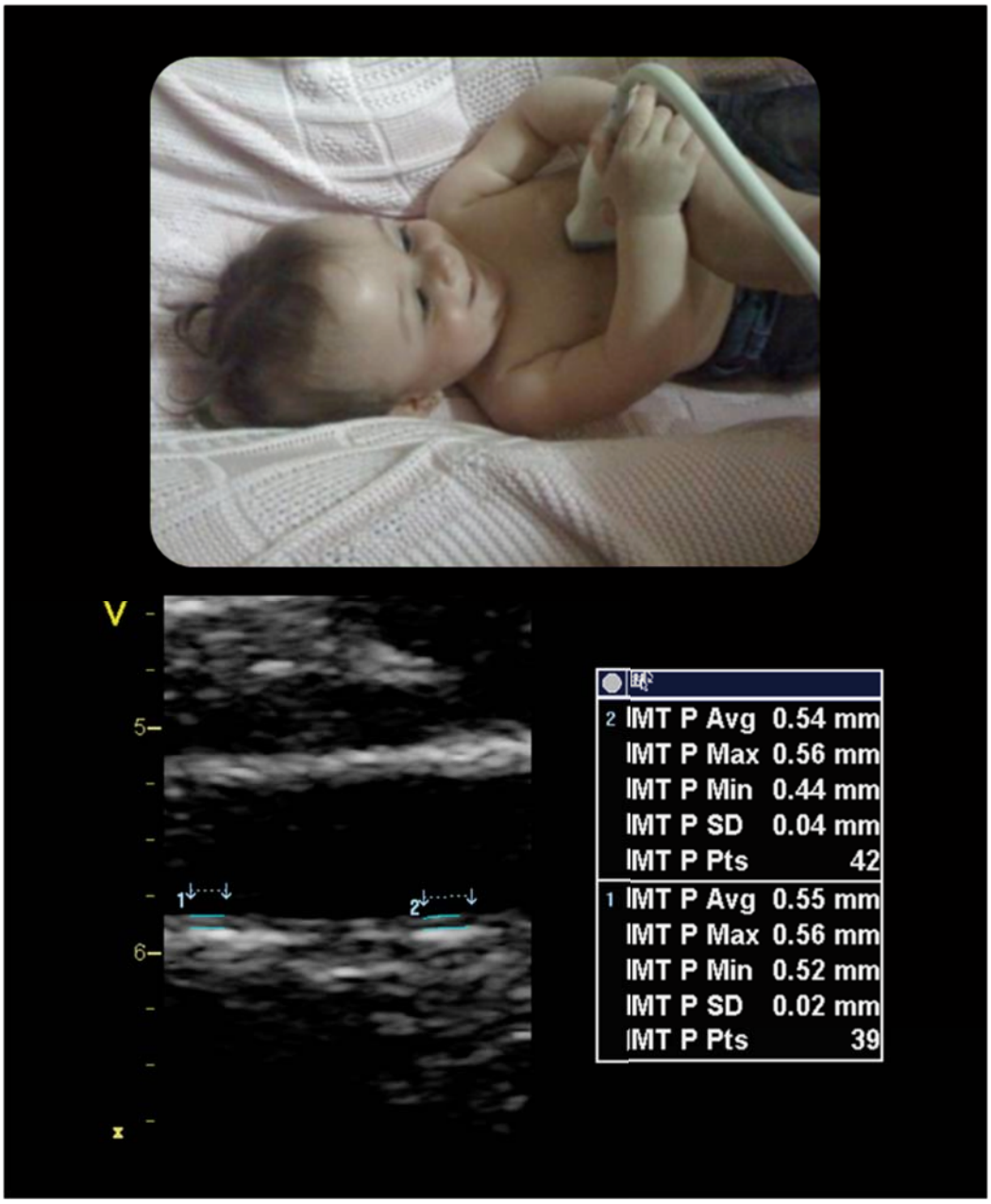

4.2.6 Infant echocardiography

Cardiovascular child evaluation was performed using Vivid Q (General Electric Healthcare, Horten, Norway). Children were studied when resting quietly or asleep. A complete two-dimensional M-mode and Doppler echocardiographic examination, with a 10S-RS phased-array 4.5-11.5 MHz transducer, was performed to assess structural heart integrity and morphometry.

Cardiovascular morphometric parameters: left atrial area, left sphericity index and wall thicknesses.

- ***Left atrial area*** was measured on a 2D image from an apical four-chamber view at end-ventricular systole (maximum point of atrial distension) [89].
- ***Left ventricular sphericity index (LSI)*** was measured on a 2D image from an apical four-chamber view at end-diastole; LSI was calculated as base-to-apex length/mid-transverse diameter [90, 91].
- Ventricular end-diastolic ***septal and left free wall thicknesses*** were measured by M-mode from a parasternal long-axis view (PLAX).

Systolic function parameters: stroke volumes, heart rate, cardiac output, shortening fraction, ejection fraction, mitral and tricuspid annular plane systolic excursion (MAPSE, TAPSE) and systolic annular peak velocities (S').

- Left and right ***stroke volumes (SV)*** were calculated as π/4*(aortic or pulmonary valve diameter)^2*(aortic or pulmonary artery systolic flow velocity-time integral). Diameters of the aortic and pulmonary valves were measured in frozen real-time images during ventricular systole by the leading-edge-to-edge method[93]; aortic diameter was obtained from the PLAX view, while the pulmonary artery diameter was obtained in a parasternal short-axis (PSAX) view. Ascending aortic flow velocity-time integral (VTI) was measured with pulsed Doppler from an apical five-chamber view, and pulmonary artery flow VTI was recorded from a standard PSAX view with the sample volume placed immediately distal to the pulmonary valve. Velocity-time integrals were calculated by manual trace of the spectral Doppler area [58].
- ***Heart rate*** was calculated in the spectral Doppler image of the aortic flow.
- Left and right ***cardiac outputs (CO)*** were calculated as left/right SV*heart rate.
- Left ***shortening fraction (SF)*** and ***ejection fraction (EF)*** were obtained from a PLAX view by M-mode, by measurement of the end-systolic and end- diastolic diameters, applying Teicholz's formula[95].
- ***Mitral and tricuspid annular plane systolic excursion (MAPSE, TAPSE)*** were measured real time in a four-chamber view, by placing the cursor at the atrioventricular junction, marked by the valve rings at the mitral or tricuspid valve. Maximum amplitude of motion was taken as the extent of displacement between end-systole and end-diastole, measured in millimeters[50].

- ***Myocardial systolic annular peak velocity (S')*** by tissue Doppler imaging (TDI) was obtained in a four-chamber-view, with the sample volume placed at the basal part of the left ventricular wall (mitral annulus), interventricular septum and right ventricular wall (tricuspid annulus) [96].

<u>*Diastolic function parameters*</u>: isovolumetric relaxation time (IRT), peak early (A) and late (A) transvalvular filling velocities, E/A ratio, E deceleration time, A wave duration time, early-diastolic (E') and atrial contraction (A') annular peak velocities, E/E' ratio, E'/A' ratio, isovolumetric relaxation time by TDI (IRT').

- ***Left isovolumetric relaxation time (IRT)*** was obtained from the pulsed Doppler waveform of the aortic blood flow, from the end of the aortic wave to the beginning of the mitral early filling wave.

- *Left and right* ***peak early (E)*** and ***late (A) transvalvular filling velocities*** were obtained from an apical four-chamber view, placing the pulsed Doppler sample volume just below the valve leaflets[58, 86].

- ***E to A ratio (E/A)*** was calculated for both left and right sides of the heart.

- ***E deceleration time (Edec)*** was measured as the time from the maximum mitral/tricuspid velocity to the baseline[97].

- ***A wave duration time (Adur)*** was measured from the beginning to the end of atrial contraction/A wave[97].

- ***Myocardial early-diastole (E') and atrial contraction (A') annular peak velocities*** by tissue Doppler imaging (TDI) were obtained in a four-chamber-view, with the sample volume placed at the basal part of the left ventricular wall (mitral annulus), interventricular septum and right ventricular wall (tricuspid annulus) [96].

- ***E to E' ratio (E/E')*** was calculated in the left and right sides of the heart[96].

- ***E' to A' ratio (E'/A')*** was calculated at interventricular septum, mitral and tricuspid annuli[96].

- ***Myocardial performance index by TDI (MPI')***, was obtained using a 2–10-MHz phased-array transducer, with frame rate above 100 fps. In a four-chamber-view,

sample volume was placed in the basal part of the left ventricular wall (mitral annulus), interventricular septum and right ventricular wall (tricuspid annulus) [96]. The following time-periods were calculated: isovolumetric contraction time (ICT'), ejection time (ET') and isovolumetric relaxation time (IRT'). Finally, left, right and septal MPI' were calculated as (ICT' + IRT')/ET'[96].

Figure 15. Parasternal long-axis view (PLAX) in a 6 month-old infant.

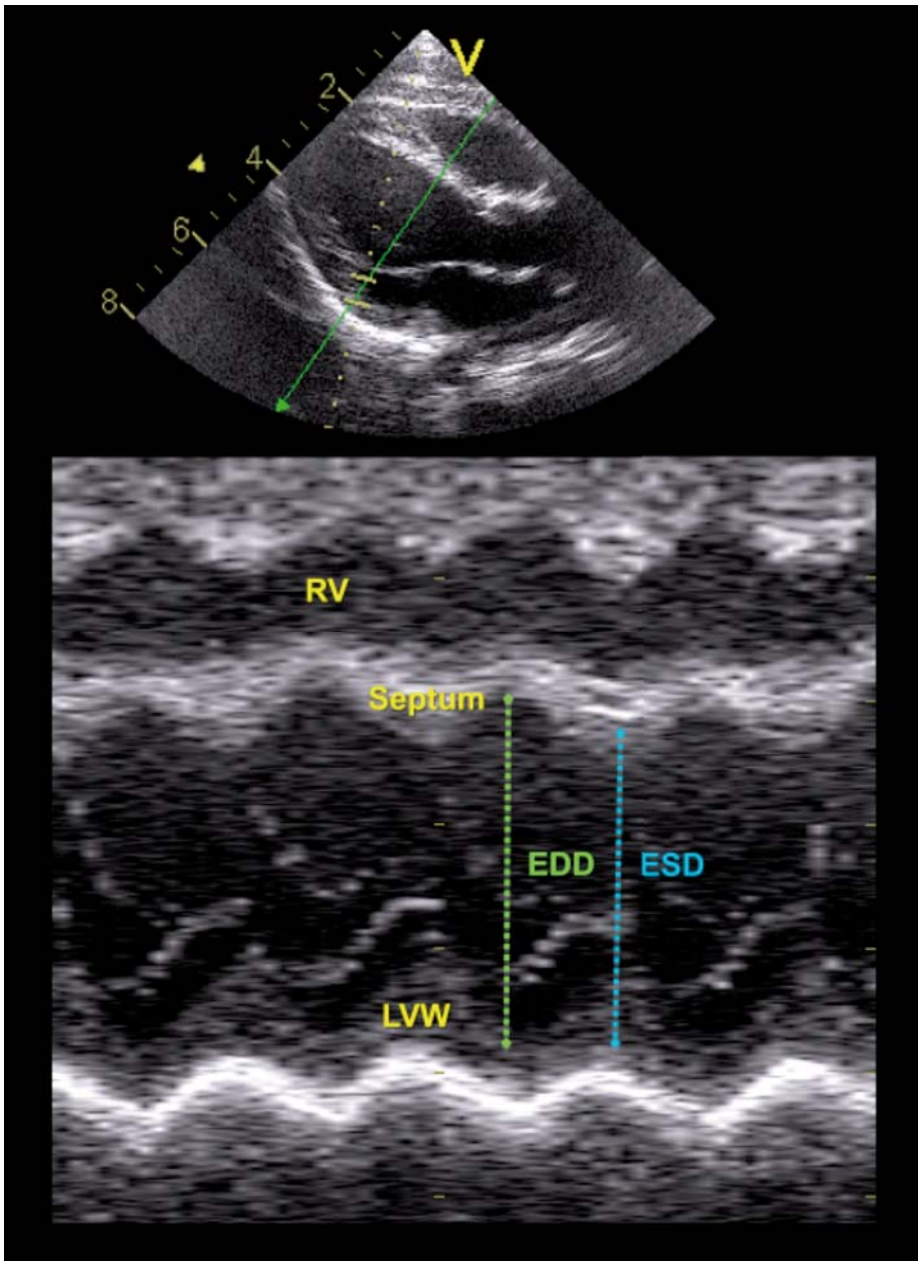

RV, right ventricle; EDD, end-diastolic diameter; ESD, end-systolic diameter; LVW, left ventricular wall.

TABLE 3. SUMMARY OF INFANT CARDIOVASCULAR EVALUATION

Plane	Measurements
Parasternal long-axis (PLAX) view	
• M-Mode	✓ Aortic valve diameter, left atrial diameter ✓ Shortening and ejection fractions, interventricular septum, left and right ventricular wall thicknesses.
Parasternal short-axis (PSAX) view	
• 2D • Pulsed Doppler	✓ Pulmonary valve diameter ✓ Pulmonary artery systolic flow
Apical 4-chamber view	
• 2D • Pulsed TDI • Pulsed Doppler • M-Mode	✓ Left atrial area, left sphericity index. ✓ Myocardial peak velocities and MPI' in mitral, septal and tricuspid annuli. ✓ Peak early (E) and late (A) transvalvular filling velocities. ✓ Mitral and tricuspid annular plane systolic excursion.
Apical 5-chamber view	
• Pulsed Doppler	✓ Aortic systolic flow and heart rate. ✓ Left isovolumetric relaxation time.
Abdominal sagittal view	
• 2D	✓ Aortic intima-media thickness.

4.3 OUTCOME DEFINITIONS

- ***Preeclampsia***

  Preeclampsia was defined according to the International Society Study of the Hypertension in Pregnancy as a resting blood pressure of ≥140/90 mm Hg on 2 occasions at least 4 hours apart and proteinuria of ≥300 mg/L or a 2+ urine dipstick >20 weeks of gestation in a previously normotensive woman[102].

- ***Neonatal morbidity***

  Neonatal morbidity was defined by the presence of bronchopulmonary dysplasia, necrotizing enterocolitis, intraventricular hemorrhage, periventricular leukomalacia, retinopathy, persistent ductus arteriosus, or sepsis[46].

- ***Perinatal mortality***

  Perinatal mortality was defined as stillbirth, intrapartum demise or death within the first 28 days of life[10].

- ***Infant hypertension***

  Infant hypertension was defined according to published guidelines, as systolic, diastolic or mean blood pressure above the 95th centile[72], at 6 months of age.

- ***Infant vascular remodeling***

  Since no reference values exist for aIMT at this age, we used centiles obtained with our control group as reference parameters. IMT values greater than or equal to the 75th percentile are considered high and indicative of increased cardiovascular risk[74]. Infant vascular remodeling was defined as an aIMT above the 75th centile.

- ***Infant cardiovascular hypertension and arterial remodeling (paper 4)*** was defined as the presence of both a mean blood pressure above 95th centile and an aIMT measurement above the 75th centile.

4.4 ETHICAL COMMITTEE APPROVAL

The study protocol was approved by the hospital ethics committee and written consent was obtained for the study from all the women.

4.5 STATISTICAL ANALYSIS

Data was analyzed using the IBM SPSS Statistics 19 statistical package and MedCalc 9.1 statistical software. Normality was evaluated by the Shapiro-Wilk test. Student's *t*-test, one-way ANOVA, Pearson χ^2 test or Fisher's exact test were used to compare quantitative and qualitative data, where appropriate. *P* values below 0.05 were considered statistically significant.

- **Study 1: Value of annular M-mode displacement versus tissue Doppler velocities to assess cardiac function in intrauterine growth restriction.**

  Doppler parameters were normalized into z-scores by previously published reference values. Echocardiographic parameters were adjusted by cardiac size, dividing the corresponding measurement between the longitudinal diameter of the heart. Comparison between study groups was performed; mean differences with 95% confidence intervals between the controls and cases' z-scores were obtained to allow comparison between M-mode and TDI.

- **Study 2: Feasibility and reproducibility of a standard protocol for 2D speckle tracking and tissue Doppler-based strain and strain rate analysis of the fetal heart.**

  In order to determine intra-observer reliability, off-line analysis was performed twice by the same operator and for inter-observer reliability once by 2 independent operators. Intra- and interobserver reproducibility was analyzed using intraclass correlation and Bland-Altman scatter plots. Correlation between TDI- and 2D-strain-derived parameters was evaluated by linear regression analysis.

- **Study 3: Risk of perinatal death in early-onset intrauterine growth restriction according to gestational age and cardiovascular Doppler indices: a multicenter study.**

  Logistic regression was used to explore the association of UA, MCA, DV, IFI and MPI as continuous variables with perinatal mortality. Gestational age at delivery was also included, as it had been shown by previous studies to be the strongest predictor of perinatal mortality described in IUGR. As a second step, multivariate analysis was

performed on all variables as dichotomized parameters, with the gestational age cut-off point defined at 28 weeks. Decision tree analysis was performed using the CHAID (χ^2 automatic interaction detection) method, which creates a tree-based classification model where, by means of regression models, the best predictor variables are selected and presented. The significance level was established at 0.05, where at each step or level CHAID chose the independent (predictor) variable that had the strongest interaction with the dependent variable (perinatal mortality).

❖ **Study 4: Fetal echocardiography to predict infant hypertension and arterial remodeling in intrauterine growth restriction.**

First, a comparative study between control and IUGR fetuses and infants was performed. Comparison of fetal echocardiographic parameters was performed by linear regression and adjusted by gender, gestational age at delivery and preeclampsia in fetuses, and also by body surface area in infants. Secondly, the association and predictive value of standard perinatal data and fetal echocardiography for infant hypertension and arterial remodeling were assessed within the IUGR group. Data was analyzed by logistic regression in order to obtain odds ratio (OR) for the cardiovascular parameters associated with the infant outcome. In order to account for changes due to gestational age, fetal parameters were included as z-scores (when available) in the model. Finally, a composite score based on the strongest predictors was generated by multivariate logistic regression, and receiver operating characteristic (ROC) curve analysis was used for calculation of area under the curve (AUC) for the score and standard perinatal parameters.

5. STUDIES

STUDY 1

Value of annular M-mode displacement *vs* tissue Doppler velocities to assess cardiac function in intrauterine growth restriction.

Cruz-Lemini M, Crispi F, Valenzuela-Alcaraz B, Figueras F, Sitges M, Gómez O, Bijnens B, Gratacós E.
Ultrasound Obstet Gynecol. 2013;42(2):175-81.
doi: 10.1002/uog.12374.

Status: Published
Impact factor: 3.557
Quartile: 1st.

Ultrasound Obstet Gynecol 2013
Published online in Wiley Online Library (wileyonlinelibrary.com). **DOI:** 10.1002/uog.12374

Value of annular M-mode displacement *vs* tissue Doppler velocities to assess cardiac function in intrauterine growth restriction

M. CRUZ-LEMINI*†, F. CRISPI*†, B. VALENZUELA-ALCARAZ*†, F. FIGUERAS*†, M. SITGES†‡, O. GÓMEZ*†, B. BIJNENS§ and E. GRATACÓS*†

**Department of Maternal-Fetal Medicine, Fetal and Perinatal Medicine Research Group Institut Clínic de Ginecologia, Obstetrícia i Neonatologia, Barcelona, Spain; †Institut d'Investigacions Biomèdiques August Pi i Sunyer and Centro de Investigación Biomédica en Red de Enfermedades Raras (CIBERER), Hospital Clínic-University of Barcelona, Barcelona, Spain; ‡Department of Cardiology, Institut Clínic del Tórax, Hospital Clinic-University of Barcelona, Barcelona, Spain; §Institució Catalana de Recerca i Estudis Avançats (ICREA), Universitat Pompeu Fabra, Barcelona, Spain*

KEYWORDS: cardiac dysfunction; fetal echocardiography; fetal growth restriction; MAPSE; TAPSE; tissue Doppler imaging

ABSTRACT

Objective *To compare the ability of two different methods for longitudinal annular motion measurement, M-mode and tissue Doppler imaging (TDI), to demonstrate cardiac dysfunction in intrauterine-growth-restricted (IUGR) fetuses.*

Methods *Cardiac longitudinal annular motion in the basal free wall of the left ventricle (mitral annulus), interventricular septum and tricuspid annulus was assessed in 23 early-onset IUGR cases and 43 controls by TDI (annular peak velocities) and M-mode (displacement).*

Results *All annular parameters were significantly decreased in the IUGR group with respect to controls using both methods. M-mode showed a trend towards equal performance as classifier between cases and controls, as compared to TDI, mainly in the tricuspid annulus.*

Conclusions *Both M-mode and TDI demonstrate annular motion changes and consequently cardiac dysfunction in IUGR fetuses. M-mode imaging is simpler to perform and could be as sensitive as TDI for detecting subtle changes.* *Copyright © 2013 ISUOG. Published by John Wiley & Sons Ltd.*

INTRODUCTION

Intrauterine growth restriction (IUGR) due to placental insufficiency remains a significant cause of perinatal death and childhood disability including suboptimal neurodevelopment and increased cardiovascular risk later in life[1–5]. The heart is a central organ in the fetal adaptive mechanisms related to placental insufficiency, and cardiac dysfunction persists postnatally as one of the main features of fetal programming[5–7]. Evaluation of cardiac function has been proposed for the early diagnosis, monitoring and prediction of longterm outcome in IUGR[6–10]. Traditionally, most echocardiographic methods for the assessment of cardiac function have been based on blood flow measurements by conventional Doppler ultrasonography. Recently, new developments in echocardiographic imaging have enabled the quantification of myocardial motion and deformation[11,12]. These parameters have been shown to be potential markers of cardiac dysfunction in fetal life[8,13–15]. In particular, longitudinal myocardial motion is a sensitive early parameter for the indication of subclinical dysfunction *in utero*[16].

Longitudinal myocardial motion in fetuses has primarily been investigated by means of tissue Doppler imaging (TDI), which permits quantitative assessment of myocardial motion by calculating myocardial velocities, and it is routinely used in children and adults[8,13,16–23]. There is now extensive experience of the use of TDI for assessing cardiac function *in utero*[13,16,19,24–30]. However, TDI is highly demanding and requires expertise in echocardiography and specific ultrasound equipment and software. In addition, normal ranges may vary with different ultrasound settings, and most equipment uses presets designed for adults that do not allow adequate magnification for the fetal heart[31]. All these factors constitute important limitations for its widespread use in the clinical setting.

Correspondence to: Dr E. Gratacós, Department of Maternal-Fetal Medicine (ICGON), Hospital Clinic, Sabino de Arana 1, 08028, Barcelona, Spain (e-mail: gratacos@clinic.ub.es)

Accepted: 10 December 2012

Longitudinal cardiac motion can also be evaluated by measuring annular displacement using M-mode imaging. This method records the atrioventricular valve annulus's descent relative to an M-mode tracking line, aligned along the axis of longitudinal displacement of the annulus, and can be performed online (real-time M-mode) or offline (anatomical M-mode)[32]. Both tricuspid and mitral annular plane systolic excursions (TAPSE and MAPSE, respectively) have been reported to correlate well with TDI velocities[33,34]. TAPSE and MAPSE have been used to characterize ventricular function in several pediatric and adult conditions, such as valvular disease and heart failure[35,36], and in children who suffered IUGR[5,34,37–39]. In fetal echocardiography, M-mode longitudinal motion has previously been described as a feasible measurement with good reproducibility, and reference ranges have been published[26,32,40]. M-mode imaging could therefore be an attractive alternative to TDI for the evaluation of cardiac function in IUGR, but, to our knowledge, no studies of annular motion have been reported in fetuses with this condition.

In this study we aimed to compare the ability of longitudinal motion, as assessed using M-mode and TDI, as methods for demonstrating cardiac dysfunction in IUGR fetuses. We assessed longitudinal annular motion in a cohort of 23 cases with early-onset IUGR and 46 control fetuses, and evaluated the magnitude of the differences and the performance in detecting cardiac dysfunction for each method.

METHODS

The study population comprised 69 women with a singleton pregnancy attending the Department of Maternal–Fetal Medicine at Hospital Clinic in Barcelona from April 2010 to February 2012. Twenty-three consecutive cases of IUGR were included, IUGR being defined as an estimated fetal weight and confirmed birth weight below the 10th centile according to local reference curves, together with umbilical artery pulsatility index (PI) above the 95th centile[41,42]. The control group consisted of 46 normal fetuses, with estimated fetal weight and birth weight above the 10th centile, matched 2-to-1 with cases by gestational age at ultrasound scan (± 1 week). In all pregnancies, gestational age was estimated based on the crown–rump length at first-trimester ultrasound[43]. A secondary analysis was also performed using a control group matched 1-to-1 with the cases by estimated fetal weight, which was calculated at the time of echocardiography according to the method of Hadlock *et al.*[44]; both estimated fetal weight and birth weight centile were calculated using local reference curves[41]. For the purpose of this study, only cases that were delivered between 26 and 34 weeks' gestation were included. Pregnancies with structural/chromosomal anomalies or evidence of fetal infection were excluded. The study protocol was approved by the local ethics committee and patients provided written informed consent.

All women underwent ultrasound examination using a Siemens Sonoline Antares machine (Siemens Medical Systems, Malvern, PA, USA), including the measurement of mean PI of the uterine arteries, umbilical artery PI, middle cerebral artery PI, ductus venosus PI, aortic isthmus PI and myocardial performance index, according to previously published methodology[45–48]. The cerebroplacental ratio was calculated by dividing the middle cerebral artery PI by the umbilical artery PI, as previously described[45]. Upon delivery, gestational age, mode of delivery, birth weight, birth-weight centile, Apgar scores, umbilical artery pH and perinatal mortality and morbidity were recorded. Perinatal mortality was defined as either intrauterine death or neonatal death up to the age of 28 days[2]. Perinatal morbidity was defined by the presence of bronchopulmonary dysplasia, respiratory distress syndrome, necrotizing enterocolitis or neonatal sepsis[2,3,49].

Cardiac annular longitudinal motion was assessed in all cases and controls by TDI (velocity) and M-mode (displacement). TDI was performed in real time using a 2–10-MHz phased-array transducer. In an apical or basal four-chamber view, sample volumes were placed in the basal free wall of the left ventricle (mitral annulus), interventricular septum and right ventricular free wall (tricuspid annulus)[50]. Annular peak velocities were measured in early diastole (E′), atrial contraction (A′) and systole (S′), and reported in cm/s.

MAPSE, TAPSE and septal annular plane systolic excursion were measured by M-mode in real-time using a 2–6-MHz linear curved-array transducer in an apical or basal four-chamber view, by placing the cursor at right angles to the atrioventricular junction, marked by the valve rings at the mitral, tricuspid and basal septum, respectively. Maximum amplitude of motion was taken as the extent of displacement between end-systole and end-diastole (measured in mm). For both measurements, insonation by the ultrasound beam was kept at an angle of $<30°$ to the orientation of the ventricular wall or the interventricular septum, with no angle correction applied (Figure 1).

Statistical analysis

Data were analyzed with the IBM SPSS Statistics 19 statistical package (IBM, New York, NY, USA). The primary outcome S′ was used to calculate sample size because of a high sensitivity reported for detecting preclinical cardiac dysfunction in children[5]. Sample size was calculated to enable us to observe a difference of 25% in S′ between cases and controls, with 80% power and a 5% type-I risk. This resulted in a required sample of 20 individuals in each group for S′. All Doppler parameters were normalized into *Z*-scores using previously published reference values[26,45–48,50,51]. Echocardiographic parameters were adjusted for cardiac size by dividing the corresponding measurement by the longitudinal diameter of the heart. Comparison

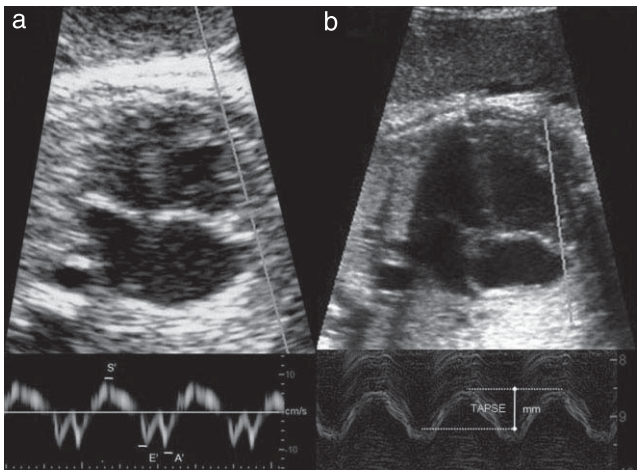

Figure 1 Ultrasound images illustrating measurement of longitudinal annular motion in fetuses using: (a) tissue Doppler imaging, showing right annular peak velocities for early diastole (E′), atrial contraction (A′) and systole (S′) (cm/s); and (b) M-mode, showing tricuspid annular plane systolic excursion (TAPSE) (mm).

between study groups was performed by Student's *t*-test for equality of means. Mean differences (with 95% confidence intervals (CI)) between the *Z*-scores of the controls and cases were calculated to allow comparison between M-mode and TDI in their ability to differentiate between these groups, and $P < 0.05$ was considered to be statistically significant.

RESULTS

Characteristics of the study populations are shown in Table 1. Baseline characteristics were similar in cases and controls, except for a higher prevalence of maternal smoking in the IUGR group than in controls. Gestational age at ultrasound was similar in both populations, while all fetoplacental Doppler parameters showed significantly worse values in the IUGR group, as expected. Also as expected, the growth-restricted group showed a significantly higher prevalence of pre-eclampsia, lower birth-weight centile and longer neonatal hospitalization in the neonatal intensive care unit. Almost all IUGR fetuses were delivered by Cesarean section, with worse 5-min Apgar scores and a non-significant trend towards worse umbilical artery pH. The IUGR cases showed 26% perinatal mortality and 65% morbidity.

Absolute values of left, right and septal annular peak velocities by TDI and displacement by M-mode are shown in Table 2. Both TDI and M-mode measurements were significantly lower in IUGR fetuses than in controls, with predominant differences observed in the tricuspid annulus in comparison to other areas. Table 3 shows all measurements normalized by longitudinal cardiac diameter (apex-to-base). When adjusted for cardiac size, only TDI A′ peak velocities, MAPSE and TAPSE showed a statistically significant difference between groups, although there was a trend towards lower values in the IUGR group for all the parameters evaluated.

Table 1 Baseline characteristics and perinatal outcomes in cases affected by intrauterine growth restriction (IUGR) delivered between 26 and 34 weeks' gestation and controls matched 2-to-1 by gestational age at ultrasound examination (US)

Characteristic	*Control group (n = 46)*	*IUGR group (n = 23)*	P
Maternal data			
Maternal age (years)	35 ± 5.2	34 ± 7.3	0.934
Caucasian	30 (65)	20 (87)	0.899
Smoker	6 (13)	6 (26)	< 0.001
Nulliparous	18 (39)	14 (61)	0.408
Fetoplacental US			
GA at US (weeks)	29.4 ± 2.5	28.7 ± 2.8	0.476
EFW (g)	1479 ± 486	750 ± 323	< 0.001
Mean UtA-PI	−0.57 ± 1.23	2.59 ± 1.78	< 0.001
UA-PI	−0.08 ± 0.48	5.00 ± 3.5	< 0.001
MCA-PI	0.46 ± 1.02	−1.80 ± 0.72	< 0.001
CPR	−0.04 ± 0.83	−3.32 ± 1.02	< 0.001
Ductus venosus PI	−0.44 ± 1.00	3.23 ± 3.78	< 0.001
Reversed aortic isthmus diastolic flow	0 (0)	10 (43)	< 0.001
MPI	0.02 ± 0.73	1.66 ± 1.04	< 0.001
Pregnancy outcomes			
Pre-eclampsia	0 (0)	10 (43)	< 0.001
GA at delivery (weeks)	39 ± 2	30 ± 2	< 0.001
Birth weight (g)	3334 ± 429	847 ± 328	< 0.001
Birth-weight centile	54 ± 28	0 ± 1	< 0.001
Cesarean section	6 (13)	22 (96)	< 0.001
5-min Apgar score < 7	0 (0)	3 (13)	0.036
UA pH	7.24 ± 1	7.20 ± 1	0.112
Perinatal mortality	0 (0)	6 (26)	< 0.001
Days in NICU	0 ± 0	64 ± 25	< 0.001
Perinatal morbidity	0 (0)	15 (65)	< 0.001

Data are expressed as mean ± SD or *n* (%). Doppler parameters expressed as *Z*-scores. CPR, cerebroplacental ratio; EFW, estimated fetal weight; GA, gestational age; MCA, middle cerebral artery; MPI, myocardial performance index; NICU, neonatal intensive care unit; PI, pulsatility index; UA, umbilical artery; UtA, uterine artery.

Examination of the mean differences between the *Z*-scores of controls and cases showed that M-mode measurements had a similar performance to TDI in demonstrating differences between the two groups (Figure 2).

In the secondary analysis using a control group matched to the cases by estimated fetal weight, the same findings were observed with regard to the differences between groups for cardiac variables assessed using M-mode and TDI (Tables S1 and S2).

DISCUSSION

Our study confirms the previous research finding that IUGR fetuses have a significant decrease in longitudinal myocardial motion as part of the fetal cardiovascular adaptation to placental insufficiency. These changes can be quantified using TDI or M-mode imaging, and the data suggest that the latter could be as sensitive as the former for detecting subtle cardiac dysfunction.

Our results showing decreased longitudinal motion, as measured by annular peak velocities in IUGR, are consistent with those of previously published

Table 2 Cardiac annular motion measurements by tissue Doppler imaging (TDI) and M-mode in cases of intrauterine growth restriction (IUGR) and controls matched 2-to-1 by gestational age

Characteristic	*Control group (n = 46)*	*IUGR group (n = 23)*	P
Annular peak velocity (cm/s) by TDI			
Left E′	7.4 ± 0.9	6.2 ± 1.3	< 0.001
Left A′	8.4 ± 1.5	6.7 ± 1.1	< 0.001
Left S′	6.9 ± 0.6	5.7 ± 1.2	< 0.001
Right E′	8.3 ± 0.8	6.9 ± 1.5	< 0.001
Right A′	11.9 ± 0.8	9.1 ± 1.6	< 0.001
Right S′	7.6 ± 1.0	6.9 ± 1.7	0.016
Septal E′	6.8 ± 1.5	5.2 ± 1.3	< 0.001
Septal A′	6.8 ± 0.8	6.2 ± 1.4	< 0.001
Septal S′	5.5 ± 0.8	5.2 ± 1.0	< 0.001
Annular displacement (mm) by M-mode			
MAPSE	5.5 ± 0.8	3.9 ± 1.2	< 0.001
TAPSE	7.6 ± 0.9	5.2 ± 1.5	< 0.001
SAPSE	4.2 ± 0.8	3.2 ± 0.8	0.004

Data are expressed as mean ± SD. A′, atrial contraction peak velocity; E′, early diastolic peak velocity; MAPSE, mitral annular plane systolic excursion; S′, systolic peak velocity; SAPSE, septal annular plane systolic excursion; TAPSE, tricuspid annular plane systolic excursion.

Table 3 Adjusted cardiac annular motion measurements by tissue Doppler imaging (TDI) and M-mode in cases of intrauterine growth restriction (IUGR) and controls matched 2-to-1 by gestational age, expressed as a ratio of raw measurement to longitudinal cardiac diameter

Characteristic	*Control group (n = 46)*	*IUGR group (n = 23)*	P
Annular peak velocity (cm/s) by TDI			
Left E′	2.16 ± 0.49	1.95 ± 0.49	0.356
Left A′	2.74 ± 0.74	2.14 ± 0.44	0.004
Left S′	2.02 ± 0.28	1.83 ± 0.50	0.102
Right E′	2.44 ± 0.44	2.25 ± 0.47	0.215
Right A′	3.29 ± 0.57	2.91 ± 0.53	0.013
Right S′	2.24 ± 0.41	2.26 ± 0.59	0.872
Septal E′	1.83 ± 0.33	1.72 ± 0.52	0.584
Septal A′	2.35 ± 0.39	2.01 ± 0.46	0.011
Septal S′	1.83 ± 0.27	1.68 ± 0.38	0.213
Annular displacement (mm) by M-mode			
MAPSE	1.39 ± 0.24	1.23 ± 0.32	0.045
TAPSE	1.86 ± 0.33	1.63 ± 0.38	0.009
SAPSE	1.13 ± 0.24	0.98 ± 0.18	0.067

Data are expressed as mean ± SD. A′, atrial contraction peak velocity; E′, early diastolic peak velocity; MAPSE, mitral annular plane systolic excursion; S′, systolic peak velocity; SAPSE, septal annular plane systolic excursion; TAPSE, tricuspid annular plane systolic excursion.

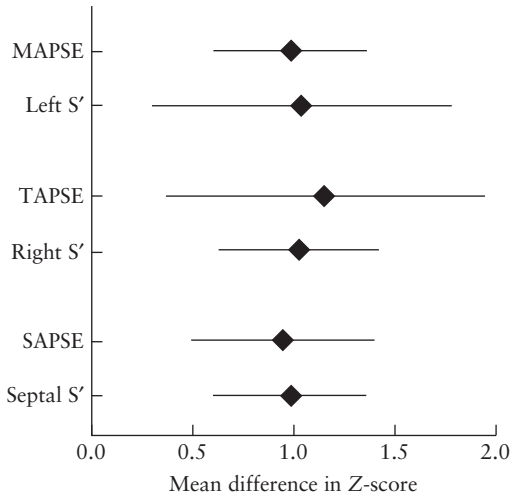

Figure 2 Plot of mean difference (♦), with 95% confidence intervals (—), of *Z*-scores between controls and cases of intrauterine growth restriction, in longitudinal annular motion as assessed by tissue Doppler and M-mode imaging. MAPSE, mitral annular plane systolic excursion; S′, systolic peak velocity; SAPSE, septal annular plane systolic excursion; TAPSE, tricuspid annular plane systolic excursion.

studies[8,16,18,52]. To our knowledge, this is the first study that has evaluated longitudinal motion using M-mode in IUGR fetuses as a potential tool for describing subclinical cardiac dysfunction in this group. M-mode and TDI results in children who had suffered IUGR[5] and reports on the fetal and adult heart show good correlation between these methods[26,33,34,53]. In this study, differences in longitudinal motion were more pronounced by M-mode in the right annulus (TAPSE). This is consistent with the results of previous studies[8,16], and with the notion that the right ventricle could be more suited to the assessment of longitudinal motion, owing to the longitudinal nature of its fibers as opposed to left ventricle fibers, which are mainly circumferential[26,54,55]. TAPSE has also shown a higher reproducibility and lower variability than other more commonly used cardiovascular measurements[37,39,53].

In our study, changes observed with M-mode showed a trend towards equal performance as TDI, and these changes remained significant following adjustment of measurements for cardiac size. The observed changes in cardiovascular parameters were small, and would qualify as indicative of subclinical cardiac dysfunction. The clinical relevance of these changes is still unknown; however, as for the concept of pre-hypertension, in which small changes in blood pressure (even within normal ranges) have been shown to increase cardiovascular risk, we believe it is reasonable to assume that small changes in cardiac function are relevant at this stage in fetal development. When the mean differences in *Z*-scores between groups were compared, a similar performance could be observed for M-mode measurements as for TDI. This could be partially explained by a higher reproducibility achieved in the clinical setting, and lesser requirements with regards to degree of expertise and ultrasound software/equipment for M-mode as compared to TDI[26,33,53]. Thus, M-mode might provide a simpler means of measuring annular motion for assessing fetal cardiac dysfunction in the context of IUGR, and possibly more generally.

In this study, crude TDI and M-mode values were adjusted by cardiac size for the first time. When performing this adjustment, significant differences between groups for many of the parameters were

lost, however, a trend towards lower values in the IUGR group was maintained. Previous studies have reported adjustment of TDI and M-mode measurements by gestational age or estimated fetal weight[16,26]. The rationale for providing adjustment by heart size comes from the fact that annular displacement and velocities depend on this parameter[50,56]. As heart size is highly correlated with body size, in normal conditions adjustment could be performed using either measurement. However, in IUGR there is relative cardiomegaly[57,58], thus we believe that cardiac size is a better parameter with which to perform adjustment.

We acknowledge that there are various strengths and limitations of our study. The selection criteria were strict, including only cases with abnormal umbilical artery Doppler and a complete echocardiographic evaluation. Doppler and cardiac evaluations were carried out by experienced examiners and results were adjusted by gestational age or cardiac size. Extreme care was taken to ensure that insonation angles were as close to 0° as possible, and to verify reliability of the measurements. On the other hand, we acknowledge the sample size as a limitation of the study, as IUGR cases born before 34 weeks' gestation are scarce in the clinical setting; further studies will be required to corroborate our findings. Another limitation is the potential interaction of confounders, such as the presence of pre-eclampsia in almost half of the IUGR population. However, we believe that the bias would be minimal, as previous studies have demonstrated that pre-eclampsia has almost no effect on fetal cardiac function in IUGR pregnancies[59]. Finally, the strict echocardiographic methodological criteria used to obtain the measurements in this study are vital for reproducibility in other settings, and future studies are warranted to confirm the external validity of our results.

In conclusion, IUGR fetuses present signs of longitudinal cardiac subclinical dysfunction, demonstrated by lower TDI and M-mode values in both the mitral and tricuspid annuli. Differences observed in our study suggest that M-mode imaging could be helpful in monitoring these fetuses owing to its lower technical demands in comparison to TDI. Further studies in IUGR and other fetal conditions are required to confirm our findings and determine the role these techniques have in assessing fetal cardiac function.

ACKNOWLEDGMENTS

The Fetal and Perinatal Medicine Research Group was supported by grants from Instituto de Salud Carlos III (ref. PI11/00051, PI11/01709) cofinanciado por el Fondo Europeo de Desarrollo Regional de la Unión Europea 'Una manera de hacer Europa'; Centro para el Desarrollo Técnico Industrial (Ref. cvREMOD 2009–2012) apoyado por el Ministerio de Economia y Competitividad y Fondo de inversión local para el empleo, Spain; Ministerio de Economia y Competitividad PN de I + D + I 2008–2011 (ref. SAF2009_08815); Cerebra Foundation for the Brain Injured Child (Carmarthen, Wales, UK) and Thrasher Research Fund (Salt Lake City, USA). M.C.L and B.V.A. wish to express their gratitude to the Mexican National Council for Science and Technology (CONACyT, Mexico City, Mexico) for supporting their predoctoral stay at Hospital Clinic, Barcelona, Spain.

REFERENCES

1. Figueras F, Gardosi J. Intrauterine growth restriction: new concepts in antenatal surveillance, diagnosis, and management. *Am J Obstet Gynecol* 2011; **204**: 288–300.
2. Baschat AA, Cosmi E, Bilardo CM, Wolf H, Berg C, Rigano S, Germer U, Moyano D, Turan S, Hartung J, Bhide A, Muller T, Bower S, Nicolaides KH, Thilaganathan B, Gembruch U, Ferrazzi E, Hecher K, Galan HL, Harman CR. Predictors of neonatal outcome in early-onset placental dysfunction. *Obstet Gynecol* 2007; **109**: 253–261.
3. Bernstein IM, Horbar JD, Badger GJ, Ohlsson A, Golan A. Morbidity and mortality among very-low-birth-weight neonates with intrauterine growth restriction. The Vermont Oxford Network. *Am J Obstet Gynecol* 2000; **182**: 198–206.
4. Figueras F, Cruz-Martinez R, Sanz-Cortes M, Arranz A, Illa M, Botet F, Costas-Moragas C, Gratacos E. Neurobehavioral outcomes in preterm, growth-restricted infants with and without prenatal advanced signs of brain-sparing. *Ultrasound Obstet Gynecol* 2011; **38**: 288–294.
5. Crispi F, Bijnens B, Figueras F, Bartrons J, Eixarch E, Le Noble F, Ahmed A, Gratacos E. Fetal growth restriction results in remodeled and less efficient hearts in children. *Circulation* 2010; **121**: 2427–2436.
6. Crispi F, Hernandez-Andrade E, Pelsers MM, Plasencia W, Benavides-Serralde JA, Eixarch E, Le Noble F, Ahmed A, Glatz JF, Nicolaides KH, Gratacos E. Cardiac dysfunction and cell damage across clinical stages of severity in growth-restricted fetuses. *Am J Obstet Gynecol* 2008; **199**: 254.e1–8.
7. Cruz-Martinez R, Figueras F, Hernandez-Andrade E, Oros D, Gratacos E. Changes in myocardial performance index and aortic isthmus and ductus venosus Doppler in term, small-for-gestational age fetuses with normal umbilical artery pulsatility index. *Ultrasound Obstet Gynecol* 2011; **38**: 400–405.
8. Comas M, Crispi F, Cruz-Martinez R, Figueras F, Gratacos E. Tissue Doppler echocardiographic markers of cardiac dysfunction in small-for-gestational age fetuses. *Am J Obstet Gynecol* 2011; **205**: 57.e1–6.
9. Cruz-Martinez R, Figueras F, Benavides-Serralde A, Crispi F, Hernandez-Andrade E, Gratacos E. Sequence of changes in myocardial performance index in relation to aortic isthmus and ductus venosus Doppler in fetuses with early-onset intrauterine growth restriction. *Ultrasound Obstet Gynecol* 2011; **38**: 179–184.
10. Acharya G, Tronnes A, Rasanen J. Aortic isthmus and cardiac monitoring of the growth-restricted fetus. *Clin Perinatol* 2011; **38**: 113–125, vi–vii.
11. Bijnens B, Cikes M, Butakoff C, Sitges M, Crispi F. Myocardial motion and deformation: What does it tell us and how does it relate to function? *Fetal Diagn Ther* 2012; **32**: 5–16.
12. Germanakis I, Gardiner H. Assessment of fetal myocardial deformation using speckle tracking techniques. *Fetal Diagn Ther* 2012; **32**: 39–46.
13. Van Mieghem T, DeKoninck P, Steenhaut P, Deprest J. Methods for prenatal assessment of fetal cardiac function. *Prenat Diagn* 2009; **29**: 1193–1203.
14. Matsui H, Germanakis I, Kulinskaya E, Gardiner HM. Temporal and spatial performance of vector velocity imaging in the human fetal heart. *Ultrasound Obstet Gynecol* 2011; **37**: 150–157.
15. Pu DR, Zhou QC, Zhang M, Peng QH, Zeng S, Xu GQ. Assessment of regional right ventricular longitudinal functions

in fetus using velocity vector imaging technology. *Prenat Diagn* 2010; **30**: 1057–1063.
16. Comas M, Crispi F, Cruz-Martinez R, Martinez JM, Figueras F, Gratacós E. Usefulness of myocardial tissue Doppler vs conventional echocardiography in the evaluation of cardiac dysfunction in early-onset intrauterine growth restriction. *Am J Obstet Gynecol* 2010; **203**: 45.e1–7.
17. Larsen LU, Sloth E, Petersen OB, PedersenTF, Sorensen K, Uldbjerg N. Systolic myocardial velocity alterations in the growth-restricted fetus with cerebroplacental redistribution. *Ultrasound Obstet Gynecol* 2009; **34**: 62–67.
18. Naujorks AA, Zielinsky P, Beltrame PA, Castagna RC, Petracco R, Busato A, Nicoloso AL, Piccoli A, Manica JL. Myocardial tissue Doppler assessment of diastolic function in the growth-restricted fetus. *Ultrasound Obstet Gynecol* 2009; **34**: 68–73.
19. Comas M, Crispi F. Assessment of fetal cardiac function using tissue Doppler techniques. *Fetal Diagn Ther* 2012; **32**: 30–38.
20. Cua CL, Cooper AL, Stein MA, Corbitt RJ, Nelin LD. Tissue Doppler changes in three neonates with congenital diaphragmatic hernia. *ASAIO J* 2009; **55**: 417–419.
21. Cui W, Roberson DA, Chen Z, Madronero LF, Cuneo BF. Systolic and diastolic time intervals measured from Doppler tissue imaging: normal values and *Z*-score tables, and effects of age, heart rate, and body surface area. *J Am Soc Echocardiogr* 2008; **21**: 361–370.
22. Dragulescu A, Mertens LL. Developments in echocardiographic techniques for the evaluation of ventricular function in children. *Arch Cardiovasc Dis* 2010; **103**: 603–614.
23. Patel N, Mills JF, Cheung MM. Assessment of right ventricular function using tissue Doppler imaging in infants with pulmonary hypertension. *Neonatology* 2009; **96**: 193–199; discussion 200–202.
24. Chan LY, Fok WY, Wong JT, Yu CM, Leung TN, Lau TK. Reference charts of gestation-specific tissue Doppler imaging indices of systolic and diastolic functions in the normal fetal heart. *Am Heart J* 2005; **150**: 750–755.
25. Di Naro E, Cromi A, Ghezzi F, Giocolano A, Caringella A, Loverro G. Myocardial dysfunction in fetuses exposed to intraamniotic infection: new insights from tissue Doppler and strain imaging. *Am J Obstet Gynecol* 2010; **203**: 459.e1–7.
26. Gardiner HM, Pasquini L, Wolfenden J, Barlow A, Li W, Kulinskaya E, Henein M. Myocardial tissue Doppler and long axis function in the fetal heart. *Int J Cardiol* 2006; **113**: 39–47.
27. Harada K, Tsuda A, Orino T, Tanaka T, Takada G. Tissue Doppler imaging in the normal fetus. *Int J Cardiol* 1999; **71**: 227–234.
28. Huhta JC, Kales E, Casbohm A. Fetal tissue Doppler—a new technique for perinatal cardiology. *Curr Opin Pediatr* 2003; **15**: 472–474.
29. Paladini D, Lamberti A, Teodoro A, Arienzo M, Tartaglione A, Martinelli P. Tissue Doppler imaging of the fetal heart. *Ultrasound Obstet Gynecol* 2000; **16**: 530–535.
30. Crispi F, Gratacos E. Fetal cardiac function: technical considerations and potential research and clinical applications. *Fetal Diagn Ther* 2012; **32**: 47–64.
31. Koopman LP, Slorach C, Manlhiot C, McCrindle BW, Friedberg MK, Mertens L, Jaeggi ET. Myocardial tissue Doppler velocity imaging in children: comparative study between two ultrasound systems. *J Am Soc Echocardiogr* 2010; **23**: 929–937.
32. Germanakis I, Pepes S, Sifakis S, Gardiner H. Fetal longitudinal myocardial function assessment by anatomic M-mode. *Fetal Diagn Ther* 2012; **32**: 65–71.
33. Papaioannou VE, Stakos DA, Dragoumanis CK, Pneumatikos IA. Relation of tricuspid annular displacement and tissue Doppler imaging velocities with duration of weaning in mechanically ventilated patients with acute pulmonary edema. *BMC Cardiovasc Disord* 2010; **10**: 20.
34. Bazaz R, Edelman K, Gulyasy B, Lopez-Candales A. Evidence of robust coupling of atrioventricular mechanical function of the right side of the heart: insights from M-mode analysis of annular motion. *Echocardiography* 2008; **25**: 557–561.
35. Lisi M, Ballo P, Cameli M, Gandolfo F, Galderisi M, Chiavarelli M, Henein MY, Mondillo S. Mitral annular longitudinal function preservation after mitral valve repair: the MARTE study. *Int J Cardiol* 2012; **157**: 212–215.
36. Wenzelburger FW, Tan YT, Choudhary FJ, Lee ES, Leyva F, Sanderson JE. Mitral annular plane systolic excursion on exercise: a simple diagnostic tool for heart failure with preserved ejection fraction. *Eur J Heart Fail* 2011; **13**: 953–960.
37. Cappelli F, Cristina Porciani M, Ricceri I, Perrotta L, Ricciardi G, Pieragnoli P, Paladini G, Michelucci A, Padeletti L. Tricuspid annular plane systolic excursion evaluation improves selection of cardiac resynchronization therapy patients. *Clin Cardiol* 2010; **33**: 578–582.
38. Giovanardi P, Tincani E, Rossi R, Agnoletto V, Bondi M, Modena MG. Right ventricular function predicts cardiovascular events in outpatients with stable cardiovascular diseases: preliminary results. *Intern Emerg Med* 2012; **7**: 251–256.
39. Koestenberger M, Nagel B, Ravekes W, Urlesberger B, Raith W, Avian A, Halb V, Cvirn G, Fritsch P, Gamillscheg A. Systolic right ventricular function in preterm and term neonates: reference values of the tricuspid annular plane systolic excursion (TAPSE) in 258 patients and calculation of *Z*-score values. *Neonatology* 2011; **100**: 85–92.
40. Carvalho JS, O'Sullivan C, Shinebourne EA, Henein MY. Right and left ventricular long-axis function in the fetus using angular M-mode. *Ultrasound Obstet Gynecol* 2001; **18**: 619–622.
41. Figueras F, Meler E, Iraola A, Eixarch E, Coll O, Figueras J, Francis A, Gratacos E, Gardosi J. Customized birthweight standards for a Spanish population. *Eur J Obstet Gynecol Reprod Biol* 2008; **136**: 20–24.
42. Arduini D, Rizzo G. Normal values of Pulsatility Index from fetal vessels: a cross-sectional study on 1556 healthy fetuses. *J Perinat Med* 1990; **18**: 165–172.
43. Robinson HP, Sweet EM, Adam AH. The accuracy of radiological estimates of gestational age using early fetal crown–rump length measurements by ultrasound as a basis for comparison. *Br J Obstet Gynaecol* 1979; **86**: 525–528.
44. Hadlock FP, Harrist RB, Shah YP, King DE, Park SK, Sharman RS. Estimating fetal age using multiple parameters: a prospective evaluation in a racially mixed population. *Am J Obstet Gynecol* 1987; **156**: 955–957.
45. Baschat AA, Gembruch U. The cerebroplacental Doppler ratio revisited. *Ultrasound Obstet Gynecol* 2003; **21**: 124–127.
46. Del Río M, Martínez JM, Figueras F, López M, Palacio M, Gómez O, Coll O, Puerto B. Reference ranges for Doppler parameters of the fetal aortic isthmus during the second half of pregnancy. *Ultrasound Obstet Gynecol* 2006; **28**: 71–76.
47. Gómez O, Figueras F, Fernández S, Bennasar M, Martínez JM, Puerto B, Gratacós E. Reference ranges for uterine artery mean pulsatility index at 11–41 weeks of gestation. *Ultrasound Obstet Gynecol* 2008; **32**: 128–132.
48. Hecher K, Campbell S, Snijders R, Nicolaides K. Reference ranges for fetal venous and atrioventricular blood flow parameters. *Ultrasound Obstet Gynecol* 1994; **4**: 381–390.
49. Papile LA, Burstein J, Burstein R, Koffler H. Incidence and evolution of subependymal and intraventricular hemorrhage: a study of infants with birth weights less than 1,500 gm. *J Pediatr* 1978; **92**: 529–534.
50. Comas M, Crispi F, Gómez O, Puerto B, Figueras F, Gratacós E. Gestational age- and estimated fetal weight-adjusted reference ranges for myocardial tissue Doppler indices at 24–41 weeks' gestation. *Ultrasound Obstet Gynecol* 2011; **37**: 57–64.
51. Cruz-Martínez R, Figueras F, Bennasar M, García-Posadas R, Crispi F, Hernández-Andrade E, Gratacós E. Normal reference ranges from 11 to 41 weeks' gestation of fetal left modified myocardial performance index by conventional Doppler with the use of stringent criteria for delimitation of the time periods. *Fetal Diagn Ther* 2012; **32**: 79–86.
52. Larsen LU, Petersen OB, Sloth E, Uldbjerg N. Color Doppler myocardial imaging demonstrates reduced diastolic tissue

velocity in growth retarded fetuses with flow redistribution. *Eur J Obstet Gynecol Reprod Biol* 2011; **155**: 140–145.
53. Papaioannou VE, Pneumatikos IA. The use of tricuspid annular plane systolic excursion and tissue Doppler imaging velocities for the estimation of pulmonary hypertension and right ventricular function in mechanically ventilated patients. In *Establishing Better Standards of Care in Doppler Echocardiography, Computed Tomography and Nuclear Cardiology*, Fleming RM (ed.) InTech: Rijeka, Croatia and Shanghai, China, 2011; 17–30.
54. Godfrey ME, Messing B, Cohen SM, Valsky DV, Yagel S. Functional assessment of the fetal heart: a review. *Ultrasound Obstet Gynecol* 2012; **39**: 131–144.
55. Ho SY, Nihoyannopoulos P. Anatomy, echocardiography, and normal right ventricular dimensions. *Heart* 2006; **92** (Suppl): i2–13.
56. Batterham A, Shave R, Oxborough D, Whyte G, George K. Longitudinal plane colour tissue-Doppler myocardial velocities and their association with left ventricular length, volume, and mass in humans. *Eur J Echocardiogr* 2008; **9**: 542–546.
57. Batton DG, Roberts C, Cacciarelli A. Cardiothoracic ratio in newborns with severe intrauterine growth retardation. *Clin Pediatr (Phila)* 1992; **31**: 564–565.
58. Bozynski ME, Hanafy FH, Hernandez RJ. Association of increased cardiothoracic ratio and intrauterine growth retardation. *Am J Perinatol* 1991; **8**: 28–30.
59. Crispi F, Comas M, Hernández-Andrade E, Eixarch E, Gómez O, Figueras F, Gratacós E. Does pre-eclampsia influence fetal cardiovascular function in early-onset intrauterine growth restriction? *Ultrasound Obstet Gynecol* 2009; **34**: 660–665.

SUPPORTING INFORMATION ON THE INTERNET

The following supporting information may be found in the online version of this article:

Table S1 Cardiac annular motion measurements by tissue Doppler imaging (TDI) and M-mode in cases of intrauterine growth restriction (IUGR) and two control groups, one matched 2-to-1 by gestational age (GA) and the other matched 1-to-1 by estimated fetal weight (EFW)

Table S2 Adjusted cardiac annular motion measurements by tissue Doppler imaging (TDI) and M-mode in cases of intrauterine growth restriction (IUGR) and two control groups, one matched 2-to-1 by gestational age (GA) and the other matched 1-to-1 by estimated fetal weight (EFW). Data are expressed as a ratio between the raw measurement and longitudinal cardiac diameter

STUDY 2

Feasibility and reproducibility of a standard protocol for 2D speckle tracking and tissue Doppler-based strain and strain rate analysis of the fetal heart.

Crispi F, Sepulveda-Swatson E, Cruz-Lemini M, Rojas-Benavente J, Garcia-Posada R, Dominguez JM, Sitges M, Bijnens B, Gratacós E.
Fetal Diagn Ther. 2012;32(1-2):96-108.
doi: 10.1159/000337329.

Status: Published
Impact factor: 1.902
Quartile: 3rd.

Original Paper: Techniques

Fetal Diagnosis and Therapy

Fetal Diagn Ther
DOI: 10.1159/000337329

Received: October 21, 2011
Accepted after revision: February 9, 2012
Published online: June 19, 2012

Feasibility and Reproducibility of a Standard Protocol for 2D Speckle Tracking and Tissue Doppler-Based Strain and Strain Rate Analysis of the Fetal Heart

Fàtima Crispi[a, c] Eduardo Sepulveda-Swatson[a, c] Monica Cruz-Lemini[a, c] Juan Rojas-Benavente[a, c] Raul Garcia-Posada[a, c] Jesus Maria Dominguez[a, c] Marta Sitges[b] Bart Bijnens[d] Eduard Gratacós[a, c]

[a]Department of Maternal-Fetal Medicine, Institut Clínic de Ginecologia, Obstetrícia i Neonatologia, and [b]Cardiology Department, Thorax Clinic Institute, Hospital Clinic – Institut d'Investigacions Biomèdiques August Pi i Sunyer, University of Barcelona, [c]Centro de Investigación Biomédica en Red en Enfermedades Raras, and [d]ICREA-Universitat Pompeu Fabra, Barcelona, Spain

Key Words
Tissue Doppler imaging · 2D speckle tracking · Reproducibililty

Abstract

Purpose: Assessment of cardiac function in the fetal heart is challenging because of its small size and high heart rate, restricted physical access to the fetus, and impossibility of fetal ECG recording. We aimed to standardize the acquisition and postprocessing of fetal echocardiography for deformation analysis and to assess its feasibility, reproducibility, and correlation for longitudinal strain and strain rate measurements by tissue Doppler imaging (TDI) and 2D speckle tracking (2D-strain) during pregnancy. ***Methods:*** Echocardiography was performed in 56 fetuses. 2D and color TDI in apical or basal four-chamber views were recorded for subsequent analysis. Caution was taken to achieve a frame rate >70 Hz for speckle tracking and >150 Hz for TDI analysis. For each acquisition, 7.5 s of noncompressed data were stored in cine loop format and analyzed offline. Since fetal ECG information is by definition not available, aortic valve closure was marked from aortic flow and the onset of each cardiac cycle was manually indicated in the 2D images. Sample volume length was standardized at the minimum size. Two observers measured the left and right ventricular peak systolic longitudinal strain and strain-rate. ***Results:*** Strain and strain rate measurements were feasible in 93% of the TDI and 2D-strain acquisitions. The mean time spent on analyzing TDI images was 18 min, with an intraclass agreement coefficient of 0.86 (95% CI 0.77–0.92), 0.83 (95% CI 0.72–0.90), 0.96 (95% CI 0.93–0.98), and 0.86 (95% CI 0.76–0.92) for basal left and right free wall peak systolic strain and strain rate, respectively. Agreement between observers using tissue Doppler also showed high reliability. The mean time spent for 2D-strain analysis was 15 min, with an intraclass agreement coefficient of 0.97 (95% CI 0.95–0.98), 0.94 (95% CI 0.89–0.96), 0.96 (95% CI 0.93–0.98), and 0.84 (95% CI 0.73–0.90) for basal left and right free wall peak systolic strain and strain rate, respectively. Agreement between observers also showed a high reliability that was similar for TDI and 2D-strain. There was a weak correlation between TDI and 2D-strain measurements. ***Conclusions:*** A standard protocol with fixed acquisition and processing settings, including manual indication of the timing events of

KARGER

Fax +41 61 306 12 34
E-Mail karger@karger.ch
www.karger.com

1015–3837/12/0000–0000$38.00/0

Accessible online at:
www.karger.com/fdt

Eduard Gratacós
Department of Maternal-Fetal Medicine (ICGON), Hospital Clinic
Sabino de Arana 1
ES–08028 Barcelona (Spain)
Tel. +34 932 279 946, E-Mail egratacos@clinic.ub.es

the cardiac cycle to correct for the lack of ECG, was feasible and reproducible for the evaluation of longitudinal ventricular strain and strain rate of the fetal heart by TDI as well as 2D-strain analysis. However, both techniques are not interchangeable as the correlation between them is relatively poor.

Introduction

Fetal echocardiography was initially used for the identification of structural congenital disease; however, more recently attention has moved to its potential in the assessment of cardiac function [1]. As the heart is a central organ in fetal adaptative mechanisms, evaluation of cardiac function has been proposed to predict outcomes and to monitor fetal well-being in several cardiac [2, 3] and extracardiac pathologies such as fetal hypoxia [4–6], hyperglycemia [7, 8], pressure or volume overload [9, 10], or cardiac compression [11]. Traditionally most echocardiographic methods were based on interrogating blood flow by Doppler or myocardial motion by M-mode [1, 12]. Recently, new developments in echocardiographic imaging technology have enabled the quantification of myocardial deformation based on tissue Doppler imaging (TDI) or 2D speckle tracking (2D-strain) which provide regional information on myocardial contractility and interaction with neighboring segments and global circulation that cannot be obtained from conventional Doppler techniques [13]. Myocardial deformation, measured as strain and strain rate, better assesses intrinsic properties of the cardiac fibers and myocytes [13] and has been demonstrated to be a very sensitive marker of cardiac dysfunction in adulthood [14–17]. These techniques also permit evaluation of the different and partially independent components of ventricular contraction and motion (longitudinal, radial, or circumferential) and can assess regional changes [13].

Both TDI and 2D-strain have demonstrated their feasibility and reproducibility in adults and have been validated in several experimental models and humans [13, 17–19]. However, their applicability in the fetal heart is challenging because of its small size and high heart rate, restricted physical access to the fetus, and impossibility of fetal ECG recording. Both techniques require postprocessing and offline analysis based on software tools designed for the adult heart and using a concomitant ECG registration. Additionally, they are dependent on the ultrasound equipment, and results using the different commercially available softwares are not fully comparable [20]. Despite these limitations, several studies in fetuses have reported myocardial motion and deformation using these techniques [21–35]. However, results are inconsistent and data on reproducibility are variable depending on the acquisition protocol and ultrasound equipment used. Finally, few reports have assessed the potential correlation between these techniques in utero [33].

We aimed to standardize the acquisition and postprocessing of fetal echocardiography for deformation analysis and to assess its feasibility and reproducibility for longitudinal strain and strain rate measurements by TDI and 2D-strain during pregnancy. A secondary aim was to evaluate the correlation between both techniques in fetal life.

Materials and Methods

Study Populations

The study population included 56 fetuses selected from women who attended the Maternal-Fetal Medicine Department at the Hospital Clinic in Barcelona (Spain) from October 2009 to September 2010. The study protocol was approved by the local Ethics Committee and patients provided their written informed consent. Exclusion criteria were structural/chromosomal anomalies, twin pregnancy, or evidence of fetal infection. All participants underwent a full morphologic examination of the fetal heart in order to exclude any cardiac structural anomaly using a Siemens Sonoline Antares (Siemens Medical Systems, Malvern, Pa., USA). Conventional feto-placental Doppler examination included the umbilical artery, middle cerebral artery, cerebro-placental ratio, ductus venosus, and left myocardial performance index. The cerebro-placental ratio was measured by dividing the middle cerebral artery and umbilical artery pulsatility indices. The ductus venosus was measured in either a midsagittal or a transverse view positioning the Doppler gate at the ductus venosus isthmic portion. The left myocardial performance index was obtained using the clicks of mitral and aorta valves as landmarks as previously described [36]. At delivery, gestational age, birth weight percentile, Apgar score, and pregnancy complications were recorded.

Ultrasound Acquisition

All patients underwent an ultrasonographic examination using a Vivid q (General Electric Healthcare, Horten, Norway) ultrasound system. A phased array sector probe of 1.4–2.5 MHz was used to obtain an apical or basal four-chamber view with the septum or free wall aligned parallel to the Doppler beam (<10° without further angle correction) in 2D for subsequent analysis. Three additional color TDI video clips were obtained from the septum and left and right free wall. If needed, a sector tilt was used to make sure that the angle between the probe and myocardial motion was <15%. No angle correction was applied offline. While recording the loop, the 2D scan area and the TDI color box were kept as small as possible to obtain the highest frame rate. The color gain was adjusted to avoid aliasing. Scans were performed

in the absence of maternal and fetal breathing or movements. Caution was taken to achieve >150 frames per second (fps) for TDI and >70 fps for 2D-strain. The frame rate/heart rate ratio was calculated for each technique. For each acquisition, 7.5 s of non-compressed data were stored in cine loop format and analyzed offline using a GE Echo Pac PC SW 108.1.x (General Electric Healthcare). The cine loops were reviewed and only those with at least 5 consecutive measurable cardiac cycles were considered valid for the study. Scans were performed by two operators (M.C.-L. and F.C.). In order to determine intraobserver reliability, offline analysis was performed twice by the same operator (J.R.-B. or E.S.-S.), and for interobserver reliability it was performed once by 2 independent operators (J.R.-B., E.S.-S. or R.G.-P.).

Tissue Doppler Imaging

TDI offline analysis of 10–13 cardiac cycles from 5–10 tissue Doppler sequences was performed following a standardized protocol as described below:

- Aortic valve closure and opening were manually marked on the spectral aortic flow.
- Mitral valve closure (corresponding to the ECG R wave) was manually indicated in the 2D clip (under the color TDI clip) in order to use it for timing events during the cardiac cycle in the absence of real ECG. Gain and velocity lowering were used in order to improve the visualization of mitral valve movement (fig. 1).
- Longitudinal peak systolic strain and strain rate were calculated offline and averaged over 5 consecutive heart cycles by placing a 2 × 3-mm sample area at the basal part of the septum and left and right ventricular free walls on the color TDI clip (fig. 2). Strain length was standardized at the minimum size (2 mm). No angle correction was applied. Caution was taken that the sample area and strain length were within the myocardium in all phases of the cycle by reviewing, and correcting where needed, region placement frame by frame all along the analyzed cardiac cycles. Linear drift compensation was applied to the deformation curves and only cycles with low drift compensation (<20%) were accepted as valid. Peak systolic strain and strain rate measurement were performed and averaged over 5 consecutive homogeneous cycles with low linear drift compensation.
- The time spent in the whole analysis including dummy ECG indication and deformation analysis in three areas (basal left and right free walls and septum) was recorded for each fetus.

2D-Strain

Offline 2D-strain analysis of 10–13 cardiac cycles from 2D grayscale cine loops was performed following a standardized protocol as described below:

- Aortic valve closure and opening were manually marked on the spectral aortic flow.
- Mitral valve closure (corresponding to the ECG R wave) was manually indicated in the 2D cine loop as described above.
- Separately, both the left and right ventricle's endocardial borders were manually traced on one arbitrary frozen frame that provided the best resolution of the endocardial border. The tracing started and ended at the mitral or tricuspid valve plane, respectively, without involvement of papillary muscles. The outer border was adjusted to approximate the epicardial border, and tracing width was kept at the minimum size (6 mm) in all cases. Next, the software automatically detected the motion of the delineated myocardium in the subsequent frames (fig. 3). Visual control of tracking quality was performed and, if required, optimized by adjusting the region of interest or manually correcting the contour to ensure adequate automatic tracking. The software then provided a profile of longitudinal peak strain and strain rate for each segment together with the global deformation (fig. 4). Spatial and temporal smoothing were kept at 0% to visually assess the strain and strain rate curve quality and then fixed at 50% to obtain the peak systolic strain and strain values at the basal left and right septal and free wall segments as well as globally.
- The time spent in the whole analysis including dummy ECG indication and deformation analysis in both ventricles was recorded for each fetus.

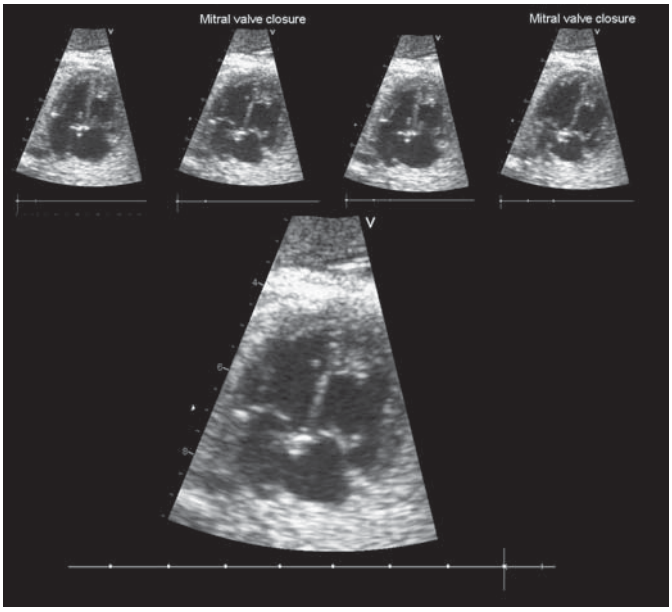

Fig. 1. Manual indication of mitral valve closure corresponding to the ECG R wave in the 2D cine loop.

Statistical Analysis

Data were analyzed with IBM SPSS Statistics version 19 and MedCalc 8.0. Intra- and interobserver reproducibility was analyzed using intraclass correlation and Bland-Altman scatter plots. Correlation between TDI- and 2D-strain-derived parameters was evaluated by linear regression analysis.

Results

Characteristics of the Study Population

The characteristics of the study population are reported in table 1. Most pregnant women were Caucasian and nonsmokers. The mean gestational age at scan time was

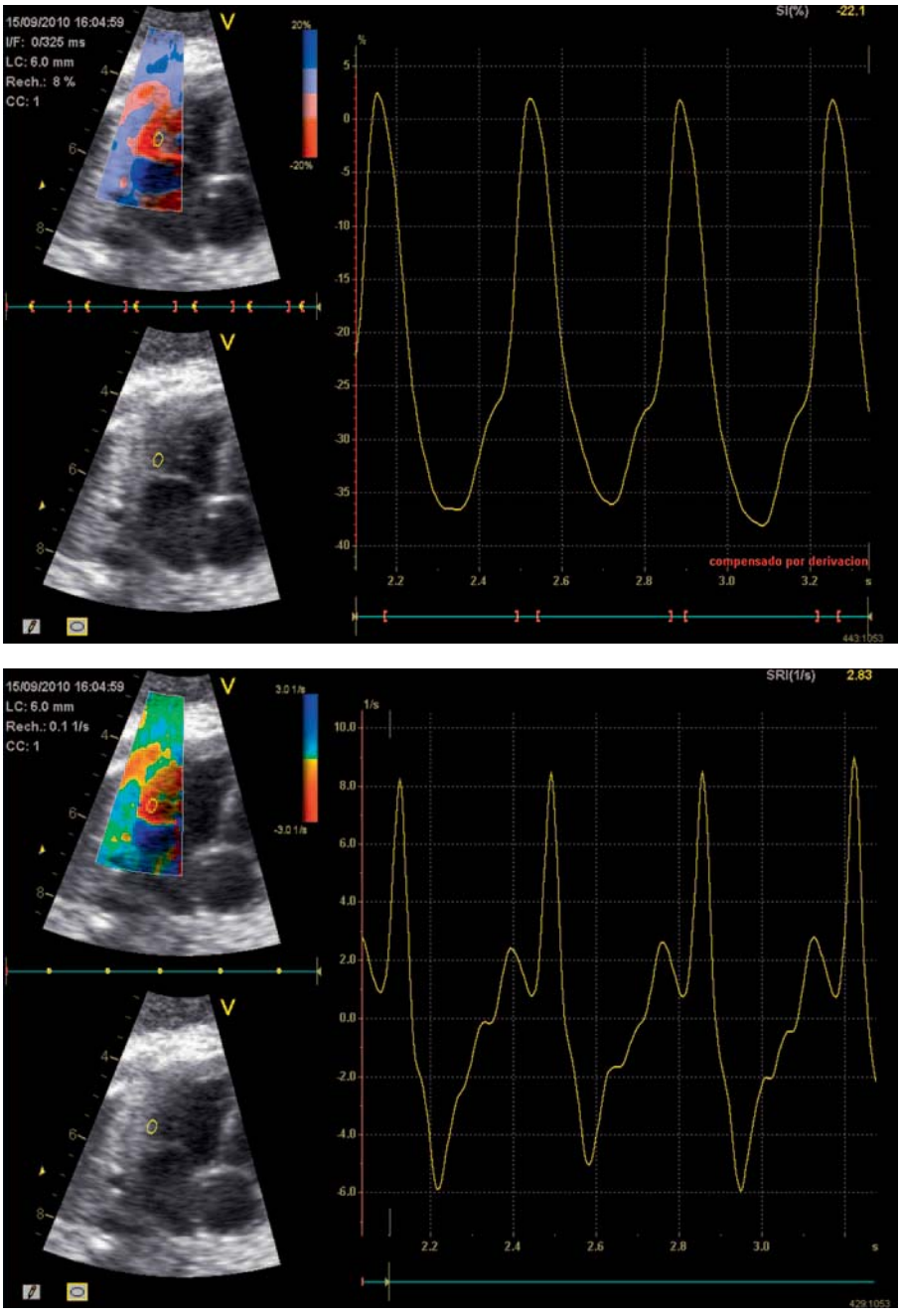

Fig. 2. Tissue Doppler-derived strain (**a**) and strain rate (**b**) waveforms.

30.5 weeks (range 23.6–40.4). The prevalence of preeclampsia was 7% and intrauterine growth restriction was 21%, with a mean gestational age at delivery of 38 weeks.

Tissue Doppler Imaging

Strain and strain rate measurements were feasible from 93% of the acquisitions. A proper acquisition could not be performed in 5 fetuses due to fetal position, oligoamnios, or maternal adiposity. The mean frame rate was 185 fps (range 158–238). The mean frame rate/heart rate ratio was 1.34 (range 1.07–1.75). The mean time spent analyzing TDI images was 18 min (range 14–25) per fetus. Intra- and interobserver agreement coefficients are shown in tables 1 and 2, respectively. A Bland-Altman plot of the difference versus the mean of the paired measurements between observers is presented in figure 5.

Table 1. Characteristics of the study population

Population characteristics	n = 56
Maternal characteristics	
Age, years	35 (22 to 47)
Caucasian	70% (40)
Smoker	2% (1)
Nulliparity	49% (28)
Feto-placental Doppler	
Gestational age at scan, weeks	30.5 (23.6 to 40.4)
Umbilical artery PI	0.42 (–0.89 to 6.19)
Middle cerebral artery PI	–0.42 (–2.89 to 2.13)
Cerebro-placental ratio	–1.04 (–4.45 to 3.28)
Ductus venosus PI	–0.02 (–2.69 to 4.63)
Left myocardial performance index	0.42 (–0.69 to 4.06)
Delivery data	
Gestational age at delivery, weeks	38.3 (25.1 to 41.6)
Birth weight, g	2,550 (400 to 3,950)
Birth weight percentile	15 (1 to 85)
5-min Apgar score <7	9% (5)
Preeclampsia[a]	7% (4)
Intrauterine growth restriction[b]	21% (12)

Data are medians (range) or proportions (%, n). Doppler parameters are expressed in Z-scores. PI = Pulsatility index.

[a] Defined as high blood pressure (two separate readings taken at least 6 h apart of 140/90 or more) and 300 mg of protein in a 24-hour urine sample developed after 20 weeks of pregnancy.

[b] Defined as birth weight <10th percentile together with umbilical artery Doppler PI above 2 SD.

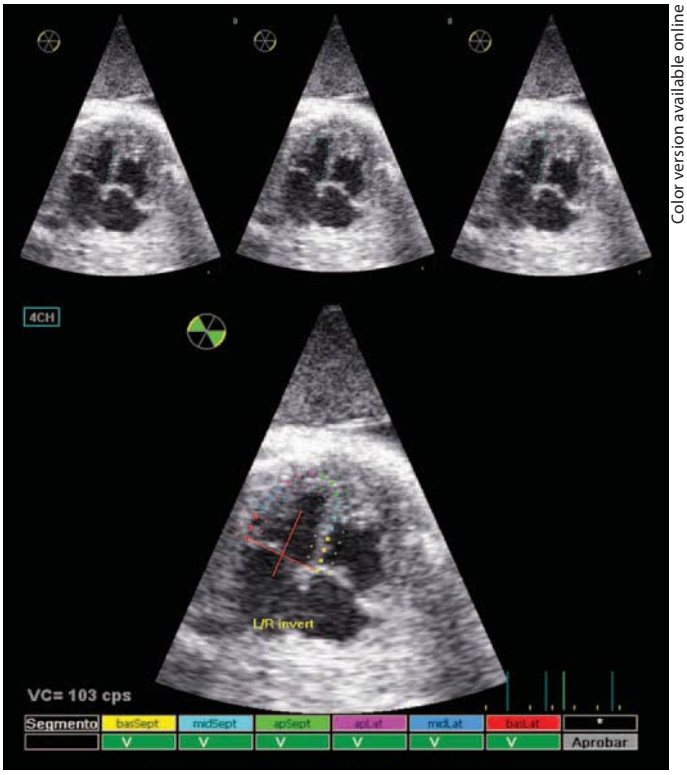

Color version available online

Fig. 3. Left ventricle's endocardial border. Manual delineation in the 2D cine loop.

Table 2. Intraobserver reliability of longitudinal peak systolic strain and strain rate by TDI and 2D-strain

	Strain	Strain rate
TDI		
Basal left free wall	0.86 (0.77–0.92)	0.83 (0.72–0.90)
Basal right free wall	0.96 (0.93–0.98)	0.86 (0.76–0.92)
Basal septum	0.96 (0.93–0.98)	0.94 (0.89–0.96)
2D-strain		
Global left ventricle	0.93 (0.88–0.96)	0.82 (0.70–0.89)
Basal left free wall	0.97 (0.95–0.98)	0.94 (0.89–0.96)
Basal left septal wall	0.93 (0.88–0.96)	0.89 (0.82–0.94)
Global right ventricle	0.89 (0.82–0.93)	0.84 (0.73–0.90)
Basal right free wall	0.96 (0.93–0.98)	0.84 (0.73–0.90)
Basal right septal wall	0.95 (0.91–0.97)	0.91 (0.84–0.94)

Data are intraclass coefficients (95% CI).

Table 3. Interobserver reliability of longitudinal peak systolic strain and strain rate by TDI and 2D-strain

	Strain	Strain rate
TDI		
Basal left free wall	0.85 (0.68–0.92)	0.83 (0.67–0.92)
Basal right free wall	0.91 (0.84–0.95)	0.86 (0.71–0.93)
Basal septum	0.88 (0.79–0.93)	0.80 (0.65–0.89)
2D-strain		
Global left ventricle	0.89 (0.81–0.93)	0.80 (0.67–0.88)
Basal left free wall	0.75 (0.60–0.85)	0.94 (0.90–0.97)
Basal left septal wall	0.82 (0.69–0.89)	0.86 (0.77–0.92)
Global right ventricle	0.87 (0.79–0.93)	0.87 (0.78–0.92)
Basal right free wall	0.90 (0.84–0.94)	0.94 (0.88–0.97)
Basal right septal wall	0.84 (0.74–0.91)	0.92 (0.84–0.95)

Data are intraclass coefficients (95% CI).

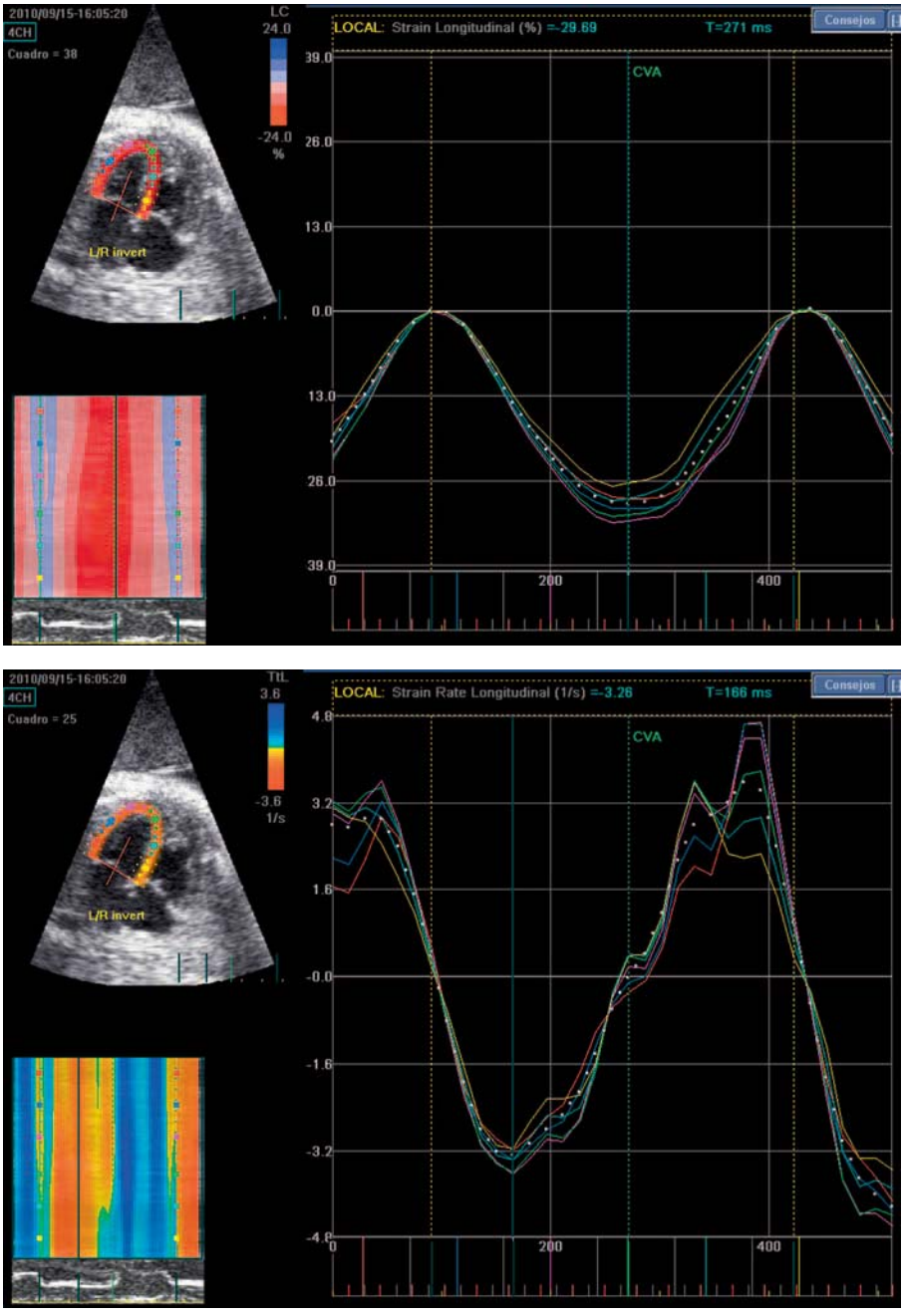

Fig. 4. Two-dimensional speckle tracking-derived strain (**a**) and strain rate (**b**) waveforms.

2D-Strain

Strain and strain rate measurements were feasible from 93% of the acquisitions. A proper acquisition could not be performed in 5 fetuses due to fetal position or maternal adiposity. The mean frame rate was 109 fps (range 72–158). The mean frame rate/heart rate ratio was 0.79 (range 0.48–1.22). The mean time spent on 2D-strain analysis was 15 min (range 12–22) per fetus. Intra- and interobserver agreement coefficients are shown in tables 1 and 2, respectively. A Bland-Altman plot of the difference versus the mean of the paired measurements between observers is presented in figure 6.

Correlation between TDI and 2D-Strain

There was a nonsignificant correlation between TDI- and 2D-strain-derived parameters (fig. 7), with R^2 values ranging from 0.002 to 0.079.

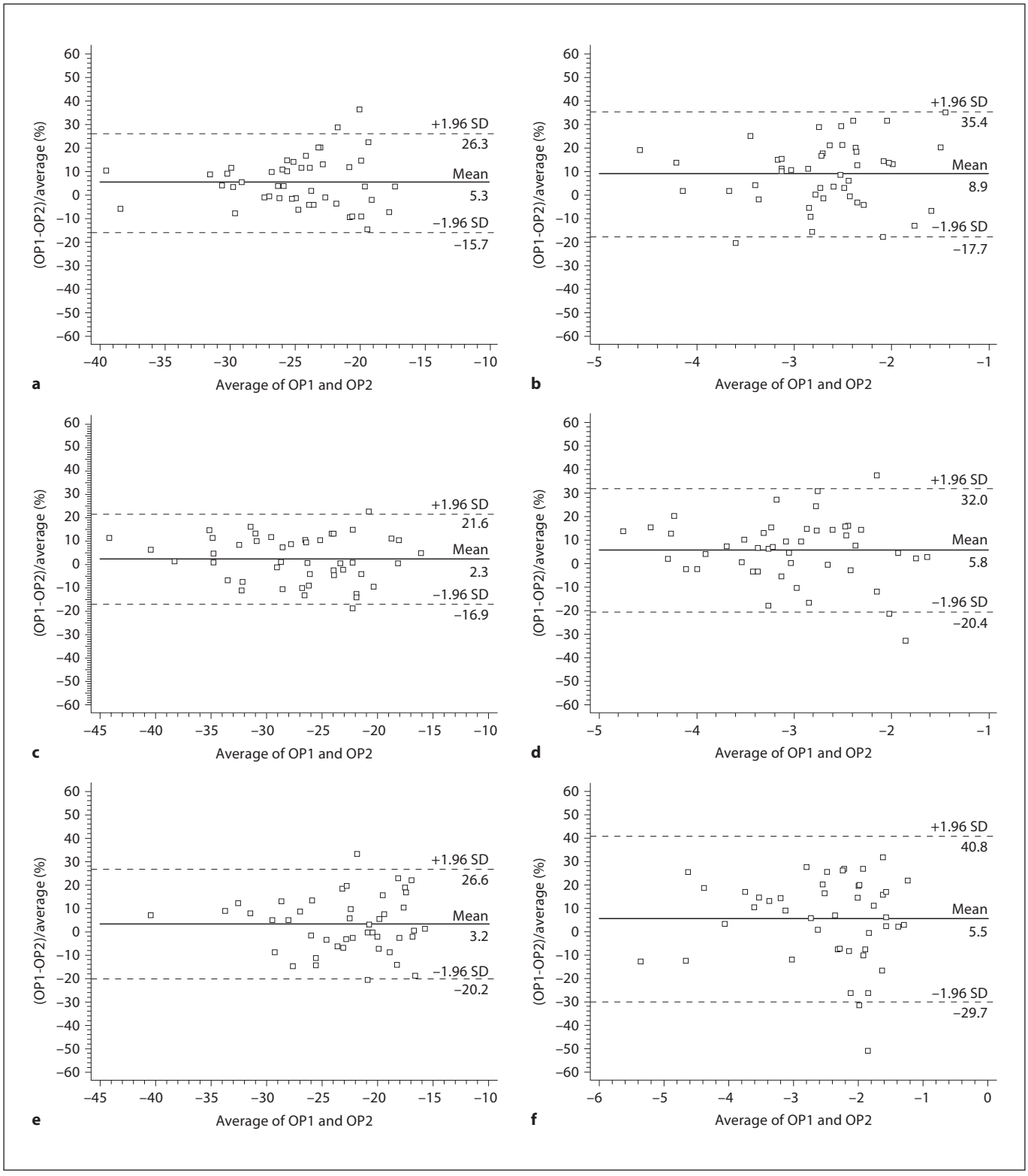

Fig. 5. Bland-Altman plot of the difference versus the mean of the paired measurements between observers of the tissue Doppler-derived parameters: peak systolic strain in the basal left free wall (**a**), peak systolic strain rate in the basal left free wall (**b**), peak systolic strain in the basal right free wall (**c**), peak systolic strain rate in the basal right free wall (**d**), peak systolic strain in the basal septum (**e**), and peak systolic strain rate in the basal septum (**f**).

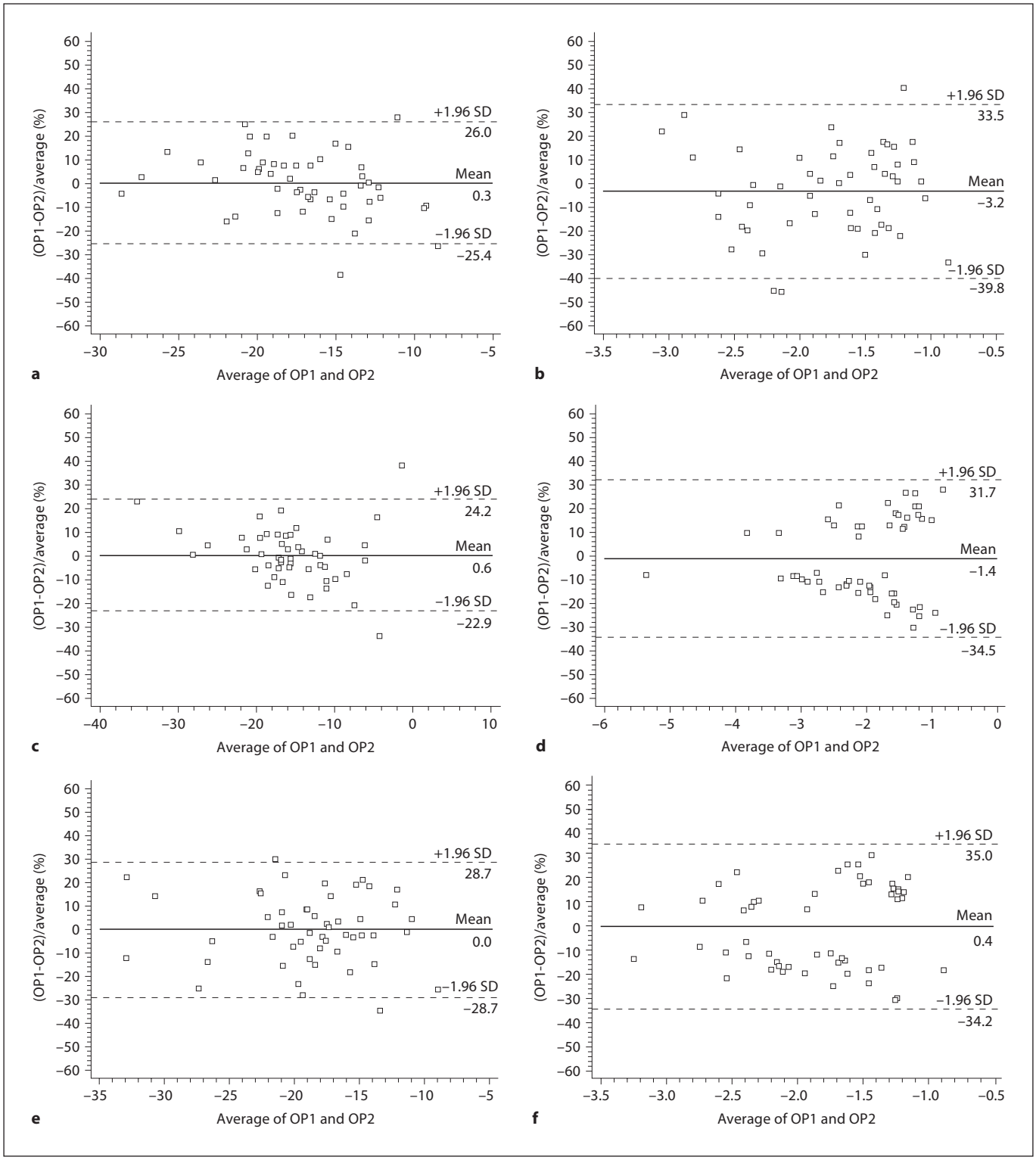

Fig. 6. Bland-Altman plot of the difference versus the mean of the paired measurements between observers of the 2D speckle tracking-derived parameters: global left ventricle peak systolic strain (**a**), global left ventricle peak systolic strain rate (**b**), peak systolic strain in the basal left free wall (**c**), peak systolic strain rate in the basal left free wall (**d**), peak systolic strain in the basal left septal wall (**e**), peak systolic strain rate in the basal left septal wall (**f**).

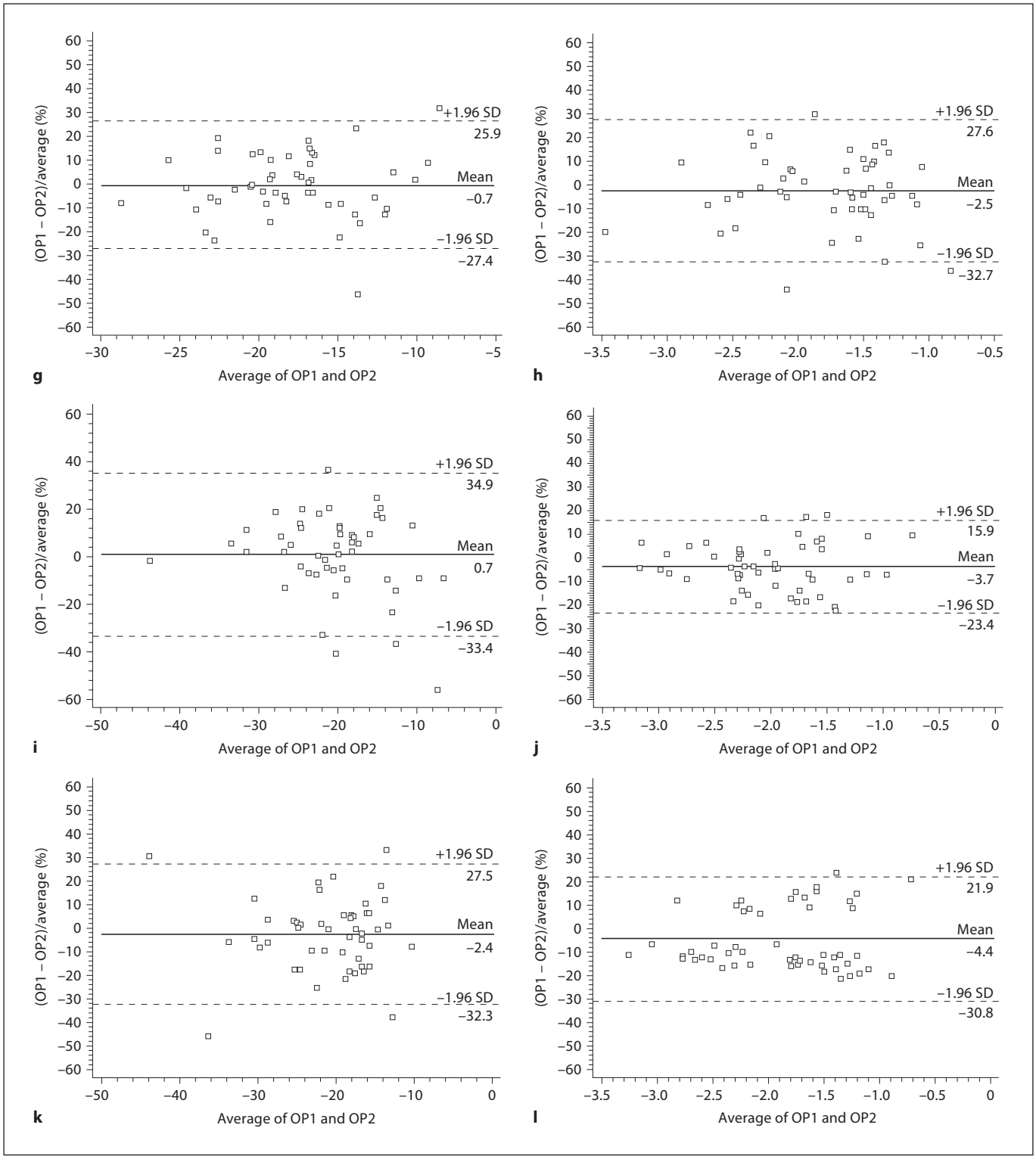

Fig. 6. Bland-Altman plot of the difference versus the mean of the paired measurements between observers of the 2D speckle tracking-derived parameters: global right ventricle peak systolic strain (**g**), global right ventricle peak systolic strain rate (**h**), peak systolic strain in the basal right free wall (**i**), peak systolic strain rate in the basal right free wall (**j**), peak systolic strain in the basal right septal wall (**k**), peak systolic strain rate in the basal right septal wall (**l**).

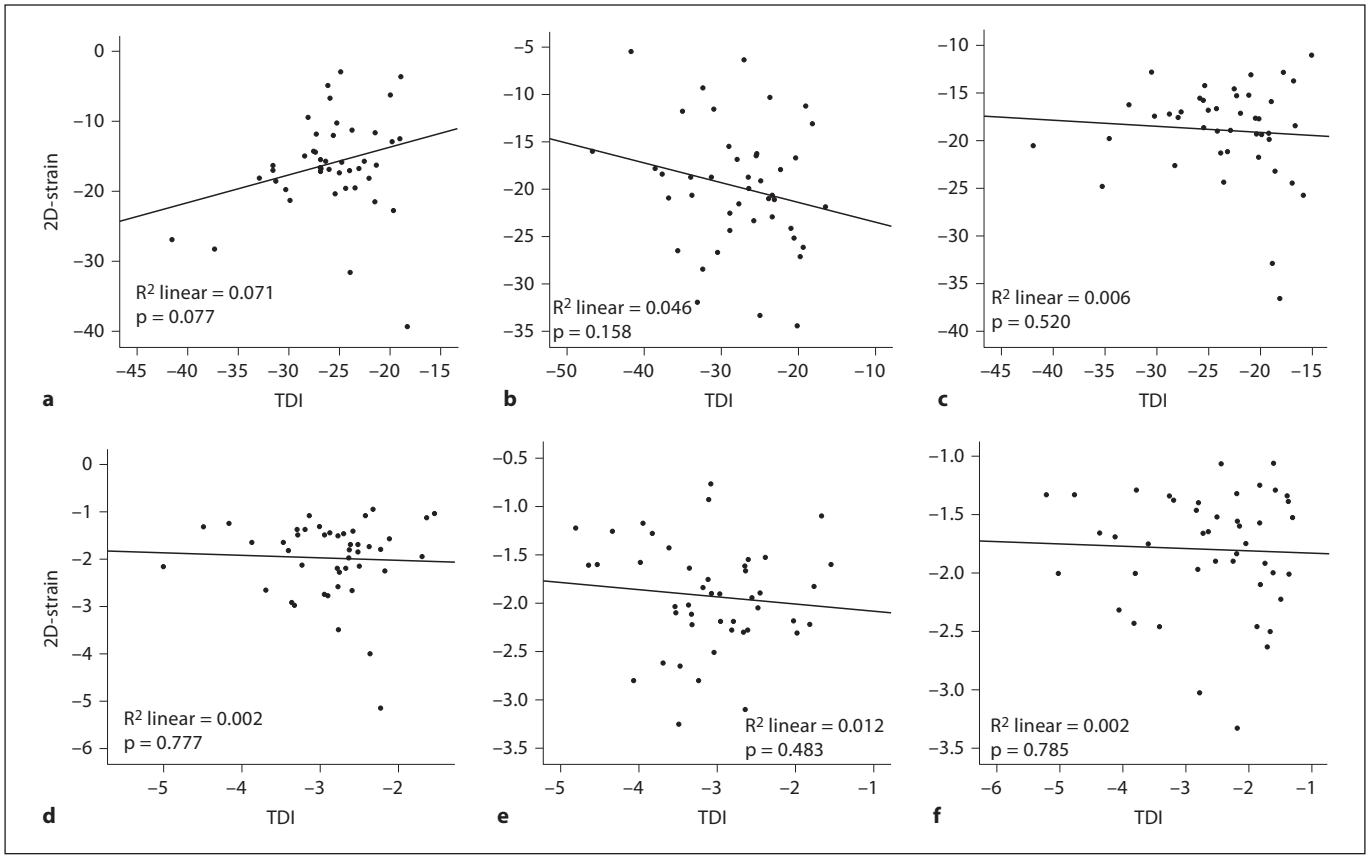

Fig. 7. Correlations comparing tissue Doppler- and 2D speckle tracking-derived parameters: peak systolic strain in the basal left free wall (**a**), peak systolic strain in the basal right free wall (**b**), peak systolic strain in the basal septum (**c**), peak systolic strain rate in the basal left free wall (**d**), peak systolic strain rate in the basal right free wall (**e**), and peak systolic strain rate in the basal septum (**f**).

Discussion

In this study, both TDI and 2D-strain were demonstrated to be feasible and reproducible to evaluate deformation parameters in the fetal heart. The study standardized a protocol of acquisition and offline analysis for TDI and 2D-strain using a dummy ECG by manually indicating the onset of each cardiac cycle based on mitral valve motion. It also demonstrates that these techniques cannot be interchanged as their correlation is relatively poor.

Evaluation of the ventricular longitudinal strain and strain rate of the fetal heart using TDI was feasible in most cases with a high intra- and interobserver reproducibility, which is concordant with studies in adults [37] and children [38] and the latest reports of TDI in fetal life [35, 39, 40]. Despite its extensive validation in the adult heart [37], the first studies on TDI [21–23, 41] in the fetus showed variable results on feasibility and reproducibility. However, these studies were based on acquisitions with very low temporal resolution (10–60 fps) which strongly limits the validity of their findings. Later on, studies using high frame rate acquisitions [35, 39, 40] showed good feasibility ranging from 93 to 99% and high agreement for TDI-derived velocities and time intervals. Recently, Perles et al. [39] reported a good repeatability for deformation TDI-derived parameters in the fetal heart. The present study showed a high repeatability with a tendency toward better agreement for strain as compared to strain rate, which is consistent with previous data [37, 38]. Additionally, there was a tendency towards better results in the right as compared to the left free wall, which is concordant with previous data in annular peak velocities [5] and may be explained by the easier insonation and dominance of the right ventricle during fetal life. Finally, the most innovative contribution of the present study is the introduction of a dummy ECG based on manual indication of the car-

diac cycle onset based on valve motion. This enables provision of a proper and physiological onset for the calculation of strain and thus results in a better definition and standardization of the maximal value and additionally offers a natural to average the traces from several heart beats. In our experience, this approach highly improves the performance and reduces the need for drift compensation (data not shown), a sign of better and more reliable strain (rate) traces. Despite that, it may account for an increase in the time required for the analysis since it is necessary to carefully review all cardiac cycles frame by frame; it results in much better estimates of deformation and therefore improves its performance and reliability.

Speckle tracking-based 2D-strain analysis also showed good feasibility and reproducibility, which was similar to TDI, in this study. Similar to TDI studies, the first reports on 2D-strain were based on low frame rate acquisitions (<50 fps) [25, 27–30] which strongly limits its validity and reproducibility as demonstrated by Matsui et al. [33]. However, results from the present study using a dummy ECG based on mitral valve motion led to a high reproducibility, similar to the more recent published data in fetuses using a high frame rate and dummy ECG by M-mode [31–34]. These results are also consistent with data in adults and children [19, 20]. Similarly to TDI, 2D-strain results also showed a higher reliability for strain as compared to strain rate analysis. In spite of the high reliability of both techniques per se, we have shown a relatively poor correlation between them. This result is consistent with recent reports in adulthood [42, 43] demonstrating a low correlation among deformation measurements which supports the notion that TDI and 2D-strain cannot be interchanged. Similarly, strain and strain rate values obtained from different ultrasound equipments or software may yield variable results which cannot be directly compared [43]. Several technical factors may account for this poor correlation. Firstly, the required frame rate is significantly different for both techniques and this may lead to the loss of fast changes in motion within the cardiac cycle and different estimates of myocardial deformation for 2D-strain. As a consequence of this lower frame rate, smoothing is larger for 2D-strain and this may result in narrower ranges of myocardial deformation values by 2D-strain as compared to those derived from TDI, which show wider ranges (fig. 7); this negatively impacts correlation. Additionally, the size of the scanned segment is larger for 2D-strain as the software averages strain within a given segment (following a 16-segment model) while TDI uses data acquired from a smaller region of interest. Despite these facts, both techniques might be useful in clinical terms. 2D-strain results in a more feasible and widely applicable method to quantify deformation, despite being less sensitive and coarser. On the other hand, TDI is a more sophisticated technique that is relatively difficult to perform and interpret but which allows more accurate and sensitive measurement of deformation in experienced hands.

Despite its high reproducibility in utero, we acknowledge that TDI and 2D-strain techniques still have several limitations when assessing the fetal heart. Firstly, the relatively small size of the fetal heart compared to the spatial resolution of the system may limit the tracking of both velocities (TDI) and grey scale speckles (2D-strain) and thus decrease accuracy. For example, when delineating the fetal heart for 2D-strain analysis, even the smallest segment width available is usually thicker than the myocardium wall. Secondly, while the required frame rate is reasonably well-defined in the adult heart, we can only assume that a higher frame rate would be necessary for the fetal heart but the optimal values have still to be defined. Thirdly, the variable fetal position makes optimal acquisition difficult, as it is not always possible to obtain an apical view. However, this study demonstrates that their feasibility is relatively high even in a high-risk population including a high proportion of intrauterine growth-restricted fetuses. Finally, no validation studies using invasive procedures can be performed to ascertain the real strain and strain rate values in the fetal heart during the maturation process.

In conclusion, evaluation of longitudinal ventricular strain and strain rate of the fetal heart is feasible by both TDI and speckle tracking-based 2D-strain echocardiography. The strength of this study is the proposal of well-defined criteria for acquisition and postprocessing, including high frame rate acquisitions, dummy ECG demarcation, and criteria for assessing the quality of the traces. We demonstrate that, despite its limitations in the fetal heart, deformation can be assessed in a reproducible manner when using the appropriate methodology.

Acknowledgements

This study was supported by grants from Instituto de Salud Carlos III (PI11/00051 and PI11/01709) cofinanciado por el Fondo Europeo de Desarrollo Regional de la Unión Europea "Una manera de hacer Europa", Spain; Centro para el Desarrollo Técnico Industrial (cvREMOD 2009-2012) apoyado por el Ministerio de Economia y Competitividad y Fondo de inversión local para el empleo, Spain; Ministerio de Economia y Competitividad PN de I+D+I 2008-2011 (SAF2009-08815), Spain; Cerebra Foundation for the Brain Injured Child (Carmarthen, Wales, UK) and Thrasher Research Fund (Salt Lake City, Utah, USA).

References

1 Tutschek B, Zimmermann T, Buck T, Bender HG: Fetal tissue Doppler echocardiography: detection rates of cardiac structures and quantitative assessment of the fetal heart. Ultrasound Obstet Gynecol 2003;21:26–32.
2 Mäkikallio K, McElhinney DB, Levine JC, et al: Fetal aortic valve stenosis and the evolution of hypoplastic left heart syndrome: patient selection for fetal intervention. Circulation 2006;113:1401–1405.
3 Clur SA, van der Wal AC, Ottenkamp J, Bilardo CM: Echocardiographic evaluation of fetal cardiac function: clinical and anatomical correlations in two cases of endocardial fibroelastosis. Fetal Diagn Ther 2010;28:51–57.
4 Crispi F, Hernandez-Andrade E, Pelsers MM, et al: Cardiac dysfunction and cell damage across clinical stages of severity in growth-restricted fetuses. Am J Obstet Gynecol 2008;199:254.e1–254.e8.
5 Comas M, Crispi F, Cruz-Martinez R, Martinez JM, Figueras F, Gratacós E: Usefulness of myocardial tissue Doppler vs conventional echocardiography in the evaluation of cardiac dysfunction in early-onset intrauterine growth restriction. Am J Obstet Gynecol 2010;203:45.e1–45.e7.
6 Makikallio K, Rasanen J, Makikallio T, Vuolteenaho O, Huhta JC: Human fetal cardiovascular profile score and neonatal outcome in intrauterine growth restriction. Ultrasound Obstet Gynecol 2008;31:48–54.
7 Gardiner HM, Pasquini L, Wolfenden J, Kulinskaya E, Li W, Henein M: Increased periconceptual maternal glycated haemoglobin in diabetic mothers reduces fetal long axis cardiac function. Heart 2006;92:1125–1130.
8 Corrigan N, Brazil DP, McAuliffe F: Fetal cardiac effects of maternal hyperglycemia during pregnancy. Birth Defects Res A Clin Molec Teratol 2009;85:523–530.
9 Van Mieghem T, Klaritsch P, Done E, et al: Assessment of fetal cardiac function before and after therapy for twin-to-twin transfusion syndrome. Am J Obstet Gynecol 2009; 200:400.e1–400.e7.
10 Byrne FA, Lee H, Kipps AK, Brook MM, Moon-Grady AJ: Echocardiographic risk stratification of fetuses with sacrococcygeal teratoma and twin-reversed arterial perfusion. Fetal Diagn Ther 2011;30:280–288.
11 Van Mieghem T, Gucciardo L, Done E, et al: Left ventricular cardiac function in fetuses with congenital diaphragmatic hernia and the effect of fetal endoscopic tracheal occlusion. Ultrasound Obstet Gynecol 2009;34: 424–429.
12 Gardiner HM, Pasquini L, Wolfenden J, Barlow A, Li W, Kulinskaya E, Henein M: Myocardial tissue Doppler and long axis function in the fetal heart. Int J Cardiol 2006;113:39–47.
13 Bijnens BH, Cikes M, Claus P, Sutherland GR: Velocity and deformation imaging for the assessment of myocardial dysfunction. Eur J Echocardiogr 2009;10:216–226.
14 Marciniak A, Claus P, Sutherland GR, Marciniak M, Karu T, Baltabaeva A, Merli E, Bijnens B, Jahangiri M: Changes in systolic left ventricular function in isolated mitral regurgitation: a strain rate imaging study. Eur Heart J 2007;28:2627–2636.
15 Cikes M, Sutherland GR, Anderson LJ, Bijnens BH: The role of echocardiographic deformation imaging in hypertrophic myopathies. Nat Rev Cardiol 2010;7:384–396.
16 Mertens L, Ganame J, Claus P, Goemans N, Thijs D, Eyskens B, et al: Early regional myocardial dysfunction in young patients with Duchenne muscular dystrophy. J Am Soc Echocardiogr 2008;21:1049–1054.
17 Sanderson JE, Wang M, Yu CM: Tissue Doppler imaging for predicting outcome in patients with cardiovascular disease. Curr Opin Cardiol 2004;19:458–463.
18 Urheim S, Edvardsen T, Torp H, Angelsen B, Smiseth OA: Myocardial strain by Doppler echocardiography: validation of a new method to quantify regional myocardial function. Circulation 2000;102:1158–1164.
19 Amundsen BH, Helle-Valle T, Edvardsen T, Torp H, Crosby J, Lyseggen E, Stoylen A, Ihlen H, Lima JA, Smiseth OA, Slordahl SA: Noninvasive myocardial strain measurement by speckle tracking echocardiography: validation against sonomicrometry and tagged magnetic resonance imaging. J Am Coll Cardiol 2006;47:789–793.
20 D'Hooge J, Heimdal A, Jamal F, Kukulski T, Bijnens B, Rademakers F, Hatle L, Suetens P, Sutherland GR: Regional strain and strain rate measurements by cardiac ultrasound: principles, implementation and limitations. Eur J Echocardiogr 2000;1:154–170
21 Paladini D, Lamberti A, Teodoro A, Arienzo M, Tartaglione A, Martinelli P: Tissue Doppler imaging of the fetal heart. Ultrasound Obstet Gynecol 2000;16:530–535.
22 Tutschek B, Zimmermann T, Buck T, Bender HG: Fetal tissue Doppler echocardiography: detection rates of cardiac structures and quantitative assessment of the fetal heart. Ultrasound Obstet Gynecol 2003;21:26–32.
23 Di Salvo G, Russo MG, Paladini D, Pacileo G, Felicetti M, Ricci C, Cardaropoli D, Palma M, Caso P, Calabro R: Quantification of regional left and right ventricular longitudinal function in 75 normal fetuses using ultrasound-based strain rate and strain imaging. Ultrasound Med Biol 2005;31:1159–1162.
24 Larsen LU, Petersen OB, Norrild K, Sorensen K, Uldbjerg N, Sloth E: Strain rate derived from color Doppler myocardial imaging for assessment of fetal cardiac function. Ultrasound Obstet Gynecol 2006;27:210–213.
25 Di Salvo G, Russo MG, Paladini D, Felicetti M, Castaldi B, Tartaglione A, di Pietto L, Ricci C, Morelli C, Pacileo G, Calabro R: Two-dimensional strain to assess regional left and right ventricular longitudinal function in 100 normal foetuses. Eur J Echocardiogr 2008;9:754–756.
26 Ta-Shma A, Perles Z, Gavri S, Golender J, Tarshansky S, Shlichter C, Bar Tov H, Rein AJ: Analysis of segmental and global function of the fetal heart using novel automatic functional imaging. J Am Soc Echocardiogr 2008;21:146–150.
27 Younoszai AK, Saudek DE, Emery SP, Thomas JD: Evaluation of myocardial mechanics in the fetus by velocity vector imaging. J Am Soc Echocardiogr 2008;21:470–474.
28 Barker PC, Houle H, Li JS, Miller S, Herlong JR, Camitta MG: Global longitudinal cardiac strain and strain rate for assessment of fetal cardiac function: novel experience with velocity vector imaging. Echocardiography 2009;26:28–36.
29 Peng QH, Zhou QC, Zeng S, Tian LQ, Zhang M, Tan Y, Pu DR: Evaluation of regional left ventricular longitudinal function in 151 normal fetuses using velocity vector imaging. Prenat Diagn 2009;29:1149–1155.
30 Pu DR, Zhou QC, Zhang M, Peng QH, Zeng S, Xu GQ: Assessment of regional right ventricular longitudinal functions in fetus using velocity vector imaging technology. Prenat Diagn 2010;30:1057–1063.
31 Van Mieghem T, Giusca S, DeKoninck P, Gucciardo L, Done E, Hindryckx A, D'Hooge J, Deprest J: Prospective assessment of fetal cardiac function with speckle tracking in healthy fetuses and recipient fetuses of twin-to-twin transfusion syndrome. J Am Soc Echocardiogr 2010;23:301–308.
32 Di Naro E, Cromi A, Ghezzi F, Giocolano A, Caringella A, Loverro G: Myocardial dysfunction in fetuses exposed to intraamniotic infection: new insights from tissue Doppler and strain imaging. Am J Obstet Gynecol 2010;203:459.e1–459.e7
33 Matsui H, Germanakis I, Kulinskaya E, Gardiner HM: Temporal and spatial performance of vector velocity imaging in the human fetal heart. Ultrasound Obstet Gynecol 2011;37:150–157.
34 Willruth AM, Geipel AK, Fimmers R, Gembruch UG: Assessment of right ventricular global and regional longitudinal peak systolic strain, strain rate and velocity in healthy fetuses and impact of gestational age using a novel speckle/feature-tracking based algorithm. Ultrasound Obstet Gynecol 2011;37: 143–149.
35 Larsen LU, Petersen OB, Sloth E, Uldbjerg N: Color Doppler myocardial imaging demonstrates reduced diastolic tissue velocity in growth retarded fetuses with flow redistribution. Eur J Obstet Gynecol Reprod Biol 2011;155:140–145.

36 Hernandez-Andrade E, López-Tenorio J, Figueroa-Diesel H, Sanin-Blair J, Carreras E, Cabero L, Gratacos E: A modified myocardial performance (Tei) index based on the use of valve clicks improves reproducibility of fetal left cardiac function assessment. Ultrasound Obstet Gynecol 2005;26:227–232.
37 Kowalski M, Kukulski T, Jamal F, D'hooge J, Weidemann F, Rademakers F, Bijnens B, Hatle L, Sutherland GR: Can natural strain and strain rate quantify regional myocardial deformation? A study in healthy subjects. Ultrasound Med Biol 2001;27:1087–1097.
38 Weidemann F, Eyskens B, Jamal F, Mertens L, Kowalski M, D'Hooge J, Bijnens B, Gewillig M, Rademakers F, Hatle L, Sutherland GR: Quantification of regional left and right ventricular radial and longitudinal function in healthy children using ultrasound-based strain rate and strain imaging. J Am Soc Echocardiogr 2002;15:20–28.
39 Perles Z, Nir A, Gavri S, Rein AJ: Assessment of fetal myocardial performance using myocardial deformation analysis. Am J Cardiol 2007;99:993–996.
40 Nii M, Hamilton RM, Fenwick L, Kingdom JC, Roman KS, Jaeggi ET: Assessment of fetal atrioventricular time intervals by tissue Doppler and pulse Doppler echocardiography: normal values and correlation with fetal electrocardiography. Heart 2006;92:1831–1837.
41 Rein AJ, O'Donnell C, Geva T, Nir A, Perles Z, Hashimoto I, Li XK, Sahn DJ: Use of tissue velocity imaging in the diagnosis of fetal cardiac arrhythmias. Circulation 2002;106:1827–1833.
42 Thorstensen A, Dalen H, Amundsen BH, Aase SA, Stoylen A: Reproducibility in echocardiographic assessment of the left ventricular global and regional function, the HUNT study. Eur J Echocardiogr 2010;11:149–156.
43 Mor-Avi V, Lang RM, Badano LP, Belohlavek M, Cardim NM, Derumeaux G, Galderisi M, Marwick T, Nagueh SF, Sengupta PP, Sicari R, Smiseth OA, Smulevitz B, Takeuchi M, Thomas JD, Vannan M, Voigt JU, Zamorano JL: Techniques for the quantitative evaluation of cardiac mechanics: ASE/EAE consensus statement on methodology and indications endorsed by the Japanese Society of Echocardiography. Eur J Echocardiogr 2011;12:167–205.

STUDY 3

Risk of perinatal death in early-onset intrauterine growth restriction according to gestational age and cardiovascular Doppler indices: a multicenter study.

Cruz-Lemini M, Crispi F, Van Mieghem T, Pedraza D, Cruz-Martínez R, Acosta-Rojas R, Figueras F, Parra-Cordero M, Deprest J, Gratacós E.
Fetal Diagn Ther. 2012;32(1-2):116-22.
doi: 10.1159/000333001.

Status: Published
Impact factor: 1.902
Quartile: 3rd.

Original Paper: Clinical Applications

Fetal Diagnosis and Therapy

Fetal Diagn Ther
DOI: 10.1159/000333001

Received: August 8, 2011
Accepted after revison: September 12, 2011
Published online: July 6, 2012

Risk of Perinatal Death in Early-Onset Intrauterine Growth Restriction according to Gestational Age and Cardiovascular Doppler Indices: A Multicenter Study

Mónica Cruz-Lemini[a] Fàtima Crispi[a] Tim Van Mieghem[b] Daniel Pedraza[c] Rogelio Cruz-Martínez[a] Ruthy Acosta-Rojas[a] Francesc Figueras[a] Mauro Parra-Cordero[c] Jan Deprest[b] Eduard Gratacós[a]

[a]Department of Maternal-Fetal Medicine (Institut Clínic de Ginecologia, Obstetrícia i Neonatologia), Hospital Clínic – Institut d'Investigacions Biomèdiques August Pi i Sunyer, University of Barcelona, and Centro de Investigación Biomédica en Red de Enfermedades Raras, Barcelona, Spain; [b]Department of Obstetrics and Gynecology, University Hospital Gasthuisberg, Leuven, Belgium; [c]Fetal Medicine Unit, Hospital Clínico Universidad de Chile, Santiago, Chile

Key Words
Intrauterine growth restriction · Perinatal mortality · Doppler · Ductus venosus · Myocardial performance index · Aortic isthmus

Abstract
Objective: To assess the value of gestational age and cardiovascular Doppler indices in predicting perinatal mortality in a multicenter cohort of early-onset intrauterine growth-restricted (IUGR) fetuses. ***Methods:*** A multicenter prospective cohort study including 157 early-onset (<34 weeks) IUGR cases with abnormal umbilical artery (UA) Doppler was conducted. Cardiovascular assessment included the ductus venosus (DV), the aortic isthmus flow index (IFI), and the myocardial performance index (MPI). Isolated and combined values to predict the risk of perinatal death were evaluated by logistic regression and by decision tree analysis, where the gestational age at delivery, UA, and middle cerebral artery (MCA) were also included as covariates. ***Results:*** Perinatal mortality was 17% (27/157). All parameters were significantly associated with perinatal death, with individual odds ratios (OR) of 25.2 for gestational age below 28 weeks, 12.1 for absent/reversed DV atrial flow, 5.3 for MCA pulsatility index <5th centile, 4.6 for UA absent/reversed diastolic end-flow, 1.8 for IFI <5th centile, and 1.6 for MPI >95th centile. Decision tree analysis identified gestational age at birth as the best predictor of death (<26 weeks, 93% mortality; 26–28 weeks, 29% mortality, and >28 weeks, 3% mortality). Between 26 and 28 weeks, DV atrial flow allowed further stratification between high (60%) and low risk (18%) of mortality. ***Conclusions:*** Gestational age largely determines the risk of perinatal mortality in early-onset IUGR before 26 weeks and later than 28 weeks of gestation. The DV may improve clinical management by stratifying the probability of death between 26 and 28 weeks of gestation.

Introduction

Intrauterine growth restriction (IUGR) due to placental insufficiency [1, 2] is a leading cause for perinatal death and long-term cardiovascular [3] and neurodevel-

KARGER

Fax +41 61 306 12 34
E-Mail karger@karger.ch
www.karger.com

1015–3837/12/0000–0000$38.00/0

Accessible online at:
www.karger.com/fdt

Eduard Gratacós
Department of Maternal-Fetal Medicine
Hospital Clinic, University of Barcelona
Sabino de Arana 1, ES–08028 Barcelona (Spain)
Tel. +34 93 227 5600, E-Mail gratacos@clinic.ub.es

opmental adverse outcomes [4]. Early-onset IUGR (<34 weeks of gestation) is associated with perinatal mortality rates as high as 46%, which warrant strict in utero monitoring to tailor planned delivery [5]. Gestational age has proven to be the strongest predictor of the probability of perinatal death in early-onset IUGR [5–7]. Therefore, the timing of delivery for early-onset IUGR fetuses is critically conditioned by the short-term risk of intrauterine or early postnatal death.

Several monitoring methods to improve the identification of severe fetal deterioration in early-onset IUGR have been suggested [8, 9]. Cardiovascular Doppler indices have long been demonstrated to have an association with the risk of perinatal death [6, 8, 9]. Among these, the ductus venosus (DV) has demonstrated the strongest short-term correlation with perinatal death, as suggested by diverse studies [2, 6, 8–11] and endorsed by a recent systematic review [7]. In addition, the DV was the best predictor of intact survival in a large cohort of IUGR fetuses delivered beyond 29 weeks of gestation [5]. However, the performance of the DV is still limited by a relatively high false-positive rate and sensitivities for perinatal mortality ranging from 30 to 70%. This has prompted research into other cardiovascular Doppler indices that might aid in refining clinical information [5, 6, 11]. Recent studies have investigated whether the aortic isthmus (AoI) and the myocardial performance index (MPI) could contribute to the prediction of mortality [12–14]. An abnormal AoI Doppler was first proposed as a potential predictor of neurological outcomes [15], but some studies also suggested a correlation with perinatal mortality [12–14]. The MPI has been shown to correlate with the progressive deterioration of heart function in early-onset IUGR fetuses [16]. In a recent study conducted on a cohort of 97 fetuses with early-onset IUGR, we evaluated the potential contribution of AoI and MPI when combined with commonly used Doppler indices in the prediction of perinatal mortality. The results suggested that AoI was of no benefit when used in combination with DV. However, MPI allowed a better stratification of the estimated probability of death in early-onset IUGR [6].

The objective of this study was to validate previous results on the prediction of perinatal mortality in early-onset IUGR in a multicenter setting in order to better estimate the differential impact of gestational age in combination with Doppler cardiovascular parameters such as DV, AoI, and MPI. To this end, we conducted a prospective multicenter study in a cohort of early-onset IUGR fetuses delivered at various institutions and followed up longitudinally until delivery.

Methods

Study Population

A multicenter prospective study was conducted in three institutions, i.e. Hospital Clínic de Barcelona (Spain), University Hospital Gasthuisberg Leuven (Belgium), and Hospital Clínico de Santiago (Chile), during a 2-year period. The study protocol was approved by the Ethics Committee at each participating center and all patients provided written informed consent. Gestational age was corrected by first-trimester ultrasound. IUGR was defined as an estimated fetal weight below the 10th centile according to local reference curves [17], together with UA-PI above the 95th centile [18, 19]. Early-onset cases were defined as cases that died or were delivered before 34 weeks of gestation. Exclusion criteria were twin pregnancies, birth weight >10th centile, and presence of fetal infection and structural or chromosomal abnormalities.

Doppler Assessment

Ultrasound assessment was performed using a Siemens Sonoline Antares (Siemens Medical Systems, Erlangen, Germany) or a Voluson 730 Expert (General Electric Medical Systems, Milwaukee, Wisc., USA) with 6- to 4-MHz or 6- to 2-MHz curved array probes. Routine ultrasound examination included a complete morphological examination, fetal weight, and amniotic fluid index calculations.

All Doppler estimations were done in the absence of fetal body movements and, if required, with maternal voluntary suspended respiration. The angle of insonation was kept <30° and the wall filter was set to 70 Hz to avoid sound artefacts. The mechanical and thermal indices were maintained below 1. All individual Doppler data was normalized by converting the measurements into Z-scores (standard deviation from the gestational age mean) according to reference ranges for each center [2, 19–26]. The following Doppler parameters were evaluated: umbilical artery (UA), middle cerebral artery (MCA), DV, AoI, and MPI. UA was evaluated in a free loop of the umbilical cord and dichotomized into present or absent/reversed end-diastolic flow (AREDF). MCA was measured in a transverse view of the fetal skull at the level of its origin from the circle of Willis and was defined as abnormal by pulsatility indices (PI) below the 5th centile [19]. DV was obtained from a mid-sagittal or alternatively a transverse section of the fetal abdomen. DV was divided into three categories according to PI and the presence of atrial flow as follows: normal (PI below the 95th centile), increased pulsatility (PI above the 95th centile with present atrial flow), and absent/reversed atrial flow (RAV) [21]. The aortic isthmus flow index (IFI) was obtained either in a sagittal view of the fetal thorax with a clear visualization of the aortic arch by placing the Doppler sample volume between the origin of the left subclavian artery and the confluence of the ductus arteriosus or in a cross section of the fetal thorax at the level of the 3-vessel and trachea view, placing the Doppler gate in the aorta just before the convergence of the arterial duct [27]. The IFI was calculated as follows: (systolic + diastolic)/systolic velocity integrals, and it was considered abnormal below the 5th centile [25]. The left MPI was obtained in a cross section of the fetal thorax in the 4-chamber view, placing the Doppler sample volume on the medial wall of the ascending aorta including the aortic and mitral valves. The valvular clicks in the Doppler wave were used as landmarks to calculate the isovolumic contraction (ICT) and relaxation times (IRT) and the ejection time (ET) [28]. The MPI

Table 1. Clinical and Doppler characteristics of the study groups

	Survivors (n = 129)	Perinatal deaths (n = 27)
Population characteristics		
Maternal age, years	32 (18 to 44)	31 (18 to 40)
Caucasian	95% (122/129)	78% (21/27)
Smoking status	57% (74/129)	56% (15/27)
Preeclampsia	75% (97/129)	52% (14/27)
Nulliparity	77% (99/129)	71% (19/27)
Doppler indices		
UA-PI	4.34 (1.63 to 22.73)	12.06 (0.05 to 41.47)*
MCA-PI	–1.07 (–2.16 to 0.99)	–1.40 (–2.72 to 1.33)*
DV-PI	1.66 (–1.97 to 10.51)	5.69 (0.07 to 21.56)*
IFI	–0.71 (–22.14 to 32.38)	–4.18 (–15.13 to 2.53)
MPI	2.24 (–2.42 to 8.72)	2.71 (–1.38 to 11.93)*
Delivery data		
Gestational age, weeks	31.1 (26.4 to 37.4)	27.4 (25.9 to 28.1)*
Birth weight, g	1,063 (460 to 2,390)	473 (370 to 530)*
5-min Apgar score <7.10	5% (7/129)	83% (10/12)*
Umbilical cord arterial pH	20% (26/129)	25% (3/12)

Data are medians (interquartile range) or proportions (%, n). Doppler parameters are expressed as Z-scores.
* $p < 0.05$ compared with survivors.

was calculated as (ICT + IRT)/ET. MPI was dichotomized as normal (below the 95th percentile) and abnormal (above the 95th percentile) [22, 26].

All Doppler parameters were converted into Z-scores according to previously published data [2, 19–26]. Only the last Doppler evaluation, performed within 72 h before delivery or death, was included in the statistical analysis.

Delivery Criteria

Indications for delivery included deterioration of fetal venous indices (absent or reversal of atrial flow in the DV), decelerative CTG, persistent abnormal BPP, and maternal complications secondary to preeclampsia [29]. When, according to these criteria, elective delivery was indicated for fetuses at gestational ages earlier than 26 weeks, the option of expectant management was discussed with parents and accepted if requested. The managing clinicians were blinded to the results of IFI and MPI. At delivery, gestational age, birth weight, Apgar scores, and umbilical pH were recorded.

Data Analysis

Data were analyzed with the SPSS 17.0 statistical package (SPSS, Chicago, Ill., USA). $p < 0.05$ was considered statistically significant. Logistic regression was used to explore the association of UA, MCA, DV, IFI, and MPI as continuous variables with perinatal mortality, defined as either intrauterine death or neonatal death within the first 28 days of life. Gestational age at delivery was also included, as it has been shown by previous studies to be the strongest predictor of perinatal mortality described in this group of fetuses. As a second step, multivariate analysis was performed on all variables as dichotomized parameters, with the gestational age cut-off point defined at 28 weeks in accordance with previous studies, as mentioned above [6].

Decision tree analysis was performed using the CHAID (χ^2 automatic interaction detection) method, which creates a tree-based classification model where, by means of regression models, the best predictor variables are selected and presented. The significance level was established at 0.05, where at each step or level CHAID chose the independent (predictor) variable that had the strongest interaction with the dependent variable (perinatal mortality).

Results

Maternal characteristics, Doppler recordings, and perinatal outcomes of the study population are shown in table 1. The median gestational age at delivery was 31 weeks and the median birth weight 977 g. Overall perinatal mortality was 17%, including 15 intrauterine and 12 neonatal deaths. All cases but the stillbirths were delivered by cesarean section.

Univariate analysis demonstrated that UA-PI, MCA-PI, DV-PI, and IFI were significantly associated with perinatal mortality (table 1). Multivariate analysis identified the UA-

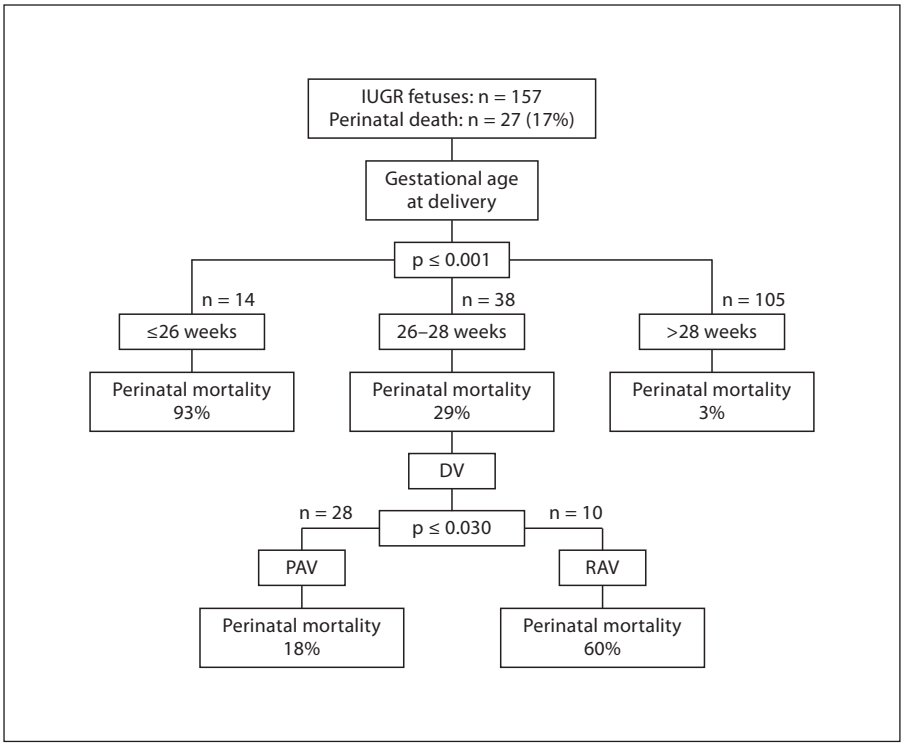

Fig. 1. Clinical algorithm for risk of death in early-onset IUGR fetuses, obtained by decision tree analysis. PAV = DV present atrial flow.

Table 2. Individual risk of death in early-onset IUGR fetuses, estimated by logistic regression (multivariate analysis)

	Estimated OR (95% CI)	p value
UA-PI	1.2 (1.1–1.4)	<0.001
MCA-PI	0.4 (0.2–0.8)	0.014
DV-PI	1.4 (1.2–1.6)	<0.001
IFI	0.9 (0.8–0.9)	0.020
MPI	1.1 (0.9–1.3)	0.373

Table 3. Individual risk of death in early-onset IUGR fetuses, estimated by logistic regression after dichotomization of variables

	Estimated OR (95% CI)	p value
GA <28 weeks	25.2 (8.3–76.1)	<0.001
DV-RAV	12.1 (4.1–35.6)	<0.001
UA-AREDF	10.2 (2.6–40.6)	0.001
MCA-PI <p5	5.3 (2.1–13.3)	<0.001
IFI <p5	1.8 (0.7–4.5)	0.232
MPI >p95	1.6 (0.7–3.8)	0.302

GA = Gestational age.

PI, MCA-PI, DV-PI, and IFI as statistically significant independent predictors for perinatal mortality (table 2). When gestational age was included in the model and the variables were dichotomized as normal/abnormal, gestational age (below 28 weeks), DV absent/reversed atrial flow (RAV), UA absent/reversed end-diastolic flow (AREDF), and MCA-PI below the 5th centile significantly and independently accounted for perinatal mortality (table 3).

Decision tree analysis was used to determine the best predictive combination of parameters for perinatal mortality (fig. 1). As expected, gestational age at delivery was the best initial predictor, with a 93% mortality rate below 26 weeks, 29% between 26–28 weeks, and 3% above 28 weeks. For cases between 26 and 28 weeks, characteristics of the DV 'a' wave (present vs. absent/reversed) allowed discrimination in two groups (18% mortality rate when it was present against 60% mortality rate when it was absent/reversed).

Discussion

This study evaluated the independent and combined contribution of fetal cardiovascular parameters to the prediction of early-onset IUGR perinatal mortality. The

study suggests an algorithm illustrating the chances of perinatal death against gestational age and DV, which might help clinical decisions in the management of early-onset IUGR fetuses.

Our data confirm previous studies showing that gestational age is the strongest predictor of perinatal mortality [5–7]. The findings are in line with studies suggesting that IUGR fetuses delivered below 26 weeks are associated with extremely high mortality rates, independently of the Doppler parameters. On the other end, IUGR fetuses delivered after 28 weeks of gestation have a much lower mortality [5, 7], which in our population was 3%. Aside from gestational age, the results confirmed previous studies suggesting DV atrial flow as the strongest Doppler predictor for perinatal mortality in preterm IUGR [6, 30, 31]. A recent systematic review confirmed that DV was the best predictor of perinatal mortality and acidemia when performed within 48 h of delivery [7]. Its value notwithstanding, it has been suggested that the DV provides limited information below 27 weeks because the mortality rate is very high in these cases anyway [5]. The current study is in line with this notion, and it further demonstrates that the DV is particularly informative in fetuses delivered between 26 and 28 weeks. In such cases the DV allows discrimination of a subgroup of fetuses with a higher mortality risk. These results support the use of the DV as a reason to indicate delivery at these gestational ages. On the contrary, the findings of this study support that the value of the DV in predicting mortality beyond 28 weeks is marginal. Nonetheless, the DV might still have a role in the prediction of morbidity and poor neurodevelopmental outcomes, as suggested by recent studies [15].

This study confirmed previous data suggesting that, when used in combination with venous Dopplers, the UA and MCA do not provide clinically useful information for the prediction of mortality [5, 8, 11]. As in previous studies, while both Doppler indices were significantly associated with the outcomes when analyzed as dichotomic variables, they were excluded from the final predictive model. Our data further confirms the lack of association between the IFI of AoI and perinatal death in multivariate models. AoI is essentially a surrogate marker of the degree of brain sparing. Consequently, and similarly to MCA Doppler, it becomes elevated very early in the sequence of fetal hemodynamic adaptation to placental insufficiency [32]. In addition, progressive changes in AoI Doppler values are strongly correlated with those occurring in the DV [32]. These reasons are proposed as determinants to explain the poor predictiveness of this vessel for perinatal mortality [8, 12–14, 33, 34]. On the contrary, AoI has been suggested to have a clear association with postnatal neurological morbidity [15, 35] since it is a marker of brain centralization. Along the same lines, the value of MCA advanced vasodilation as a predictor of neurobehavioral disruption among preterm newborns with IUGR is being increasingly suggested [36].

The present study could not demonstrate any additive value of MPI with respect to DV in the prediction of perinatal mortality. MPI failed to improve the prediction of DV by itself in the multivariate analysis despite its significant association with perinatal mortality. We could therefore not confirm our previous findings suggesting that inclusion of MPI could marginally improve the performance of gestational age and DV [6]. This discrepancy may be explained by differences in the study population characteristics, the statistical approach, or the limited external validity of MPI. The statistical analysis used in the present study was based on a CHAID model that automatically chooses the independently associated parameters for decision making, while our previous analysis was performed manually for each group. A recent longitudinal study on cardiovascular changes in IUGR showed that the MPI becomes altered at an earlier stage than the DV [33], and this may explain a weaker association with perinatal mortality. These results do not preclude the clinical value of MPI but illustrate that larger studies should be conducted in order to refine the assessment of the potential contribution of the MPI to monitoring of early-onset IUGR.

Our study presents various strengths and limitations. The selection criteria were strict and we included only early-onset cases with abnormal UA Doppler with at least one examination performed within 72 h of delivery or death. Perinatal mortality was defined as stillbirth or death within 28 days of life. This may lead to some discrepancies with other studies reporting neonatal mortality or intact survival as an outcome, and which exclude prenatal death [5, 9, 10]. Doppler values were assessed against normal reference curves and they were measured by experienced examiners. Patients were obtained from three different centers. We acknowledge that this may have introduced variability and consequently may have potentially affected the internal consistency of some measurements, although results were similar among centers. At the same time, the multicenter nature of the study reinforces the external validity of the results. The statistical or decision tree analysis is a strong model that performs a series of regressions in

order to adequately choose the strongest predictive variables associated with an outcome. Among other limitations of the study, we acknowledge that the criteria used to indicate elective delivery, which included DV measurements, are an insurmountable inherent bias of this type of studies. However, ethical reasons prevented us from blinding DV results to clinicians. Additionally, other non-Doppler parameters that have demonstrated their usefulness in predicting perinatal mortality, such as biophysical profile or computerized non-stress test, were not evaluated in a consistent manner among centers in this cohort and consequently were not included in the analysis.

In conclusion, cardiovascular Doppler parameters are significantly associated with perinatal mortality in early-onset IUGR. Our study confirms previous findings that gestational age at delivery is the strongest predictor of mortality in this group of fetuses. The results of this study suggest that before 26 weeks and after 28 weeks, gestational age alone is the strongest and almost unique predictor of perinatal mortality in early-onset IUGR. However, in the group between 26 and 28 weeks of gestation, the DV may provide useful information and allow stratification between high and low risks of perinatal mortality. This information may be of help in the decision-making process in this subgroup of fetuses. Our data may add to previous and future studies to further refine management guidelines for early-onset IUGR.

Acknowledgements

This study was supported by grants from the Fondo de Investigación Sanitaria (PI/060347 and PI/0690152; Spain), the Ministerio de Ciencia e Innovación (SAF2009-08815; Spain), the Centro para el Desarrollo Técnico Industrial (CENIT 20092012, supported by the Ministerio de Ciencia e Innovación, and the Fondo de Inversión Local para el Empleo; Spain), the Cerebra Foundation for the Brain Injured Child (Carmarthen, UK), and the Thrasher Research Fund (Salt Lake City, Utah, USA). Fátima Crispi is supported by a Rio Hortega research grant (CM07/00076) from the Carlos III Institute of Health (Spain). Rogelio Cruz-Martínez is supported by Marie Curie Host Fellowships for Early Stage Researchers, FETAL-MED-019707-2.

References

1 Gardosi J: Intrauterine growth restriction: new standards for assessing adverse outcome. Best Pract Res Clin Obstet Gynaecol 2009;23:741–749.

2 Baschat AA, Gembruch U, Weiner CP, Harman CR: Qualitative venous Doppler waveform analysis improves prediction of critical perinatal outcomes in premature growth-restricted fetuses. Ultrasound Obstet Gynecol 2003;22:240–245.

3 Crispi F, Bijnens B, Figueras F, Bartrons J, Eixarch E, Le Noble F, Ahmed A, Gratacos E: Fetal growth restriction results in remodeled and less efficient hearts in children. Circulation 2010;121:2427–2436.

4 Jang DG, Jo YS, Lee SJ, Kim N, Lee GS: Perinatal outcomes and maternal clinical characteristics in IUGR with absent or reversed end-diastolic flow velocity in the umbilical artery. Arch Gynecol Obstet 2011;284:73–8.

5 Baschat AA, Cosmi E, Bilardo CM, Wolf H, Berg C, Rigano S, Germer U, Moyano D, Turan S, Hartung J, Bhide A, Muller T, Bower S, Nicolaides KH, Thilaganathan B, Gembruch U, Ferrazzi E, Hecher K, Galan HL, Harman CR: Predictors of neonatal outcome in early-onset placental dysfunction. Obstet Gynecol 2007;109:253–261.

6 Hernandez-Andrade E, Crispi F, Benavides-Serralde JA, Plasencia W, Diesel HF, Eixarch E, Acosta-Rojas R, Figueras F, Nicolaides K, Gratacos E: Contribution of the myocardial performance index and aortic isthmus blood flow index to predicting mortality in preterm growth-restricted fetuses. Ultrasound Obstet Gynecol 2009;34:430–436.

7 Morris RK, Selman TJ, Verma M, Robson SC, Kleijnen J, Khan KS: Systematic review and meta-analysis of the test accuracy of ductus venosus Doppler to predict compromise of fetal/neonatal wellbeing in high risk pregnancies with placental insufficiency. Eur J Obstet Gynecol Reprod Biol 2010;152:3–12.

8 Del Rio M, Martinez JM, Figueras F, Bennasar M, Olivella A, Palacio M, Coll O, Puerto B, Gratacos E: Doppler assessment of the aortic isthmus and perinatal outcome in preterm fetuses with severe intrauterine growth restriction. Ultrasound Obstet Gynecol 2008;31:41–47.

9 Turan S, Turan OM, Berg C, Moyano D, Bhide A, Bower S, Thilaganathan B, Gembruch U, Nicolaides K, Harman C, Baschat AA: Computerized fetal heart rate analysis, Doppler ultrasound and biophysical profile score in the prediction of acid-base status of growth-restricted fetuses. Ultrasound Obstet Gynecol 2007;30:750–756.

10 Alves SK, Francisco RP, Miyadahira S, Krebs VL, Vaz FA, Zugaib M: Ductus venosus Doppler and postnatal outcomes in fetuses with absent or reversed end-diastolic flow in the umbilical arteries. Eur J Obstet Gynecol Reprod Biol 2008;141:100–103.

11 Bilardo CM, Wolf H, Stigter RH, Ville Y, Baez E, Visser GH, Hecher K: Relationship between monitoring parameters and perinatal outcome in severe, early intrauterine growth restriction. Ultrasound Obstet Gynecol 2004;23:119–125.

12 Figueras F, Benavides A, Del Rio M, Crispi F, Eixarch E, Martinez JM, Hernandez-Andrade E, Gratacos E: Monitoring of fetuses with intrauterine growth restriction: longitudinal changes in ductus venosus and aortic isthmus flow. Ultrasound Obstet Gynecol 2009;33:39–43.

13 Rizzo G, Capponi A, Vendola M, Pietrolucci ME, Arduini D: Relationship between aortic isthmus and ductus venosus velocity waveforms in severe growth restricted fetuses. Prenat Diagn 2008;28:1042–1047.

14 Fouron JC: The unrecognized physiological and clinical significance of the fetal aortic isthmus. Ultrasound Obstet Gynecol 2003;22:441–447.

15 Cruz-Martinez R, Figueras F, Tenorio V, Valsky DV, Arranz A, Crispi F, Hernández-Andrade E, Gratacos E: Combination of the aortic isthmus with ductus venosus improves the prediction of neurological damage in early-onset intrauterine growth restricted fetuses. Ultrasound Obstet Gynecol 2010;36:40.
16 Crispi F, Hernandez-Andrade E, Pelsers MM, Plasencia W, Benavides-Serralde JA, Eixarch E, Le Noble F, Ahmed A, Glatz JF, Nicolaides KH, Gratacos E: Cardiac dysfunction and cell damage across clinical stages of severity in growth-restricted fetuses. Am J Obstet Gynecol 2008;199:254.e1–254.e8.
17 Figueras F, Meler E, Iraola A, Eixarch E, Coll O, Figueras J, Francis A, Gratacos E, Gardosi J: Customized birthweight standards for a spanish population. Eur J Obstet Gynecol Reprod Biol 2008;136:20–24.
18 Baschat AA, Weiner CP: Umbilical artery Doppler screening for detection of the small fetus in need of antepartum surveillance. Am J Obstet Gynecol 2000;182:154–158.
19 Arduini D, Rizzo G: Normal values of pulsatility index from fetal vessels: a cross-sectional study on 1,556 healthy fetuses. J Perinat Med 1990;18:165–172.
20 Del Rio M, Martinez JM, Figueras F, Lopez M, Palacio M, Gomez O, Coll O, Puerto B: Reference ranges for Doppler parameters of the fetal aortic isthmus during the second half of pregnancy. Ultrasound Obstet Gynecol 2006;28:71–76.
21 Hecher K, Campbell S, Snijders R, Nicolaides K: Reference ranges for fetal venous and atrioventricular blood flow parameters. Ultrasound Obstet Gynecol 1994;4:381–390.
22 Hernandez-Andrade E, Figueroa-Diesel H, Kottman C, Illanes S, Arraztoa J, Acosta-Rojas R, Gratacos E: Gestational-age-adjusted reference values for the modified myocardial performance index for evaluation of fetal left cardiac function. Ultrasound Obstet Gynecol 2007;29:321–325.
23 Mari G, Deter RL, Carpenter RL, Rahman F, Zimmerman R, Moise KJ Jr, Dorman KF, Ludomirsky A, Gonzalez R, Gomez R, Oz U, Detti L, Copel JA, Bahado-Singh R, Berry S, Martinez-Poyer J, Blackwell SC: Noninvasive diagnosis by Doppler ultrasonography of fetal anemia due to maternal red-cell alloimmunization. Collaborative group for Doppler assessment of the blood velocity in anemic fetuses. N Engl J Med 2000;342:9–14.
24 Rizzo G, Capponi A, Talone PE, Arduini D, Romanini C: Doppler indices from inferior vena cava and ductus venosus in predicting ph and oxygen tension in umbilical blood at cordocentesis in growth-retarded fetuses. Ultrasound Obstet Gynecol 1996;7:401–410.
25 Ruskamp J, Fouron JC, Gosselin J, Raboisson MJ, Infante-Rivard C, Proulx F: Reference values for an index of fetal aortic isthmus blood flow during the second half of pregnancy. Ultrasound Obstet Gynecol 2003;21:441–444.
26 Van Mieghem T, Gucciardo L, Lewi P, Lewi L, Van Schoubroeck D, Devlieger R, De Catte L, Verhaeghe J, Deprest J: Validation of the fetal myocardial performance index in the second and third trimesters of gestation. Ultrasound Obstet Gynecol 2009;33:58–63.
27 Del Rio M, Martinez JM, Figueras F, Bennasar M, Palacio M, Gomez O, Coll O, Puerto B, Cararach V: Doppler assessment of fetal aortic isthmus blood flow in two different sonographic planes during the second half of gestation. Ultrasound Obstet Gynecol 2005;26:170–174.
28 Hernandez-Andrade E, Lopez-Tenorio J, Figueroa-Diesel H, Sanin-Blair J, Carreras E, Cabero L, Gratacos E: A modified myocardial performance (Tei) index based on the use of valve clicks improves reproducibility of fetal left cardiac function assessment. Ultrasound Obstet Gynecol 2005;26:227–232.
29 Report of the national high blood pressure education program working group on high blood pressure in pregnancy. Am J Obstet Gynecol 2000;183:S1–S22.
30 Robertson MC, Murila F, Tong S, Baker LS, Yu VY, Wallace EM: Predicting perinatal outcome through changes in umbilical artery Doppler studies after antenatal corticosteroids in the growth-restricted fetus. Obstet Gynecol 2009;113:636–640.
31 Baschat AA: Doppler application in the delivery timing of the preterm growth-restricted fetus: another step in the right direction. Ultrasound Obstet Gynecol 2004;23:111–118.
32 Cruz-Martinez R, Figueras F, Hernandez-Andrade E, Oros D, Gratacos E: Changes in myocardial performance index, aortic isthmus and ductus venosus in term, small-for-gestational age fetuses with normal umbilical artery Doppler. Ultrasound Obstet Gynecol 2011;38:400–405.
33 Cruz-Martinez R, Figueras F, Benavides-Serralde A, Crispi F, Hernandez-Andrade E, Gratacos E: Sequence of changes in myocardial performance index in relation with aortic isthmus and ductus venosus Doppler in fetuses with early-onset intrauterine growth restriction. Ultrasound Obstet Gynecol 2011;38:179–184.
34 Makikallio K: Is it time to add aortic isthmus evaluation to the repertoire of Doppler investigations for placental insufficiency? Ultrasound Obstet Gynecol 2008;31:6–9.
35 Fouron JC, Gosselin J, Amiel-Tison C, Infante-Rivard C, Fouron C, Skoll A, Veilleux A: Correlation between prenatal velocity waveforms in the aortic isthmus and neurodevelopmental outcome between the ages of 2 and 4 years. Am J Obstet Gynecol 2001;184:630–636.
36 Figueras F, Cruz-Martinez R, Sanz-Cortes M, Arranz A, Illa M, Botet F, Costas-Moragas C, Gratacos E: Neurobehavioral outcomes in preterm, growth-restricted infants with and without prenatal advanced signs of brain-sparing. Ultrasound Obstet Gynecol 2011;38:288–294.

STUDY 4

Fetal echocardiography to predict infant hypertension and arterial remodeling in intrauterine growth restriction.

Cruz-Lemini M, Crispi F, Valenzuela-Alcaraz B, Figueras F, Gómez O, Sitges M, Bijnens B, Gratacós E.

Am J Obstet Gynecol 2013.

Status: Submitted

Impact factor: 3.877

Quartile: 1st.

TITLE PAGES

A fetal cardiovascular score to predict infant hypertension and arterial remodeling in intrauterine growth restriction

Mónica CRUZ-LEMINI, MD[1]; Fátima CRISPI, MD, PhD[1]; Brenda VALENZUELA-ALCARAZ, MD[1]; Francesc FIGUERAS, MD, PhD[1]; Olga GÓMEZ, MD, PhD[1]; Marta SITGES, MD, PhD[2]; Bart BIJNENS, PhD[3]; Eduard GRATACÓS, MD, PhD[1].

[1]Department of Maternal-Fetal Medicine (Institut Clínic de Ginecologia, Obstetrícia i Neonatologia), Hospital Clínic - Institut d'Investigacions Biomèdiques August Pi i Sunyer, Universitat de Barcelona and Centro de Investigación Biomédica en Red en Enfermedades Raras, Barcelona, Spain. [2]Department of Cardiology (Institut Clínic del Tòrax), Hospital Clínic - Institut d'Investigacions Biomèdiques August Pi i Sunyer, Universitat de Barcelona, Barcelona, Spain. [3]ICREA - Universitat Pompeu Fabra, Barcelona, Spain.

Corresponding author:

Eduard Gratacós MD, PhD.

Head & Professor, Department of Maternal-Fetal Medicine

Institut Clínic de Ginecologia, Obstetrícia i Neonatologia (ICGON), Hospital Clínic, University of Barcelona. Sabino de Arana 1, 08028 Barcelona, Spain.

Telephone: +34 93 227 9931; Fax: +34 93 227 5612. E-mail: gratacos@clinic.ub.es

DISCLOSURE: The authors report no conflict of interest.

This research was presented at the 12th World Congress in Fetal Medicine, Marbella, Spain; June 23-27, 2013.

Funding: This work was supported by grants from Instituto de Salud Carlos III [grant number PI11/00051, PI12/00801, PI11/01709], cofinanced by the Fondo Europeo de Desarrollo Regional de la Unión Europea "Una manera de hacer Europa", Spain; Centro para el Desarrollo Técnico Industrial [cvREMOD 2009-2012] supported by the Ministerio de Economía y Competitividad y Fondo de Inversión Local para el Empleo, Spain; Ministerio de Economía y Competitividad PN de I+D+I 2008-2011 [SAF2009-08815], Spain; Cerebra Foundation for the Brain Injured Child (Carmarthen, Wales, UK) and Thrasher Research Fund (Salt Lake City, USA). M.C.L. and B.V.A. wish to express their gratitude to the Mexican National Council for Science and Technology (CONACyT, Mexico City, Mexico) for supporting their predoctoral stay at Hospital Clínic, Barcelona, Spain.

Reprints: Eduard Gratacós MD, PhD. Institut Clínic de Ginecologia, Obstetrícia i Neonatologia (ICGON), Hospital Clínic, University of Barcelona. Sabino de Arana 1, 08028 Barcelona, Spain. E-mail: gratacos@clinic.ub.es

Manuscript word count: 3985.

Abstract word count: 236.

CONDENSATION AND SHORT VERSION OF TITLE

Condensation:

Fetal echocardiography identifies a high-risk group within the IUGR fetuses, which could be targeted for early screening of blood pressure and other cardiovascular risk factors postnatally.

Short version of title: Fetal echocardiography to predict postnatal hypertension in IUGR.

ABSTRACT AND KEYWORDS

OBJECTIVE

Intrauterine growth restricted (IUGR) fetuses suffer cardiovascular remodeling which persists into infancy and has been related to cardiovascular outcomes in adulthood. Hypertension in infancy has been demonstrated to be a strong risk factor for later cardiovascular disease. Close monitoring together with dietary interventions have shown to improve cardiovascular health in hypertensive children; however, not all IUGR show increased blood pressure. We evaluated the potential of fetal echocardiography for predicting hypertension and arterial remodeling in 6 month old IUGR infants.

STUDY DESIGN

100 consecutive IUGR and 100 control fetuses were followed-up into infancy. Fetal assessment included perinatal Doppler, cardiac morphometry, ejection fraction, cardiac output, isovolumic relaxation time (IVRT), tricuspid annular-plane systolic excursion (TAPSE) and tissue Doppler. Infant hypertension and arterial remodeling were defined as mean blood pressure >95th centile together with aortic intima-media thickness >75th centile at 6 months of age. Odds ratio were obtained for fetal parameters associated with infant outcomes.

RESULTS

Fetal TAPSE, right sphericity index, IVRT and cerebroplacental ratio were the strongest predictors for postnatal vascular remodeling. A cardiovascular risk score based on fetal TAPSE, cerebroplacental ratio, right sphericity index and IVRT was highly predictive of infant hypertension and arterial remodeling (area under the curve 0.87, 95% CI 0.79 – 0.93, $p<0.001$)).

CONCLUSIONS

Fetal echocardiographic parameters identify a high-risk group within the IUGR fetuses, which could be targeted for early screening of blood pressure and other cardiovascular risk factors, as well as for promoting healthy diet and physical exercise.

Keywords: cardiovascular risk; fetal echocardiography; fetal programming; hypertension; intrauterine growth restriction.

MAIN TEXT

INTRODUCTION

Intrauterine growth restriction (IUGR) is defined as an estimated fetal weight below the 10th centile for gestational age. Evidence from large epidemiological studies has long suggested a strong association between IUGR and increased cardiovascular mortality in adulthood[1]. Recent prospective studies have described that fetuses with IUGR have cardiac remodeling and dysfunction, which persists into infancy in the form of remodeled hearts, hypertension and increased intima-media thickness[2-5]. Hypertension in childhood is a strong risk factor for later cardiovascular disease[6, 7] and is considered an indication for lifestyle modifications[7, 8]. Detection of IUGR may constitute an opportunity to apply preventive cardiovascular interventions from early life[9]. However, IUGR may affect up to 5-10% of the whole population, and only a fraction will display the cardiovascular features above described during childhood. Therefore, personalized medicine approaches are required to allow selection of subjects at high risk.

Perinatal selection of cases at risk would allow an efficient approach to detect fetuses that may later benefit for early screening and intervention in infancy[7, 9]. Perinatal criteria conventionally used to establish the severity of IUGR, such as gestational age at onset or fetoplacental Doppler changes, have shown a weak association with postnatal cardiovascular findings. Thus, a remarkable proportion of fetuses with relatively benign forms of IUGR may still present with hypertension and cardiovascular remodeling in childhood[4, 10, 11]. Fetal echocardiography is a potential and so far unexplored approach to achieve prenatal detection of cardiovascular remodeling persisting into childhood. Several functional and morphometric echocardiographic parameters show remarkable

differences in IUGR with respect to normally grown fetuses[2, 4, 5, 11, 12]. However, the relationship of these changes with cardiovascular findings in childhood has not been determined. It is unknown to what extent prenatal changes are only a direct reflection of fetal deterioration due to hypoxia and undernutrition occurring in IUGR[3]. In addition, events during the neonatal period might exert influences in later cardiovascular function.

We conducted a prospective cohort study including 100 IUGR fetuses and 100 normally grown fetuses. Subjects were evaluated prenatally with comprehensive echocardiography and followed-up into 6 months of age to assess blood pressure and aortic intima-media thickness. We evaluated the correlation of fetal echocardiographic parameters with postnatal cardiovascular features and explored whether a cardiovascular score was predictive of infant hypertension and arterial remodeling.

MATERIALS AND METHODS

Study population

The study design was a prospective cohort study including fetuses with IUGR and controls, identified *in utero* and followed into infancy. The source population comprised pregnancies from April 2010 to September 2012 who attended the Department of Maternal–Fetal Medicine at Hospital Clínic in Barcelona, Spain. Pregnancies with structural/chromosomal anomalies, evidence of fetal infection or achieved by assisted reproduction technologies were excluded from the study. IUGR was defined as an estimated fetal weight, and (later) confirmed birth weight, below the 10th centile according to local reference curves[13]. In total, 132 IUGR fetuses were included for the study in prenatal life; 4 cases were later excluded because of Down's syndrome (2) and pulmonary stenosis (2), 5 cases died before delivery and 11 in the neonatal period. From the remaining 112 patients, 12 were lost on follow-up leaving us with 100 IUGR cases. The reference cohort of fetuses with normal estimated fetal weight and birth weight (>10th percentile) were randomly sampled from pregnancies

at our institution and paired with IUGR cases by gestational age at scan (±1 week). The study was approved by our institution's Ethics Committee, and written parental consent was obtained for all study participants. The study protocol included fetal standard obstetric assessment and echocardiography, record of delivery data and postnatal vascular assessment at 6 months of age.

Baseline and perinatal characteristics

Upon fetal examination, maternal characteristics such as height, weight, body mass index, smoking during pregnancy and parity were recorded. Gestational age at scan was calculated based on the crown-rump length obtained at first trimester screening. All women underwent ultrasonographic examination using a Siemens Sonoline Antares machine (Siemens Medical Systems, Malvern, PA, USA) which included estimation of fetal weight and standard obstetric Doppler evaluation comprising measurement of the pulsatility index (PI) for the uterine arteries, umbilical artery, middle cerebral artery, ductus venosus and aortic isthmus. Estimated fetal weight was calculated according to the method of Hadlock et al; both estimated fetal weight and birth weight centile were calculated using local reference curves[13]. Uterine artery evaluation was performed with the probe placed on the lower quadrant of the abdomen, angled medially, with identification by color Doppler imaging of the apparent crossover with the external iliac artery. Mean uterine artery PI was calculated as the average PI of right and left arteries[14]. Umbilical artery was evaluated in a free loop of the umbilical cord; middle cerebral artery was measured in a transverse view of the fetal skull at the level of its origin from the circle of Willis[15]. Cerebroplacental ratio was calculated by dividing middle cerebral artery and umbilical artery PI[16]. Ductus venosus was obtained from a mid-sagittal or alternatively a transverse section of the fetal abdomen, prior to its entrance into the inferior vena cava, positioning the Doppler gate at the isthmic portion[17]. The aortic isthmus was obtained either in a sagittal view of the fetal thorax with a clear visualization of the aortic arch by placing the Doppler sample volume between the origin of the left subclavian artery and the confluence of the ductus arteriosus or in a

cross section of the fetal thorax at the level of the 3-vessel and trachea view, placing the Doppler gate in the aorta just before the convergence of the arterial duct[18]. Upon delivery, gestational age, birth weight, birth weight centile, mode of delivery, Apgar scores, presence of preeclampsia and length of stay at the neonatal intensive care unit were recorded.

Fetal echocardiography

Upon IUGR diagnosis, a complete two-dimensional echocardiographic examination was performed initially to assess structural heart integrity using a Siemens Sonoline Antares machine (Siemens Medical Systems, Malvern, PA, USA). Cardiovascular evaluation was performed using a curved-array 2-6 MHz transducer, with the exception of tissue Doppler measurements that required a phased-array 2-10 MHz transducer. The following measurements were performed:

Cardiac morphometry included cardiothoracic ratio, atrial areas, ventricular sphericity indexes and myocardial wall thicknesses. The cardiothoracic ratio was measured from a four-chamber view, by the area method previously described[19]. Left and right atrial areas were delineated on 2D images from an apical or basal four-chamber view at end-ventricular systole (maximum point of atrial distension)[20]. Ventricular base-to-apex lengths and transverse diameters were measured on 2D images from an apical four-chamber view at end-diastole. Ventricular sphericity indexes were calculated as base-to-apex length/transverse diameter of the left and right ventricles respectively[21, 22]. Ventricular end-diastolic septal and free wall thicknesses were measured by M-mode from a transverse four-chamber view.

Systolic function evaluation included ejection fraction (EF), stroke volumes (SV), cardiac outputs (CO), cardiac index (CI), mitral/tricuspid annular-plane systolic excursion (MAPSE/TAPSE), systolic annular peak velocities (S') and the isovolumic contraction (IVCT) and ejection times (ET). Left and right EF were obtained from a transverse four-chamber view by M-mode, using Teicholz's formula[23]. Left and right SV were calculated as $\pi/4$*(aortic or pulmonary

valve diameter)2*(aortic or pulmonary artery systolic flow velocity-time integral). Fetal heart rate was calculated in the spectral Doppler image of the aortic or pulmonary flow. Aortic systolic flow was obtained in an apical or basal 5-chamber view of the heart, and the pulmonary artery systolic flow was obtained in a right ventricle outflow tract view; both at angles as close to 0º as possible. Velocity-time integrals were calculated by manual trace of the spectral Doppler area[24]. Left and right CO were calculated as left/right SV*fetal heart rate. Diameters of the aortic and pulmonary valves were measured in frozen real-time images during systole by the leading edge-to-edge method[25]. CI was obtained by the formula (left CO + right CO)/estimated fetal weight, and expressed in mL/min/Kg[26]. MAPSE and TAPSE assessed by M-mode, were measured real time in an apical or basal four-chamber view, by placing the cursor at a right angle to the atrioventricular junction, marked by the valve rings at the mitral or tricuspid valves[5, 27]; maximum amplitude of motion was taken as the extent of displacement between end-systole and end-diastole, measured in millimeters. Tissue Doppler imaging was applied in spectral Doppler mode at mitral and tricuspid lateral annuli from an apical or basal four-chamber view, to record S' in cm/s[12]. The IVCT and ET were obtained in a cross section of the fetal thorax at the 4-chamber view, placing the Doppler sample volume on the medial wall of the ascending aorta, including the aortic and mitral valve; valvular clicks in the Doppler wave were used as landmarks to calculate each[28]. The IVCT was measured from the closure of the mitral valve to the opening of the aortic valve, and the ET was measured from opening to closure of the aortic valve.

Diastolic function was evaluated by peak early/late transvalvular filling velocities (E/A) ratio, E deceleration time, early diastolic annular peak velocity (E'), E/E' ratio and left isovolumic relaxation time (IVRT). Atrioventricular flow velocities were obtained from a basal or apical four-chamber view, placing the pulsed Doppler sample volume just below the valve leaflets[24, 29]. E deceleration time was measured as the time from the maximum mitral/tricuspid velocity to the baseline[30]. Tissue Doppler imaging was applied in spectral Doppler mode at the mitral and tricuspid

lateral annuli, from an apical or basal four-chamber view, to record E' in cm/s[12]. Left IVRT was measured in the same plane as IVCT and ET, from the closure of the aortic valve to the opening of the mitral valve[28].

Anthropometric and vascular assessment at 6 months of age

Postnatal assessment was scheduled at 6 months of age including anthropometric data, blood pressure and vascular ultrasound assessment.

Anthropometric data included the infant's height, weight, body mass index and body surface area measured at the time of the examination.

Systolic and diastolic blood pressures were obtained at the beginning of the medical evaluation by a trained physician from the brachial artery using a validated ambulatory automated Omron 5 Series device, while the infant was resting.

Vascular assessment by ultrasound was performed using Vivid Q (General Electric Healthcare, Horten, Norway), with a 12L-RS linear-array 6.0-13.0 MHz transducer. Infants were studied when resting quietly or asleep. Longitudinal clips of the far wall of the proximal abdominal aorta in the upper abdomen were obtained, and aIMT measurements were performed offline according to a standardized protocol based on a trace method with the assistance of commercially available software (GE EchoPAC PC 108.1.x, General Electric Healthcare). To obtain aIMT, three end-diastolic frames were selected across a length of 10 mm and analyzed for mean and maximum aIMT, and the average reading from these three frames was calculated[31, 32].

Cardiovascular endpoint: hypertension and arterial remodeling

To define hypertension and arterial remodeling, we sought those parameters reported in literature as sensitive for detecting preclinical cardiovascular dysfunction in infants. Thus, the cardiovascular endpoint of hypertension and arterial remodeling at 6 months of age was defined as

presence of both a mean blood pressure above 95th centile and maximum aIMT above the 75th centile[31]. Blood pressure centiles were calculated according to published reference values[6]. Since no reference values exist for aIMT at this age, we used centiles obtained with our control group as reference parameters.

Statistical analysis

Data was analyzed using the IBM SPSS Statistics 19 and MedCalc 9.1 statistical software. Sample size was calculated to enable to observe a difference of 10% in fetal TAPSE values for IUGR as compared to controls. Fetal TAPSE was chosen because of its high sensitivity for preclinical cardiac dysfunction in fetuses and children[5, 27, 33]. For a power of 80% and alpha risk of 0.05, a minimum of 97 subjects per study group was required.

First, a comparative study between control and IUGR fetuses and infants was performed and presented as mean ± standard deviation (SD) or percentage (%). Normality was evaluated by the Shapiro-Wilk test. Baseline and perinatal characteristics were compared in cases and controls by Student's *t* test. Comparison of fetal echocardiographic parameters was performed by linear regression and adjusted by gender, gestational age at delivery and preeclampsia in fetuses, and also by body surface area in infants. *P* values below 0.05 were considered statistically significant.

Second, the association and predictive value of standard perinatal data and fetal echocardiography for infant hypertension and arterial remodeling were assessed within the IUGR group. Infant hypertension and arterial remodeling at 6 months of age were defined as mean blood pressure above the 95th centile along with aIMT above 75th centile[7, 31, 32, 34]. Data was analyzed by logistic regression in order to obtain odds ratio (OR) for the cardiovascular parameters associated with the infant vascular outcome. In order to account for changes due to gestational age, fetal parameters were included as z-scores (when available) in the model[12, 15-18, 25, 27, 35, 36]. Finally, a composite score based on the strongest predictors was generated by multivariate logistic regression,

and receiver operating characteristic (ROC) curve analysis was used for calculation of area under the curve (AUC) for the score and standard perinatal parameters.

RESULTS

Baseline perinatal and delivery characteristics

Baseline characteristics of the pregnant group are shown in Table 1. Maternal characteristics and gestational age at scan were similar in IUGR cases and controls. As expected, estimated fetal weight and fetoplacental Doppler parameters were significantly worse in the IUGR group. The growth restricted group showed an earlier gestational age at delivery, with lower birth weight centile and worse perinatal outcomes, shown by a higher incidence of preeclampsia, caesarean section and longer neonatal hospitalization.

Fetal echocardiography

Results of fetal echocardiography in the study groups are shown in Table 2. Cardiac shape and size showed significant differences between groups. Cardiothoracic ratio and atrial areas were increased in the IUGR fetuses as compared to controls. Left and right sphericity indexes were significantly decreased in IUGR fetuses when compared to controls, with thicker myocardial walls. Both EF and heart rate showed no differences between groups. Both SV and CO were reduced in the IUGR fetuses; however when corrected by estimated fetal weight (cardiac index), IUGR fetuses showed a trend to higher values as compared to controls. Longitudinal function assessed by MAPSE, TAPSE and S' was significantly reduced in the IUGR fetuses as compared to controls. Both the IVCT and ET were increased in the IUGR group. Diastolic function parameters also showed differences, with decreased E' velocities and increased E/A and E/E' ratios, IVRT and E deceleration time in IUGR fetuses as compared to controls.

Anthropometric and vascular assessment at 6 months of age

Follow-up characteristics of the 6-month old infants were evaluated are shown in Table 3. IUGR infants showed lower height, weight, body mass index and body surface area as compared to controls with no significant difference in age at assessment or gender. Both systolic and diastolic blood pressures were significantly higher in the IUGR infants, with 2% of cases presenting systolic hypertension and 41% diastolic hypertension. Mean blood pressure was also significantly increased, with 41% infants above the 95th centile. Both mean and maximum aIMT measurements were significantly increased in IUGR infants as compared to controls. Seventy-three percent of the IUGR infants presented maximum aIMT above the 75th centile and thirty-seven percent above the 95th centile.

Prediction of hypertension and arterial remodeling in IUGR cases

We analyzed the association of the different perinatal and echocardiographic parameters for the prediction of infant hypertension and arterial remodeling within the IUGR cases, defined by the presence of both a mean blood pressure above 95th centile and maximum aIMT above the 75th centile. Thirty-one (31%) IUGR infants had both criteria present at 6 months of age.

Table 4 and Figure 1 show the predictive value (as OR) of fetal parameters for hypertension and arterial remodeling, assessed by univariate regression analysis. Neither gestational age at delivery, nor birth weight centile were predictors of the presence of this combined cardiovascular endpoint within the IUGR group. Umbilical, middle cerebral and uterine artery Doppler showed a significant association, however ductus venosus and aortic isthmus showed none. Several fetal echocardiographic parameters were associated with hypertension and arterial remodeling, with morphometric and longitudinal motion parameters having the highest predictive values: decreased TAPSE (OR 10.2) and lower right sphericity index (OR 5.6) demonstrated the strongest associations.

In order to assess the potential interaction among the different parameters, a multivariate

analysis was performed including TAPSE (the parameter showing the strongest association with hypertension and arterial remodeling in the univariate analysis) with other significant predictors of risk (supplementary material). Most parameters continued showing independent predictive values for the combined cardiovascular endpoint: cerebroplacental ratio (OR 2.2 (95% CI 1.5 – 3.1, p<0.001)), right sphericity index (OR 2.8 (95% CI 1.4 – 10.9, p<0.015)) and IVRT (OR 2.2 (95% CI 1.4 – 3.5, p0.001)) having the highest OR. Finally, a composite score, based on the best perinatal and fetal echocardiographic predictors was generated by combining these variables in a regression analysis. This fetal cardiovascular score was comprised of TAPSE (z-score), cerebroplacental ratio (z-score), right sphericity index (crude value) and IVRT (z-score) (Figure 2), and yielded the following equation: 1.907 + (TAPSE*-0.589) + (cerebroplacental ratio*-0.286) + (right sphericity index*-1.938) + (IVRT*0.342) ≥0.1253. The equation resulted in 90% sensitivity, 77% specificity, 63% positive predictive value, 95% negative predictive value, 3.9 positive likelihood ratio and 0.1 negative likelihood ratio, to detect those IUGR cases with infant hypertension and arterial remodeling. ROC curve comparison was performed to estimate area under the curve for isolated and combined parameters with the highest OR. The average AUC for the fetal cardiovascular score was 0.87 (95% CI 0.79 – 0.93, p<0.001), higher than fetal TAPSE alone (0.64 (95% CI 0.56 – 0.73, p=0.030), fetal EF (0.57 (95% CI 0.48 – 0.65, p=0.072) and perinatal factors (Figure 3).

COMMENT

This study supports that a fetal cardiovascular score is strongly associated with the presence of postnatal hypertension and arterial remodeling at 6 months of age in IUGR. Echocardiographic parameters demonstrated a far better performance than perinatal factors and fetoplacental Doppler used for establishing the severity of IUGR.

Echocardiographic measurements in fetuses were consistent with previous studies demonstrating significant differences in cardiac function under IUGR[1-3, 5, 11, 12, 32, 37-40]. Likewise,

increased blood pressure and aIMT had previously been reported in IUGR neonates and children[3, 32, 38, 40-42]. The present study expands previous findings. Longitudinal follow-up demonstrated the relationship between prenatal echocardiography and postnatal cardiovascular findings.

As expected, gestational age and birth weight centile showed no association with the occurrence of hypertension and arterial remodeling in childhood. Likewise, fetoplacental Doppler parameters used in fetal management because of their association with perinatal outcome, had only a weak association with postnatal cardiovascular outcome. The absence of a direct relationship between these factors, which are widely accepted severity criteria and bear a strong association with perinatal and neurological outcome[43-45] suggests that cardiovascular programming may require the presence of predisposing factors. In line with this notion, fetal echocardiographic parameters showed a strong association with hypertension and arterial remodeling. This might indicate that, irrespective of conventional perinatal criteria, there is a fraction of subjects displaying more pronounced adaptative cardiovascular changes under IUGR, and in which these changes persist postnatally. The cardiovascular score developed in this study could identify this high-risk subgroup with a sensitivity of 90%.

Our proposed score logically combines information for cardiovascular remodeling, namely the severity of the IUGR (cerebroplacental ratio), cardiac morphology (sphericity index), systolic function (TAPSE) and diastolic function (IVRT). All indices comprised by the score can be obtained with any obstetrical ultrasound device equipped with M-mode, conventional pulsed and color Doppler, and are reproducible in fetuses[16, 27, 28]. TAPSE has been used in fetuses to describe cardiovascular dysfunction in IUGR, reflecting subclinical longitudinal dysfunction of the right ventricle[5]. Postnatally, TAPSE has been reported as a good predictor for mortality in Eisenmenger's syndrome, or to monitor postoperatory function in resychronisation therapy[33, 46]. Changes in sphericity index had been previously described in IUGR children by our group[3, 11], showing more

globular hearts probably due to cavity dilation secondary to hypoxia; in this study we first report that these changes are already present in utero. IVRT is a known parameter for the evaluation of diastolic dysfunction due to poor myocardial relaxation, and is used commonly in fetal echocardiography[24, 28, 35].

Overall, our results show that fetal echocardiography can predict mid-term cardiovascular risk factors and support the concept of including the selected IUGR population as a high-risk group for early screening in cardiovascular guidelines[3]. From a clinical perspective, this study opens a line that may find new applications for echocardiography in fetal life. Considering that diagnosis of IUGR is established in about 5-10% of pregnancies, the findings of this study would affect thousands of children per year. In addition, recent prospective validation with long term follow-up is required to confirm the value of predictive scores based on fetal echocardiography with a clear clinical application. If these expectations are confirmed, prediction of hypertension and arterial remodeling from perinatal life would represent a public health opportunity for intervention. It is recognized that mild cardiovascular changes that remain subclinical during childhood may represent significant health issues if combined with additional behaviors or stressors during adulthood[47]. Hypertension in the child has been associated with substantial long-term health risks and considered an indication for lifestyle modifications[6]. In addition, aIMT measurement allows detection of increased cardiovascular risk as an indicator of arterial remodeling in children[31, 32, 38]. Interventions in this target group could go from blood pressure monitoring before 3 years of age, recommending lack of exposure to other risk factors (secondary smoking, obesity), surveillance of catch-up growth or administration of hypotensors[7, 9] and specially, promoting exercise and physical activity. Particularly, high intake of dietary long-chain ω-3 fatty acids is associated with lower blood pressure and may prevent progression of subclinical atherosclerosis in children born with low birth weight[48]. A recent randomized trial in a large cohort of children suggest that the inverse association of fetal growth with arterial wall thickness in childhood can be prevented by dietary ω-3 fatty acid supplementation over

the first 5 years of life[49].

Among the strengths of this study was the longitudinal workup of structural and functional echocardiographic findings from fetal life to infancy. This allowed to prospectively examine the effects of impaired fetal growth, while controlling for postnatal confounders as much as possible. Examination at 6 months of age was decided because it is a reasonable point in time to avoid the effects of neonatal cardiovascular transition to postnatal life and potential interference with temporary blood pressure changes. While we acknowledge that longer term evaluation would provide more robust data on the long term prediction value, this would entail the need for correction of potential confounders associated with diet, exercise or socioeconomic factors. In addition, there is strong evidence on the longer term effects of IUGR in children and adolescents[7, 38, 48]. Notwithstanding these comments, we acknowledge that longer term follow up is necessary to validate the clinical value of echocardiographic scores to predict hypertension and other cardiovascular outcomes in childhood. Likewise, we acknowledge that there is no standard definition for increased cardiovascular risk at 6 months of age and that an ideal outcome for this type of study would be information of cardiovascular disease or clinical events at adult age, such as myocardial infarction, heart failure or death. Therefore, further long term follow-up of an extended cohort to validate the findings here reported is warranted.

In conclusion, this study provides evidence that a score based on fetal echocardiographic findings allows prediction of postnatal hypertension and arterial remodeling. Identification of high-risk groups within IUGR fetuses and other conditions described to be associated with cardiovascular programming[50] would lead to new clinical applications for echocardiography in pregnancy, and would represent a step forward in personalized fetal and pediatric cardiology. If these results are validated by other authors this research could open the door for designing targeted interventions to reduce the risks of cardiovascular disease from perinatal life.

TABLES

Table 1. Baseline and perinatal characteristics of the study groups.

	Controls (n=100)	IUGR (n=100)	*p*-value
Maternal characteristics			
Height (cm)	162 ± 7	161 ± 6	0.279
Weight (Kg)	61 ± 11	59 ± 13	0.242
Body mass index (Kg/m2)	22 ± 4	23 ± 5	0.120
Smoking (%)	21	24	0.735
Nulliparity (%)	57	67	0.190
Fetoplacental ultrasound evaluation			
Gestational age at ultrasound (weeks)	35.3 ± 5.1	35.8 ± 3.6	0.424
Estimated fetal weight (grams)	2270 ± 889	1960 ± 626	0.005
Estimated fetal weight centile	52 ± 24	2 ± 3	<0.001
Mean uterine artery PI	0.68 ± 0.18	0.88 ± 0.43	0.001
Umbilical artery PI	1.03 ± 0.21	1.25 ± 0.58	0.002
Middle cerebral artery PI	2.01 ± 0.35	1.56 ± 0.48	<0.001
Cerebroplacental ratio	2.02 ± 0.53	1.46 ± 0.73	<0.001
Ductus venosus PI	0.52 ± 0.16	0.55 ± 0.19	0.229
Aortic isthmus PI	2.67 ± 0.36	3.92 ± 2.87	<0.001
Pregnancy outcomes			
Gestational age at delivery (weeks)	40.1 ± 1.5	37.2 ± 3.5	<0.001
Birth weight (grams)	3373 ± 412	2153 ± 664	<0.001
Birth weight centile	50 ± 25	3 ± 3	<0.001
Cesarean section (%)	16	42	<0.001
5-minute Apgar score <7 (%)	0	1	1.000
Preeclampsia (%)	1	10	0.013
Days in neonatal intensive care unit	1 ± 4	11 ± 22	<0.001

Data shown as mean ± SD or percentage. *P*-value calculated by Student's t test or χ^2 test where appropriate. IUGR, intrauterine growth restriction; PI, pulsatility index.

Table 2. Fetal echocardiography data from the study groups.

	Controls (n=100)	IUGR (n=100)	Adjusted *p*-value
Gestational age at evaluation (weeks)	35.3 ± 5.1	35.8 ± 3.6	0.082
Cardiac morphometry			
Cardiothoracic ratio	0.27 ± 0.05	0.33 ± 0.05	<0.001
Left atrial area (cm2)	1.61 ± 0.62	1.75 ± 0.58	0.004
Right atrial area (cm2)	1.84 ± 0.76	2.02 ± 0.60	0.003
Left sphericity index	2.06 ± 0.37	1.87 ± 0.42	0.005
Right sphericity index	1.85 ± 0.39	1.57 ± 0.28	<0.001
Left wall thickness (mm)	2.91 ± 0.67	3.48 ± 0.74	<0.001
Right wall thickness (mm)	3.06 ± 0.68	3.63 ± 0.70	<0.001
Interventricular septum (mm)	2.69 ± 0.62	3.38 ± 0.81	<0.001
Systolic function			
Left ejection fraction (%)	70.9 ± 8.8	71.3 ± 9.9	0.843
Right ejection fraction (%)	67.5 ± 8.1	68.5 ± 9.9	0.896
Heart rate (BPM)	140 ± 10	138 ± 12	0.168
Left stroke volume (mL)	4.1 ± 1.7	3.3 ± 1.5	0.107
Left cardiac output (mL/min)	559 ± 236	449 ± 195	0.116
Right stroke volume (mL)	4.8 ± 1.8	4.3 ± 1.9	0.018
Right cardiac output (mL/min)	667 ± 228	593 ± 260	0.018
Cardiac index (mL/min/Kg)	498 ± 145	536 ± 162	0.086
MAPSE (mm)	5.5 ± 1.3	5.0 ± 1.1	0.014
TAPSE (mm)	7.2 ± 1.3	6.6 ± 1.3	0.018
Mitral S' (cm/s)	7.1 ± 1.3	6.2 ± 1.1	0.010
Tricuspid S' (cm/s)	7.9 ± 1.4	7.4 ± 1.3	<0.001
Isovolumic contraction time (ms)	29 ± 4	36 ± 8	<0.001
Ejection time (ms)	171 ± 10	158 ± 11	<0.001
Diastolic function			
Mitral E/A ratio	0.74 ± 0.13	0.81 ± 0.15	0.002
Tricuspid E/A ratio	0.74 ± 0.10	0.80 ± 0.18	0.011
Mitral E deceleration time (ms)	87 ± 34	97 ± 27	0.063
Tricuspid E deceleration time (ms)	83 ± 30	91 ± 26	0.086
Mitral E' (cm/s)	7.9 ± 1.8	6.8 ± 1.4	0.001
Tricuspid E' (cm/s)	8.7 ± 1.5	7.9 ± 1.4	0.018
Mitral E/E'	4.8 ± 1.3	5.4 ± 1.4	0.002
Tricuspid E/E'	4.9 ± 1.1	5.6 ± 1.5	<0.001
Isovolumic relaxation time (ms)	46 ± 8	52 ±8	<0.001

Data shown as mean ± SD. P-value of IUGR compared with controls, calculated by linear regression adjusted by gestational age at delivery, preeclampsia and gender. IUGR, intrauterine growth restriction; BPM, beats per minute; MAPSE, mitral annular plane systolic excursion; TAPSE, tricuspid annular plane systolic excursion; S', systolic peak velocity; E', early-diastole peak velocity.

Table 3. Anthropometric and vascular characteristics at 6 months of age.

	Controls (n=100)	IUGR (n=100)	Adjusted p-value
Age at assessment (months)	6.5 ± 0.5	6.4 ± 0.6	0.202
Male (%)	47	57	0.203
Heart rate (BPM)	133 ± 12	132 ± 12	0.556
Anthropometric characteristics			
Height (cm)	67.8 ± 2.7	64.7 ± 2.7	<0.001
Weight (grams)	7722 ± 722	6800 ± 900	<0.001
Body mass index (Kg/m2)	16.9 ± 1.9	16.2 ± 1.7	0.007
Body surface area (m2)	0.36 ± 0.02	0.33 ± 0.03	<0.001
Blood pressure			
Systolic blood pressure (mmHg)	76 ± 11	86 ± 8	<0.001
Systolic blood pressure above 95th centile (%)	0	2	0.646
Diastolic blood pressure (mmHg)	54 ± 8	64 ± 8	<0.001
Diastolic blood pressure above 95th centile (%)	3	41	<0.001
Mean blood pressure (mmHg)	61 ± 8	71 ± 7	<0.001
Mean blood pressure above 95th centile (%)	5	41	0.002
aIMT			
Mean aIMT (mm)	0.485 ± 0.066	0.569 ± 0.065	<0.001
Maximum aIMT (mm)	0.564 ± 0.071	0.665 ± 0.070	<0.001
Maximum aIMT above 75th centile (%)	25	73	<0.001

Data shown as mean ± SD or percentage. P-value calculated by Student's t test or $\chi 2$ test where appropriate. Blood pressure and aIMT p values calculated by linear regression adjusting by gestational age at delivery, preeclampsia, gender, body mass index and body surface area. IUGR, intrauterine growth restriction; BPM, beats per minute; aIMT, aortic intima-media thickness.

Table 4. Univariate analysis to assess the association between perinatal and fetal echocardiographic parameters with hypertension and arterial remodeling at 6 months of age in IUGR cases.

Study population: IUGR cases (n=100)

Hypertension and arterial remodeling defined as mean blood pressure above 95th centile and aortic intima media above 75th centile at 6 months of age (31%).

	Odds Ratio	95% CI	p
Standard perinatal parameters			
Gestational age at delivery (weeks)$^{-1}$	1.3	1.1 – 1.4	0.051
Birth weight centile^{-1}	1.2	0.9 – 1.4	0.054
Mean uterine artery PI (z-score)	1.4	1.0 – 1.9	0.022
Umbilical artery PI (z-score)	1.6	1.2 – 2.1	0.002
Middle cerebral artery PI (z-score)$^{-1}$	1.8	1.1 – 2.8	0.014
Cerebroplacental ratio (z-score)$^{-1}$	1.8	1.3 – 2.6	0.001
Ductus venosus PI (z-score)	1.4	0.9 – 1.9	0.106
Aortic isthmus PI (z-score)	1.0	0.9 – 1.1	0.186
Fetal echocardiographic parameters			
Cardiac morphometry			
Cardiothoracic ratio	2.3	1.5 – 3.6	<0.001
Left atrial area (cm2)	2.3	1.5 – 3.7	<0.001
Right atrial area (cm2)	2.4	1.6 – 3.8	<0.001
Left sphericity index^{-1}	3.9	2.1 – 7.0	<0.001
Right sphericity index^{-1}	5.6	2.6 – 12.1	<0.001
Left wall thickness (mm)	1.3	1.1 – 1.4	<0.001
Right wall thickness (mm)	1.3	1.1 – 1.4	<0.001
Interventricular septum thickness (mm)	1.3	1.1 – 1.4	<0.001
Systolic function			
Left ejection fraction (%)	1.0	0.9 – 1.1	0.890
Right ejection fraction (%)	0.9	0.9 – 1.1	0.928
Left stroke volume (mL)	0.9	0.6 – 1.2	0.402
Left cardiac output (mL/min)	0.9	1.0 – 1.0	0.309
Right stroke volume (mL)	0.7	0.5 – 1.1	0.085
Right cardiac output (mL/min)	1.0	1.0 – 1.0	0.058
Cardiac index (mL/min/Kg)	0.9	0.9 – 1.0	0.093
MAPSE (z-score)$^{-1}$	2.2	1.4 – 3.8	0.001
TAPSE (z-score)$^{-1}$	10.2	4.2 – 36.1	<0.001
Mitral S' (z-score)$^{-1}$	3.0	1.2 – 6.4	0.012
Tricuspid S' (z-score)$^{-1}$	7.5	1.4 – 35.2	0.041
Isovolumic contraction time (z-score)	1.7	1.1 – 2.7	0.028
Ejection time (z-score)$^{-1}$	2.5	1.6 – 3.9	0.001
Diastolic function			
Mitral E/A ratio	3.5	2.1 – 6.1	<0.001

Tricuspid E/A ratio	3.0	1.7 – 4.9	<0.001
Mitral E deceleration time (ms)	1.0	1.0 – 1.1	<0.001
Tricuspid E deceleration time (ms)	1.0	1.0 – 1.1	<0.001
Mitral E' (z-score)$^{-1}$	1.6	1.2 – 2.1	<0.001
Tricuspid E' (z-score)	1.2	1.0 – 1.5	0.096
Mitral lateral E/E' (z-score)	1.1	0.8 – 1.4	0.642
Tricuspid E/E' (z-score)	0.8	0.6 – 1.0	0.036
Isovolumic relaxation time (z-score)	2.4	1.4 – 3.9	<0.001

IUGR, intrauterine growth restriction; PI, pulsatility index; MAPSE, mitral annular plane systolic excursion; TAPSE, tricuspid annular plane systolic excursion; S', systolic peak velocity; E', early-diastole peak velocity.

6. RESULTS

6. RESULTS

6.1 Study 1: Value of annular M-mode displacement *vs* tissue Doppler velocities to assess cardiac function in intrauterine growth restriction.

Baseline characteristics were similar in cases and controls, with the exception of higher maternal smoking prevalence in the IUGR group as compared to controls. Gestational age at ultrasound was similar in both populations, while all fetoplacental Doppler parameters showed significant worse values in the IUGR group, as expected. Also as expected, the growth restricted group showed significantly higher prevalence of preeclampsia, lower birth weight centile, and longer neonatal hospitalization in the neonatal intensive care unit. Almost all IUGR fetuses where delivered by cesarean section with a non-significant trend to worse 5-minute Apgar scores and umbilical artery pH. IUGR showed 26% perinatal mortality and 65% morbidity.

Absolute values of left, right and septal annular peak velocities by TDI and displacement by M-mode are shown in Table 6.1.1. Both TDI and M-mode measurements were significantly lower in IUGR fetuses when compared to controls, with predominant differences observed in the tricuspid annulus in comparison to other areas. Table 6.1.2 shows all measurements normalized by cardiac longitudinal (apex-to-base) diameter. When adjusted by cardiac size, only TDI A' peak velocities, MAPSE and TAPSE showed a statistically significant difference between groups, although there was a trend to lower values for all parameters evaluated. Mean differences between controls and cases' z-scores showed that M-mode measurements had similar performance in demonstrating differences between the two groups, as compared to TDI.

Table 6.1.1. Fetal cardiac longitudinal annular motion results by TDI and M-mode in control and IUGR.

	Controls n = 46	IUGR n = 23	*p* value
Annular peak velocities by TDI			
Left E' (cm/s)	7.4 ± 0.9	6.2 ± 1.3	*<0.001*
Left A' (cm/s)	8.4 ± 1.5	6.7 ± 1.1	*<0.001*
Left S' (cm/s)	6.9 ± 0.6	5.7 ± 1.2	*<0.001*
Right E' (cm/s)	8.3 ± 0.8	6.9 ± 1.5	*<0.001*
Right A' (cm/s)	11.9 ± 0.8	9.1 ± 1.6	*<0.001*
Right S' (cm/s)	7.6 ± 1.0	6.9 ± 1.7	*0.016*
Septal E' (cm/s)	6.8 ± 1.5	5.2 ± 1.3	*<0.001*
Septal A' (cm/s)	6.8 ± 0.8	6.2 ± 1.4	*<0.001*
Septal S' (cm/s)	5.5 ± 0.8	5.2 ± 1.0	*<0.001*
Annular displacement by M-mode			
MAPSE (mm)	5.5 ± 0.8	3.9 ± 1.2	*<0.001*
TAPSE (mm)	7.6 ± 0.9	5.2 ± 1.5	*<0.001*
SAPSE (mm)	4.2 ± 0.8	3.2 ± 0.8	*0.004*

Data expressed as mean ± SD.

Table 6.1.2. Fetal cardiac longitudinal annular motion results by TDI and M-mode in control and IUGR. Data is shown as a ratio, (measurement/cardiac longitudinal diameter).

	Controls n = 46	IUGR n = 23	*p* value
Annular peak velocities by TDI			
Left E'	2.16 ± 0.49	1.95 ± 0.49	*0.356*
Left A'	2.74 ± 0.74	2.14 ± 0.44	*0.004*
Left S'	2.02 ± 0.28	1.83 ± 0.50	*0.102*
Right E'	2.44 ± 0.44	2.25 ± 0.47	*0.215*
Right A'	3.29 ± 0.57	2.91 ± 0.53	*0.013*
Right S'	2.24 ± 0.41	2.26 ± 0.59	*0.872*
Septal E'	1.83 ± 0.33	1.72 ± 0.52	*0.584*
Septal A'	2.35 ± 0.39	2.01 ± 0.46	*0.011*
Septal S'	1.83 ± 0.27	1.68 ± 0.38	*0.213*
Annular displacement by M-mode			
MAPSE	1.39 ± 0.24	1.23 ± 0.32	*0.045*
TAPSE	1.86 ± 0.33	1.63 ± 0.38	*0.009*
SAPSE	1.13 ± 0.24	0.98 ± 0.18	*0.067*

Data expressed as mean ± SD.

Figure 6.1. Measurement of longitudinal-axis motion in the right fetal heart by tissue Doppler and M-mode.

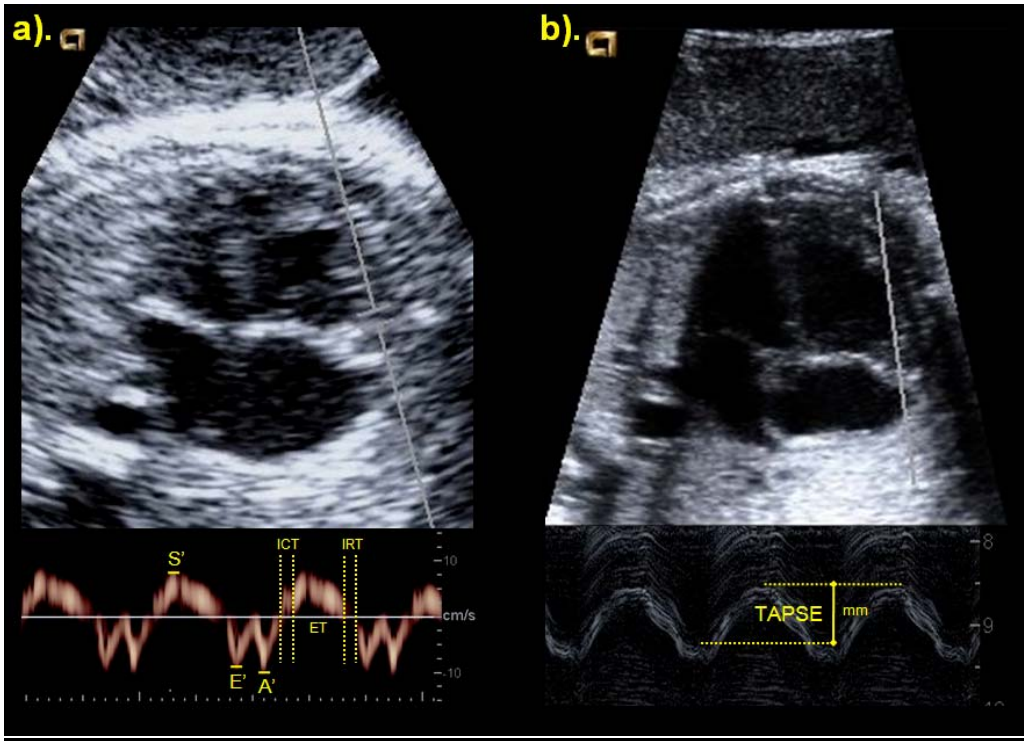

a) Tissue Doppler annular peak velocities for early diastole (E'), atrial contraction (A') and systole (S') in centimeters per second. Components for the myocardial performance index (MPI') are also shown.

b) M-mode TAPSE (tricuspid annular plane systolic excursion) in millimeters.

6.2 Study 2: Feasibility and reproducibility of a standard protocol for 2D speckle tracking and tissue Doppler-based strain and strain rate analysis of the fetal heart.

In this population, most pregnant women were Caucasian and non-smokers. Mean gestational age at scan was 30.5 weeks. The prevalence of preeclampsia was 7% and IUGR 21%, with a mean gestational age at delivery of 38 weeks.

TDI

Strain and strain-rate measurements were feasible in 93% of the acquisitions. A proper acquisition could not be performed in 5 fetuses due to fetal position, oligohydramnios or maternal adiposity. Mean frame rate was 185 fps (range 158-238 fps). Mean frame rate/heart rate ratio was 1.34 (range 1.07-1.75). Mean time spent analyzing TDI images was 18 minutes (range 14-25 minutes) per fetus. Intra- and inter-observer agreement coefficients are shown in Tables 6.2.1 and 6.2.2 respectively. A Bland Altman plot of the difference versus the mean of the paired measurements between observers is presented in Figure 6.2.1.

2D-strain

Strain and strain-rate measurements were feasible from 93% of the acquisitions. A proper acquisition could not be performed in 5 fetuses due to fetal position or maternal adiposity. Mean frame rate was 109 fps (range 72-158 fps). Mean frame rate/heart rate ratio was 0.79 (range 0.48-1.22). Mean time spent for 2D-strain analysis was 15 minutes (range 12-22 minutes) per fetus. Intra- and inter-observer agreement coefficients are shown in Tables 6.2.1 and 6.2.2 respectively. A Bland Altman plot of the difference versus the mean of the paired measurements between observers is presented in Figure 6.2.2.

Correlation between TDI and 2D-strain

There was a non-significant correlation between TDI and 2D-strain derived parameters (Figure 6.2.3) with R^2 values ranging from 0.002 to 0.079.

Table 6.2.1. Intra-observer reliability of longitudinal peak systolic strain and strain-rate by TDI and 2D-strain of the fetal heart.

	Strain	Strain-rate
TDI		
Basal left free wall	0.86 (0.77-0.92)	0.83 (0.72-0.90)
Basal right free wall	0.96 (0.93-0.98)	0.86 (0.76-0.92)
Basal septum	0.96 (0.93-0.98)	0.94 (0.89-0.96)
2D-strain		
Global left ventricle	0.93 (0.88-0.96)	0.82 (0.70-0.89)
Basal left free wall	0.97 (0.95-0.98)	0.94 (0.89-0.96)
Basal left septal wall	0.93 (0.88-0.96)	0.89 (0.82-0.94)
Global right ventricle	0.89 (0.82-0.93)	0.84 (0.73-0.90)
Basal right free wall	0.96 (0.93-0.98)	0.84 (0.73-0.90)
Basal right septal wall	0.95 (0.91-0.97)	0.91 (0.84-0.94)

Data are intraclass coefficient (95% confidence interval). TDI, tissue Doppler imaging; 2D-strain, 2D speckle tracking imaging.

Table 6.2.2. Inter-observer reliability of longitudinal peak systolic strain and strain-rate by TDI and 2D-strain of the fetal heart.

	Strain	Strain-rate
TDI		
Basal left free wall	0.85 (0.68-0.92)	0.83 (0.67-0.92)
Basal right free wall	0.91 (0.84-0.95)	0.86 (0.71-0.93)
Basal septum	0.88 (0.79-0.93)	0.80 (0.65-0.89)
2D-strain		
Global left ventricle	0.89 (0.81-0.93)	0.80 (0.67-0.88)
Basal left free wall	0.75 (0.60-0.85)	0.94 (0.90-0.97)
Basal left septal wall	0.82 (0.69-0.89)	0.86 (0.77-0.92)
Global right ventricle	0.87 (0.79-0.93)	0.87 (0.78-0.92)
Basal right free wall	0.90 (0.84-0.94)	0.94 (0.88-0.97)
Basal right septal wall	0.84 (0.74-0.91)	0.92 (0.84-0.95)

Data are intraclass coefficient (95% confidence interval). TDI, tissue Doppler imaging; 2D-strain, 2D speckle tracking imaging.

Figure 6.2.1. Bland–Altman plot of the difference versus the mean of the paired measurements between observers of the tissue Doppler derived parameters of the fetal heart: (A) peak systolic strain in basal left free wall, (B) peak systolic strain-rate in basal left free wall, (C) peak systolic strain in basal right free wall, (D) peak systolic strain-rate in basal right free wall, (E) peak systolic strain in basal septum, (F) peak systolic strain-rate in basal septum.

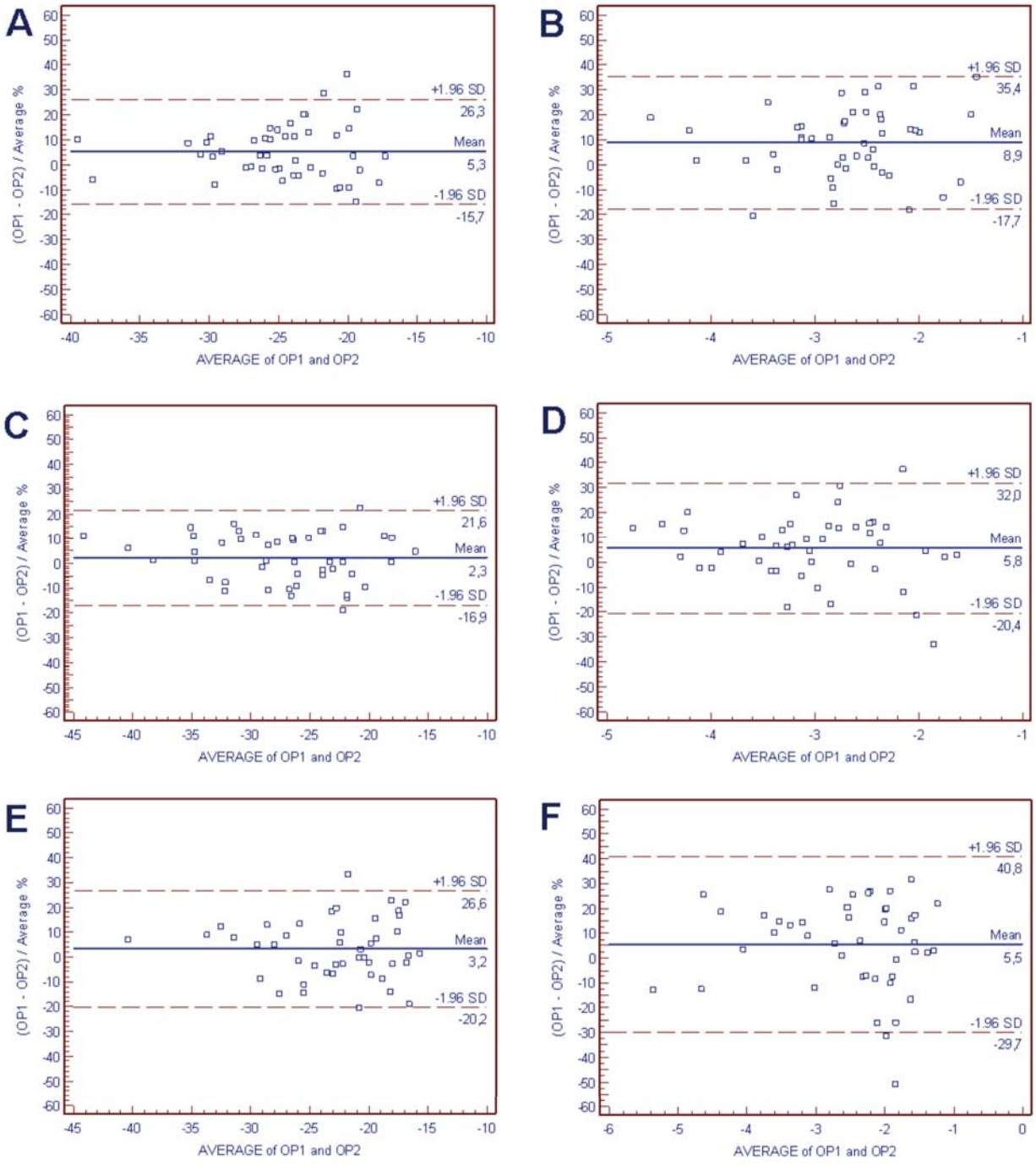

Figure 6.2.2. Bland–Altman plot of the difference versus the mean of the paired measurements between observers of the 2D speckle tracking derived parameters of the fetal heart: (A) global left ventricle peak systolic strain, (B) global left ventricle peak systolic strain-rate, (C) peak systolic strain in basal left free wall, (D) peak systolic strain-rate in basal left free wall, (E) peak systolic strain in basal left septal wall, (F) peak systolic strain-rate in basal left septal wall.

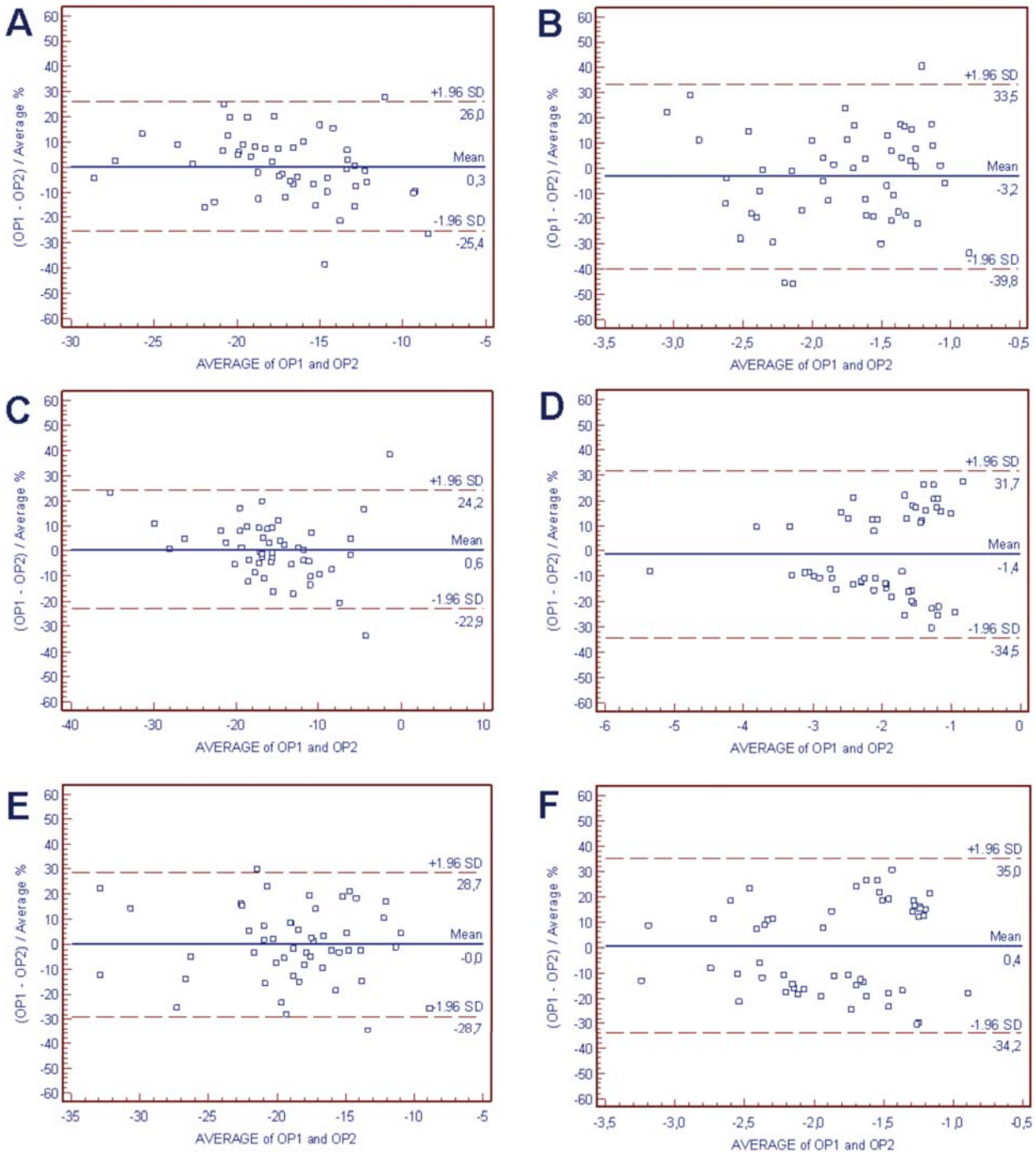

Figure 6.2.2 (cont.) Bland–Altman plot of the difference versus the mean of the paired measurements between observers of the 2D speckle tracking derived parameters of the fetal heart: (G) global right ventricle peak systolic strain, (H) global right ventricle peak systolic strain-rate, (I) peak systolic strain in basal right free wall, (J) peak systolic strain-rate in basal right free wall, (K) peak systolic strain in basal right septal wall, (L) peak systolic strain-rate in basal right septal wall.

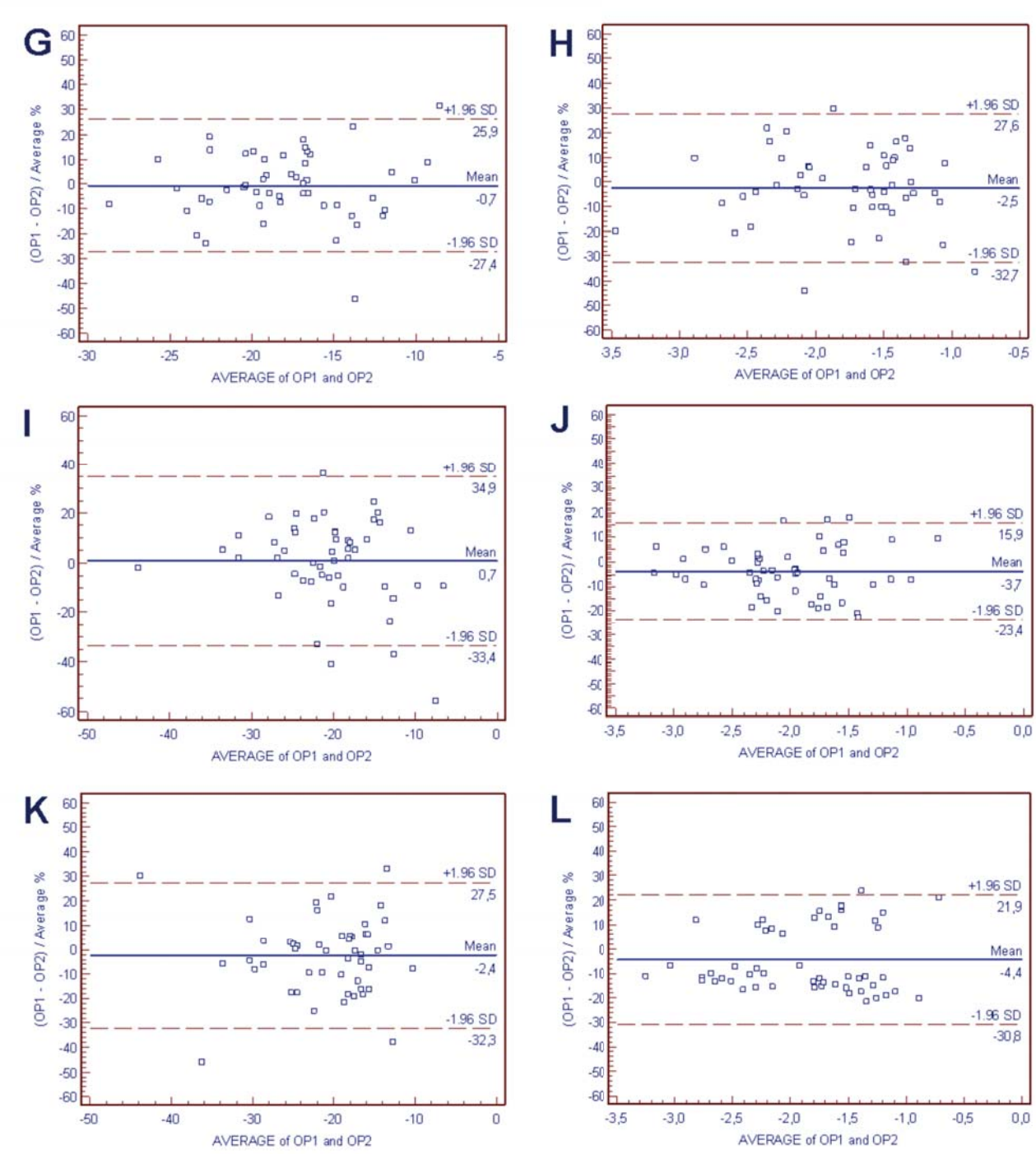

Figure 6.2.3. Correlations comparing tissue Doppler and 2D speckle tracking derived parameters of the fetal heart: (A) peak systolic strain in basal left free wall, (B) peak systolic strain in basal right free wall, (C) peak systolic strain in basal septum, (D) peak systolic strain-rate in basal left free wall, (E) peak systolic strain-rate in basal right free wall, and (F) peak systolic strain-rate in basal septum.

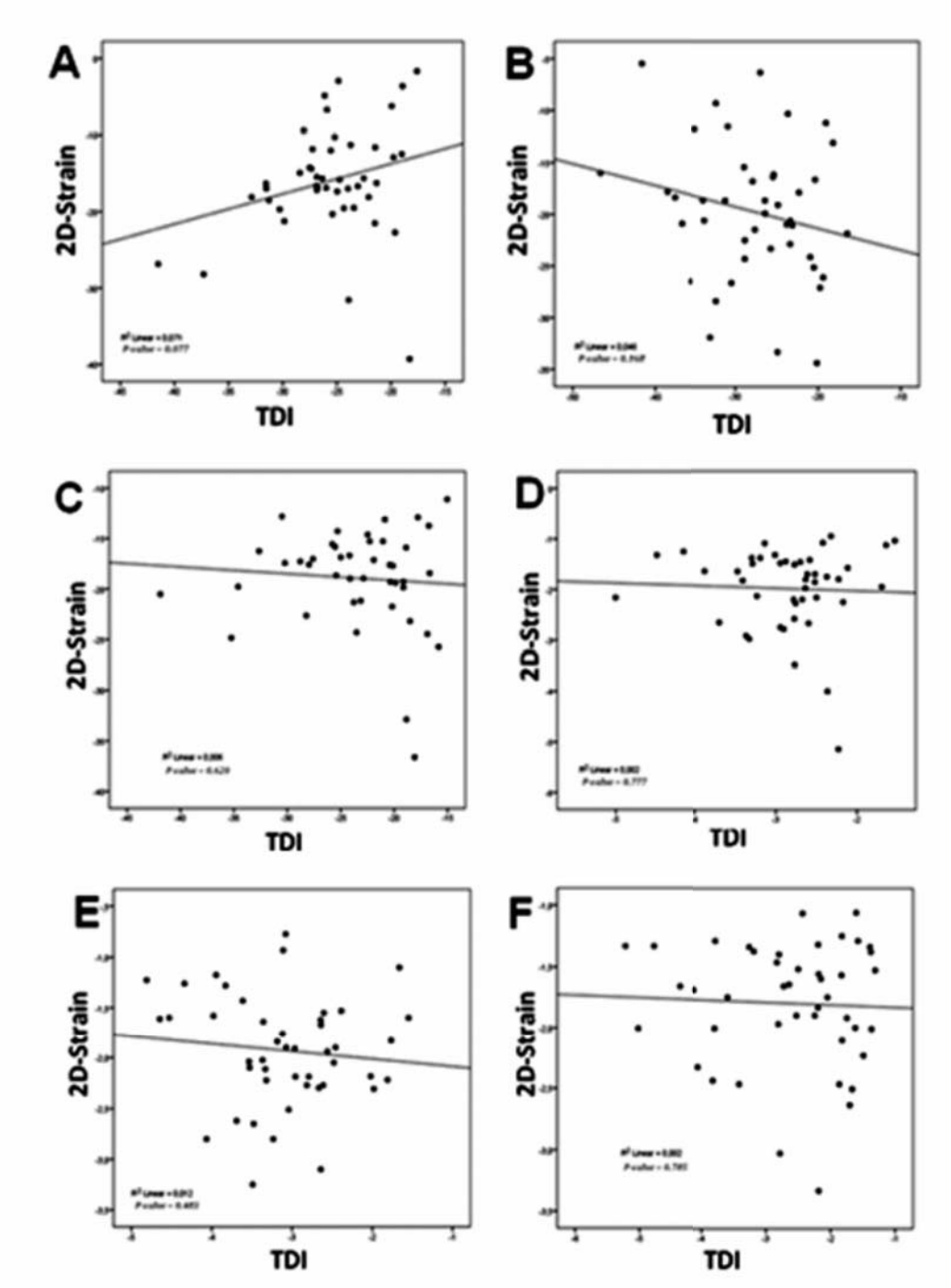

6.3 Study 3: Risk of perinatal death in early-onset intrauterine growth restriction according to gestational age and cardiovascular Doppler indices: a multicenter study.

Median gestational age at delivery was 31 weeks and median birth weight 977 grams. Overall perinatal mortality was 17%, including 15 intrauterine and 12 neonatal deaths. All cases but the stillbirths were delivered by caesarean section.

Univariate analysis demonstrated that UA PI, MCA PI, DV PI and IFI were significantly associated with perinatal mortality; multivariate analysis identified as statistically significant independent predictors for perinatal mortality the UA PI, MCA PI, DV PI and IFI (Table 6.3.1). When gestational age was included in the model and variables were dichotomized as normal/abnormal, gestational age (below 28 weeks), DV atrial flow (RAV), UA end-diastolic flow and MCA PI below 5th centile, significantly and independently accounted for perinatal mortality (Table 6.3.2).

Decision tree analysis was used to determine the best predictive combination of parameters for perinatal mortality (Figure 6.3). As expected, gestational age at delivery was the best initial predictor, with a 93% mortality rate below 26 weeks, 29% between 26-28 weeks and 3% above 28 weeks. For cases between 26 and 28 weeks, characteristics of DV “a” wave (present vs. absent/reversed) allowed discrimination in two groups; 18% mortality rate when it was present against 60% mortality rate when it was absent/reversed.

Table 6.3.1. Individual risk of death in early-onset IUGR fetuses estimated by logistic regression (multivariate analysis).

	Estimated Odds Ratio (95% Confidence Interval)	p-value
UA-PI	1.2 (1.1 to 1.4)	<0.001
MCA-PI	0.4 (0.2 to 0.8)	0.014
DV-PI	1.4 (1.2 to 1.6)	<0.001
IFI	0.9 (0.8 to 0.9)	0.020
MPI	1.1 (0.9 to 1.3)	0.373

PI, pulsatility index; UA, umbilical artery; MCA, middle cerebral artery; DV, ductus venosus; IFI, aortic isthmus flow index; MPI, myocardial performance index.

Table 6.3.2. Individual risk of death in early-onset IUGR fetuses estimated by logistic regression after dichotomization of variables.

	Estimated Odds Ratio (95% Confidence Interval)	p-value
GA <28 weeks	25.2 (8.3 to 76.1)	<0.001
DV-RAV	12.1 (4.1 to 35.6)	<0.001
UA-RAV	10.2 (2.6 to 40.6)	0.001
MCA-PI <p5	5.3 (2.1 to 13.3)	<0.001
IFI <p5	1.8 (0.7 to 4.5)	0.232
MPI >p95	1.6 (0.7 to 3.8)	0.302

GA, gestational age; PI, pulsatility index; RAV, reverse/absent end diastolic/atrial flow; UA, umbilical artery; MCA, middle cerebral artery; DV, ductus venosus; IFI, isthmus flow index; MPI, myocardial performance index.

Figure 6.3. Clinical algorithm for risk of death in early-onset intrauterine growth restricted (IUGR) fetuses, obtained by decision tree analysis. PAV, ductus venosus present atrial flow; RAV, ductus venosus absent/reversed atrial flow.

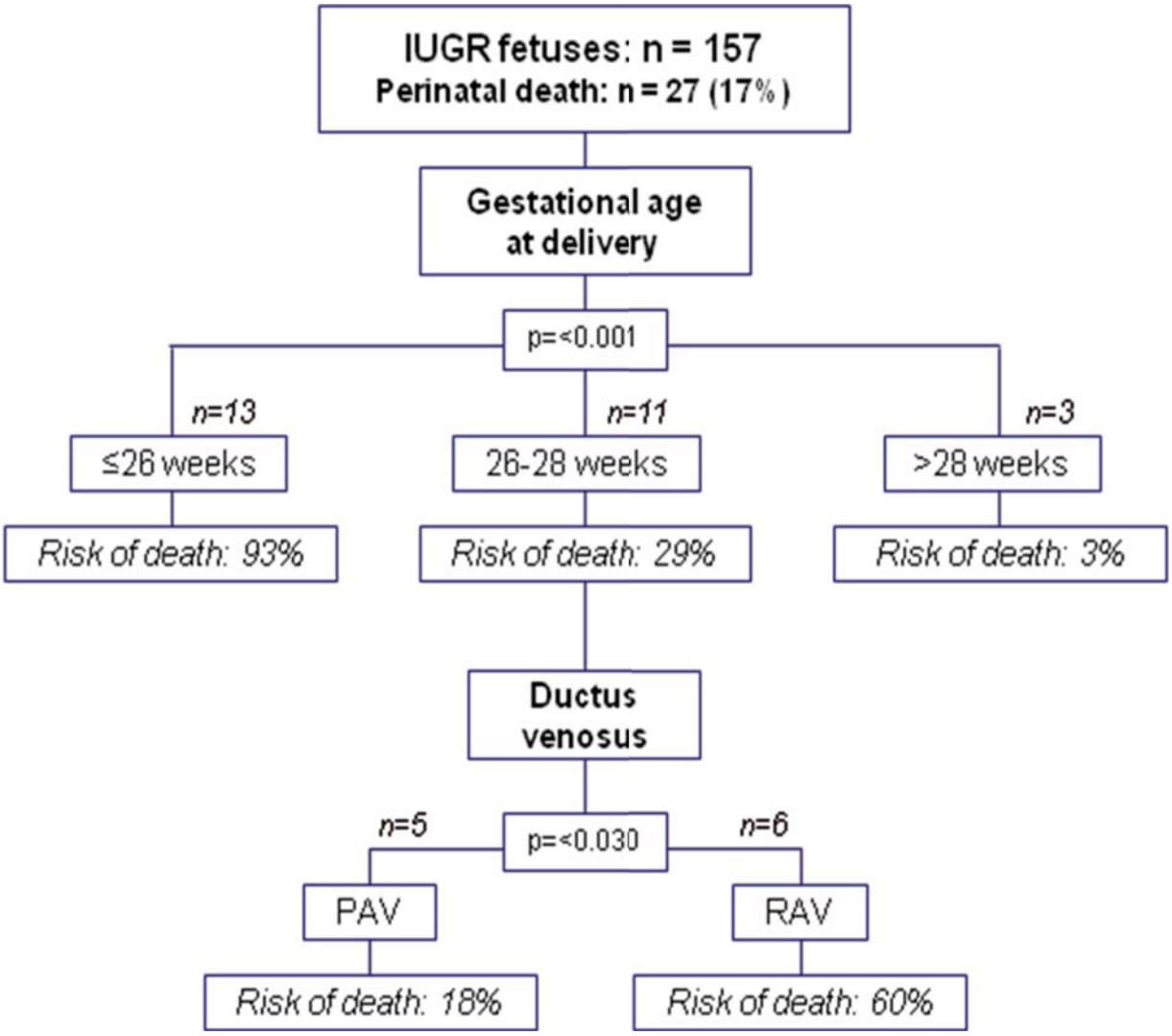

6.4 Study 4: Fetal echocardiography to predict infant hypertension and arterial remodeling in intrauterine growth restriction.

Baseline perinatal and delivery characteristics

Maternal characteristics and gestational age at scan were similar in IUGR cases and controls. As expected, estimated fetal weight and fetoplacental Doppler parameters were significantly worse in the IUGR group. The growth restricted group showed an earlier gestational age at delivery, with lower birth weight centile and worse perinatal outcomes.

Fetal echocardiography

Results of fetal echocardiography in the study groups are shown in Table 6.4.1. Cardiac shape and size showed significant differences between groups. Cardiothoracic ratio and atrial areas were increased in the IUGR fetuses as compared to controls. Left and right sphericity indexes were significantly decreased in IUGR fetuses when compared to controls, with thicker myocardial walls. EF and heart rate showed no differences between groups. Both SV and CO were reduced in the IUGR fetuses, however when corrected by estimated fetal weight (cardiac index), IUGR fetuses showed a trend to higher values as compared to controls. Longitudinal function demonstrated by MAPSE, TAPSE and S' was significantly reduced in the IUGR fetuses as compared to controls. Both the ICT and ET were increased in the IUGR group. Diastolic function parameters also showed differences, with decreased E' velocities and increased E/A and E/E' ratios, IRT and E deceleration times in IUGR fetuses as compared to controls.

Anthropometric and vascular assessment at 6 months of age

IUGR infants showed lower height, weight and body surface area as compared to controls with no significant difference in age at assessment, gender or body mass index. Both systolic and diastolic blood pressures were significantly higher in the IUGR infants, with 2% of cases presenting systolic hypertension and 41% diastolic hypertension. Mean blood pressure was also significantly increased, with 41% infants above the 95th centile. Both mean and maximum aIMT measurements were significantly increased in IUGR infants when compared to controls. Seventy-three percent of the IUGR infants presented maximum aIMT above the 75th centile and thirty-seven percent above the 95th centile.

Prediction of hypertension and arterial remodeling in IUGR cases

We analyzed the association of the different perinatal and echocardiographic parameters for the prediction of infant hypertension and arterial remodeling within the IUGR cases, defined by the presence of both a mean blood pressure above 95th centile and maximum aIMT above the 75th centile. Thirty-one IUGR infants had both criteria present at 6 months of age.

Table 6.4.3 and Figure 6.4.1 show the predictive value (as OR) of fetal parameters for hypertension and arterial remodeling, assessed by univariate regression analysis. Neither gestational age at delivery, nor birth weight centile were predictors of cardiovascular risk factors within the IUGR group. Umbilical, middle cerebral and uterine artery Doppler showed a significant association, however ductus venosus and aortic isthmus showed none. Several fetal echocardiographic parameters were associated with hypertension and arterial remodeling, with morphometric and longitudinal motion parameters having the highest OR: decreased TAPSE (OR 10.2) and lower right sphericity index (OR 5.6) demonstrated the strongest associations.

In order to assess the potential interaction among the different parameters, a multivariate analysis was performed including TAPSE (the parameter showing the strongest association with hypertension and arterial remodeling in the univariate analysis) with other significant predictors of risk. Most parameters continued their associations to cardiovascular risk factors.

Finally, a composite score, based on the best standard perinatal and fetal echocardiographic predictors was generated by combining these variables in a regression analysis. This fetal cardiovascular score comprised of TAPSE (z-score), cerebroplacental ratio (z-score), right sphericity index (crude value) and IVRT (z-score) and yielded the following equation: 1.907 + (TAPSE*-0.589) + (cerebroplacental ratio*-0.286) + (right sphericity index*-1.938) + (IVRT*0.342) ≥0.1253. The equation resulted in 90% sensitivity, 77% specificity, 42% positive predictive value, 98% negative predictive value, 3.9 positive likelihood ratio and 0.1 negative likelihood ratio to detect those IUGR cases with infant hypertension and arterial remodeling. ROC curve analysis was performed to estimate area under the curve for isolated and combined parameters with the highest OR. The average AUC for the fetal cardiovascular score was 0.87 (95% CI 0.80 – 0.92, p<0.001), higher than fetal TAPSE alone (0.64 (95% CI 0.56 – 0.73, p=0.030), fetal EF (0.57 (95% CI 0.48 – 0.65, p=0.072) and perinatal criteria (Figure 6.4.2).

Table 6.4.1. Fetal echocardiography data from the study groups.

	Controls (n=100)	IUGR (n=100)	*p*
Gestational age at evaluation (weeks)	35.3 ± 5.1	35.8 ± 3.6	0.082
Cardiac morphometry			
Cardiothoracic ratio	0.27 ± 0.05	0.33 ± 0.05	<0.001
Left atrial area (cm^2)	1.61 ± 0.62	1.75 ± 0.58	0.004
Right atrial area (cm^2)	1.84 ± 0.76	2.02 ± 0.60	0.003
Left sphericity index	2.06 ± 0.37	1.87 ± 0.42	0.005
Right sphericity index	1.85 ± 0.39	1.57 ± 0.28	<0.001
Left wall thickness (mm)	2.91 ± 0.67	3.48 ± 0.74	<0.001
Right wall thickness (mm)	3.06 ± 0.68	3.63 ± 0.70	<0.001
Interventricular septum (mm)	2.69 ± 0.62	3.38 ± 0.81	<0.001
Systolic function			
Left ejection fraction (%)	70.9 ± 8.8	71.3 ± 9.9	0.843
Right ejection fraction (%)	67.5 ± 8.1	68.5 ± 9.9	0.896
Heart rate (BPM)	140 ± 10	138 ± 12	0.168
Left stroke volume (mL)	4.1 ± 1.7	3.3 ± 1.5	0.107
Left cardiac output (mL/min)	559 ± 236	449 ± 195	0.116
Right stroke volume (mL)	4.8 ± 1.8	4.3 ± 1.9	0.018
Right cardiac output (mL/min)	667 ± 228	593 ± 260	0.018
Cardiac index (mL/min/Kg)	498 ± 145	536 ± 162	0.086
MAPSE (mm)	5.5 ± 1.3	5.0 ± 1.1	0.014
TAPSE (mm)	7.2 ± 1.3	6.6 ± 1.3	0.018
Mitral S' (cm/s)	7.1 ± 1.3	6.2 ± 1.1	0.010
Tricuspid S' (cm/s)	7.9 ± 1.4	7.4 ± 1.3	<0.001
Isovolumic contraction time (ms)	29 ± 4	36 ± 8	<0.001
Ejection time (ms)	171 ± 10	158 ± 11	<0.001
Diastolic function			
Mitral E/A ratio	0.74 ± 0.13	0.81 ± 0.15	0.002
Tricuspid E/A ratio	0.74 ± 0.10	0.80 ± 0.18	0.011
Mitral E deceleration time (ms)	87 ± 34	97 ± 27	0.063
Tricuspid E deceleration time (ms)	83 ± 30	91 ± 26	0.086
Mitral E' (cm/s)	7.9 ± 1.8	6.8 ± 1.4	0.001
Tricuspid E' (cm/s)	8.7 ± 1.5	7.9 ± 1.4	0.018
Mitral E/E'	4.8 ± 1.3	5.4 ± 1.4	0.002
Tricuspid E/E'	4.9 ± 1.1	5.6 ± 1.5	<0.001
Isovolumic relaxation time (ms)	46 ± 8	52 ±8	<0.001

Data shown as mean ± SD. P-value of IUGR compared with controls, calculated by linear regression adjusted by gestational age at delivery, preeclampsia and gender. IUGR, intrauterine growth restriction; BPM, beats per minute; MAPSE, mitral annular plane systolic excursion; TAPSE, tricuspid annular plane systolic excursion; S', systolic peak velocity; E', early-diastole peak velocity.

Table 6.4.2. Anthropometric and vascular characteristics at 6 months of age.

	Controls (n=100)	IUGR (n=100)	*p*
Age at assessment (months)	6.5 ± 0.5	6.4 ± 0.6	0.562
Male (%)	47	57	0.117
Heart rate (BPM)	133 ± 12	132 ± 12	0.855
Anthropometric characteristics			
Height (cm)	67.8 ± 2.7	64.7 ± 2.7	<0.001
Weight (grams)	7722 ± 722	6800 ± 900	<0.001
Body mass index (Kg/m^2)	16.9 ± 1.9	16.2 ± 1.7	0.078
Body surface area (m^2)	0.36 ± 0.02	0.33 ± 0.03	<0.001
Blood pressure			
Systolic blood pressure (mmHg)	76 ± 11	86 ± 8	<0.001
Systolic blood pressure above 95th centile (%)	0	2	0.646
Diastolic blood pressure (mmHg)	54 ± 8	64 ± 8	<0.001
Diastolic blood pressure above 95th centile (%)	3	41	<0.001
Mean blood pressure (mmHg)	61 ± 8	71 ± 7	<0.001
Mean blood pressure above 95th centile (%)	5	41	0.002
aIMT			
Mean aIMT (mm)	0.485 ± 0.066	0.569 ± 0.065	<0.001
Maximum aIMT (mm)	0.564 ± 0.071	0.665 ± 0.070	<0.001
Maximum aIMT above 75th centile (%)	25	73	<0.001

Data shown as mean ± SD or percentage. P-value calculated by linear regression adjusted by gestational age at delivery, preeclampsia, gender and body surface area. IUGR, intrauterine growth restriction; BPM, beats per minute; aIMT, aortic intima-media thickness.

Table 6.4.3. Univariate analysis to assess the association between perinatal and fetal echocardiographic parameters with hypertension and arterial remodeling at 6 months of age in IUGR cases.

Study population: IUGR cases (n=100)
Hypertension and arterial remodeling defined as mean blood pressure above 95th centile and aortic intima media above 75th centile at 6 months of age (31%).

	Odds Ratio	95% CI	*p*
Standard perinatal parameters			
Gestational age at delivery (weeks) $^{-1}$	1.3	1.1 – 1.4	0.051
Birth weight centile^{-1}	1.2	0.9 – 1.4	0.054
Mean uterine artery PI (z-score)	1.4	1.0 – 1.9	0.022
Umbilical artery PI (z-score)	1.6	1.2 – 2.1	0.002
Middle cerebral artery PI (z-score)$^{-1}$	1.8	1.1 – 2.8	0.014
Cerebroplacental ratio (z-score) $^{-1}$	1.8	1.3 – 2.6	0.001
Ductus venosus PI (z-score)	1.4	0.9 – 1.9	0.106
Aortic isthmus PI (z-score)	1.0	0.9 – 1.1	0.186
Fetal echocardiographic parameters			
Cardiac morphometry			
Cardiothoracic ratio	2.3	1.5 – 3.6	<0.001
Left atrial area (cm^2)	2.3	1.5 – 3.7	<0.001
Right atrial area (cm^2)	2.4	1.6 – 3.8	<0.001
Left sphericity index^{-1}	3.9	2.1 – 7.0	<0.001
Right sphericity index^{-1}	5.6	2.6 – 12.1	<0.001
Left wall thickness (mm)	1.3	1.1 – 1.4	<0.001
Right wall thickness (mm)	1.3	1.1 – 1.4	<0.001
Interventricular septum thickness (mm)	1.3	1.1 – 1.4	<0.001
Systolic function			
Left ejection fraction (%)	1.0	0.9 – 1.1	0.890
Right ejection fraction (%)	0.9	0.9 – 1.1	0.928
Left stroke volume (mL)	0.9	0.6 – 1.2	0.402
Left cardiac output (mL/min)	0.9	1.0 – 1.0	0.309
Right stroke volume (mL)	0.7	0.5 – 1.1	0.085
Right cardiac output (mL/min)	1.0	1.0 – 1.0	0.058
Cardiac index (mL/min/Kg)	0.9	0.9 – 1.0	0.093
MAPSE (z-score) $^{-1}$	2.2	1.4 – 3.8	0.001
TAPSE (z-score) $^{-1}$	10.2	4.2 – 36.1	<0.001
Mitral S' (z-score) $^{-1}$	3.0	1.2 – 6.4	0.012
Tricuspid S' (z-score) $^{-1}$	7.5	1.4 – 35.2	0.041
Isovolumic contraction time (z-score)	1.7	1.1 – 2.7	0.028
Ejection time (z-score) $^{-1}$	2.5	1.6 – 3.9	0.001
Diastolic function			
Mitral E/A ratio	3.5	2.1 – 6.1	<0.001
Tricuspid E/A ratio	3.0	1.7 – 4.9	<0.001
Mitral E deceleration time (ms)	1.0	1.0 – 1.1	<0.001
Tricuspid E deceleration time (ms)	1.0	1.0 – 1.1	<0.001
Mitral E' (z-score) $^{-1}$	1.6	1.2 – 2.1	<0.001
Tricuspid E' (z-score)	1.2	1.0 – 1.5	0.096
Mitral lateral E/E' (z-score)	1.1	0.8 – 1.4	0.642
Tricuspid E/E' (z-score)	0.8	0.6 – 1.0	0.036
Isovolumic relaxation time (z-score)	2.4	1.4 – 3.9	<0.001

IUGR, intrauterine growth restriction; PI, pulsatility index; MAPSE, mitral annular plane systolic excursion; TAPSE, tricuspid annular plane systolic excursion; S', systolic peak velocity; E', early-diastole peak velocity.

Figure 6.4.1. Univariate analysis for the association between standard perinatal and fetal echocardiographic parameters with hypertension and arterial remodeling at 6 months of age. Fetal parameters included as z-scores when available. Odds ratio and 95% confidence intervals shown.

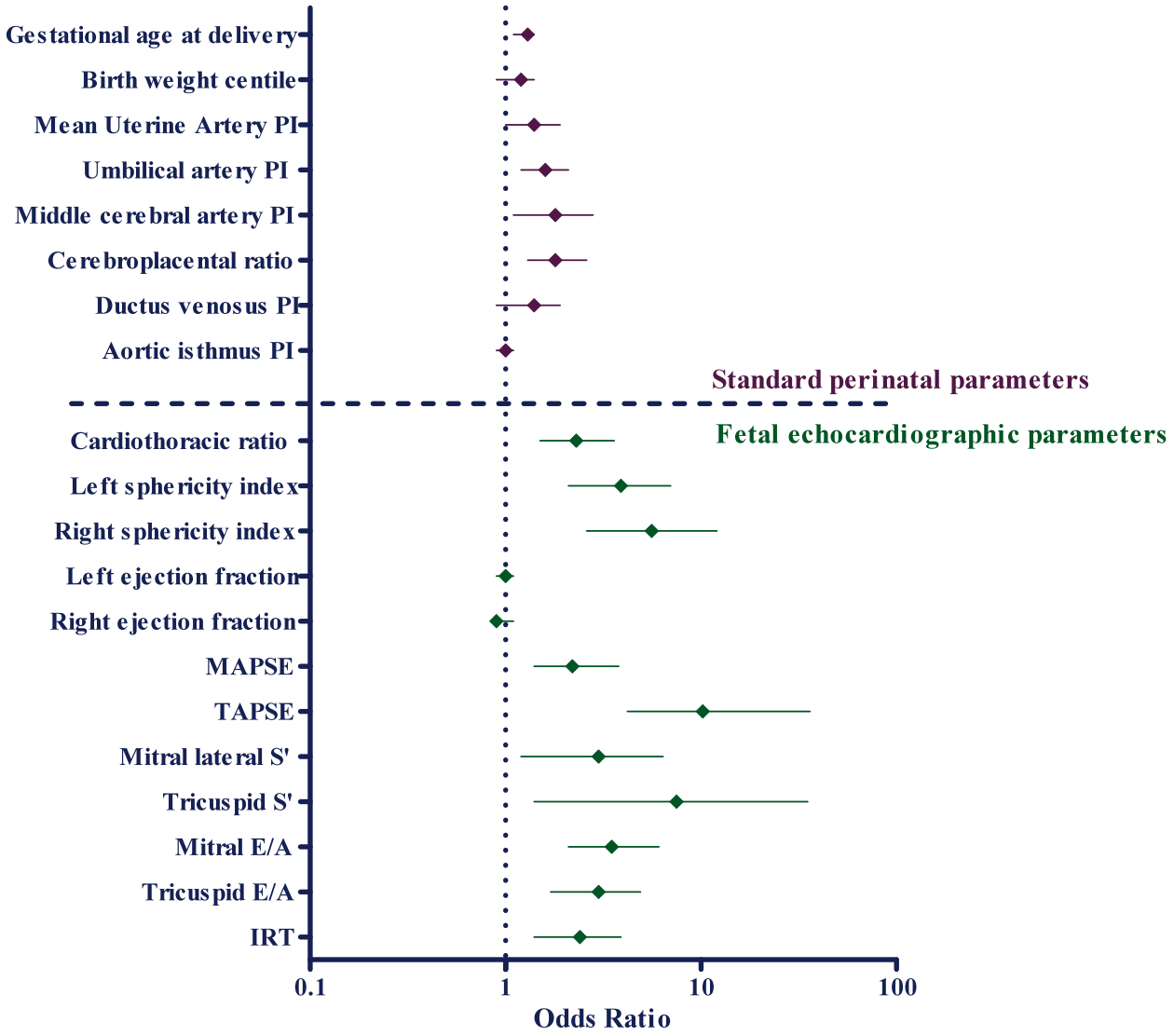

Figure 6.4.2. ROC curves illustrating the predictive value of fetal cardiovascular score (Fetal CV score) compared with (a) TAPSE and ejection fraction, and (b) standard perinatal criteria (gestational age at delivery, birth weight centile and umbilical artery PI) for hypertension and arterial remodeling at 6 month of age.

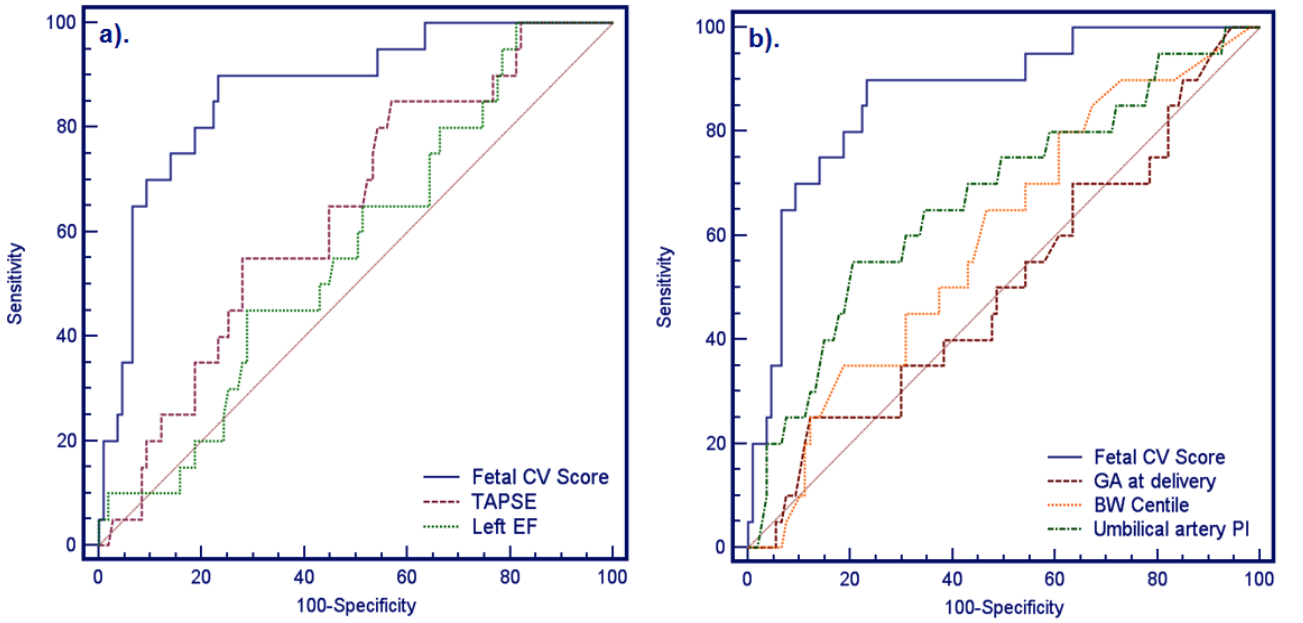

Fetal Cardiovascular Score AUC: 0.87 (95% CI 0.79 – 0.93, p<0.001)
TAPSE AUC: 0.64 (95% CI 0.56 – 0.73, p=0.030)
Left ejection fraction AUC: 0.57 (95% CI 0.48 – 0.65, p=0.072)

Fetal Cardiovascular Score AUC: 0.87 (95% CI 0.79 – 0.93, p<0.001)
GA at delivery AUC: 0.51 (95% CI 0.42 – 0.60, p=0.070)
Birthweight centile AUC: 0.60 (95% CI 0.51 – 0.68, p=0.066)
Umbilical artery PI AUC: 0.67 (95% CI 0.59 – 0.75, p=0.070)

Fetal CV Score [1.907 + (TAPSE*-0.589) + (CPR*-0.286) + (RSI*-1.938) + (IRT*0.342)]

Figure 6.4.2. Illustration showing the components of the fetal cardiovascular score for prediction of infant hypertension and arterial remodeling.

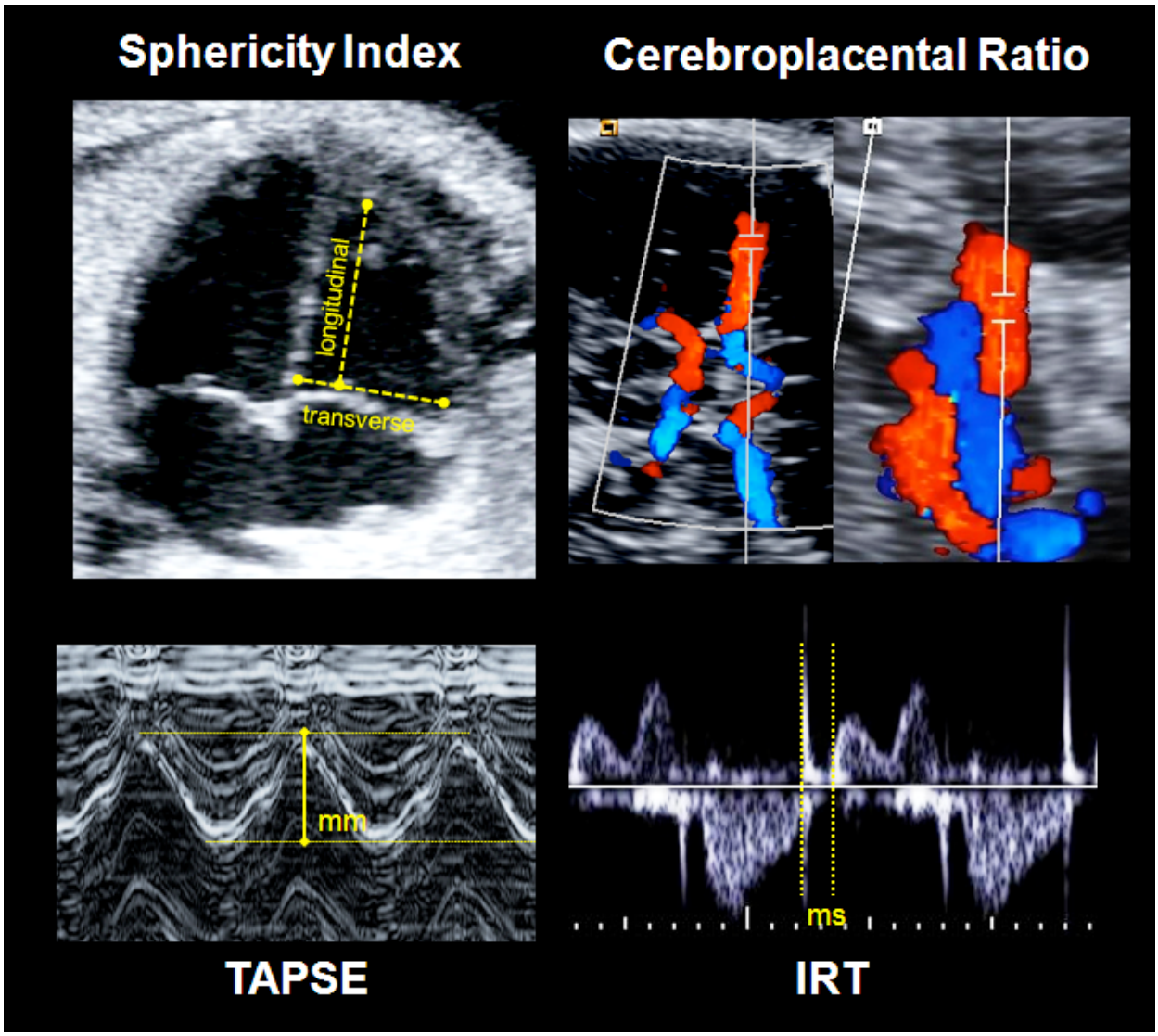

TAPSE, tricuspid annular plane systolic excursion; IRT, isovolumetric relaxation time

6.5 Study 5 (unpublished data): Infant echocardiography.

Anthropometric and vascular assessment at 6 months of age

The study population was the same for ***study 4***; baseline characteristics and vascular data of these are shown in table 6.4.2. IUGR infants showed lower height, weight and body surface area as compared to controls with no significant difference in age at assessment, gender or body mass index. Both systolic and diastolic blood pressures were significantly higher in the IUGR infants, with 2% of cases presenting systolic hypertension and 41% diastolic hypertension. Mean blood pressure was also significantly increased, with 41% infants above the 95th centile. Both mean and maximum aIMT measurements were significantly increased in IUGR infants when compared to controls. Seventy-three percent of the IUGR infants presented maximum aIMT above the 75th centile and thirty-seven percent above the 95th centile.

Infant echocardiography

Results of infant echocardiography in the study groups are shown in Table 6.5.1. Systolic function parameters such as stroke volume and cardiac output showed no differences between groups; left shortening and ejection fractions were higher in the IUGR group. Longitudinal parameters MAPSE, TAPSE and S' peak velocities were all significantly decreased in the IUGR group with respect to controls. Diastolic function parameters such as the IRT or transvalvular filling A velocities were higher in the IUGR group, while all tissue Doppler velocities E' and A' were significantly decreased. Cardiac shape and size showed significant differences between groups. Atrial areas were increased in the IUGR infants as compared to controls, and left sphericity index was significantly decreased, with thicker myocardial walls.

Table 6.5.1. Echocardiographic evaluation at 6 months of age.

	Controls (n=100)	IUGR (n=100)	*p*	*Adjusted P values*
Systolic function				
Left ventricle				
Heart rate (bpm)	134 ± 13	132 ± 12	0.255	0.815
Left stroke volume (mL)	18.1 ± 5.1	20.2 ± 6.9	0.035	0.335
Left cardiac output (L/min)	2.4 ± 0.7	2.7 ± 0.9	0.057	0.253
Normalized left cardiac output (L/min/m^2)*	6.6 ± 1.8	7.9 ± 2.9	0.001	0.097
Left ejection fraction (%)	65.5 ± 8.1	68.4 ± 9.8	0.048	0.017
Left shortening fraction (%)	34.3 ± 6.4	37.0 ± 7.7	0.020	0.018
MAPSE (mm)	10.8 ± 1.9	9.8 ± 1.5	<0.001	0.011
Normalized MAPSE (mm/√BSA)	17.9 ± 3.2	16.9 ± 2.7	0.021	0.027
Mitral lateral S' peak velocity (cm/s)	7.1 ± 1.3	6.3 ± 1.1	<0.001	0.045
Mitral septal S' peak velocity (cm/s)	6.3 ± 1.1	5.7 ± 0.9	<0.001	0.036
Right ventricle				
Right stroke volume (mL)	14.3 ± 3.8	12.9 ± 4.4	0.036	0.128
Right cardiac output (L/min)	1.9 ± 0.5	1.7 ± 0.5	0.010	0.095
Normalized right cardiac output (L/min/m^2)*	5.3 ± 1.5	4.9 ± 1.6	0.282	0.109
TAPSE (mm)	15.9 ± 1.8	14.2 ± 1.8	<0.001	<0.001
Normalized TAPSE (mm/√BSA)	26.5 ± 3.0	24.5 ± 2.9	<0.001	<0.001
Tricuspid S' peak velocity (cm/s)	7.9 ± 1.4	7.4 ± 1.3	0.029	0.030
Diastolic function				
Left ventricle				
Isovolumetric relaxation time (ms)	50 ± 11	57 ± 10	<0.001	0.028
Mitral E wave velocity (cm/s)	108 ± 18	116 ± 20	0.017	0.079
Mitral A wave velocity (cm/s)	81 ± 16	89 ± 18	0.003	0.029
Mitral E/A ratio	1.37 ± 0.27	1.33 ± 0.30	0.460	0.755
Mitral E deceleration time (ms)	89 ± 28	96 ± 25	0.111	0.716
Mitral A duration time (ms)	98 ± 21	107 ± 23	0.014	0.443
Mitral lateral E' peak velocity (cm/s)	12.9 ± 2.5	11.0 ± 2.1	<0.001	0.057
Mitral lateral A' peak velocity (cm/s)	8.9 ± 3.0	6.9 ± 1.9	<0.001	0.049
Mitral septal E' peak velocity (cm/s)	11.6 ± 2.5	10.3 ± 1.8	<0.001	0.019
Mitral septal A' peak velocity (cm/s)	8.2 ± 2.4	7.3 ± 2.1	0.012	0.014
Mitral E'/E	8.7 ± 2.3	10.7 ± 2.0	<0.001	0.031
Mitral IVRT' (ms)	49 ± 8	50 ± 7	0.090	0.724
Right ventricle				
Tricuspid E wave velocity (cm/s)	70 ± 21	74 ± 16	0.161	0.267
Tricuspid A wave velocity (cm/s)	69 ± 21	77 ± 15	0.004	0.006
Tricuspid E/A ratio	1.07 ± 0.32	0.97 ± 0.20	0.025	0.053
Tricuspid E deceleration time (ms)	89 ± 31	97 ± 27	0.093	0.601
Tricuspid A duration time (ms)	102 ± 25	114 ± 17	0.001	0.699
Tricuspid E' peak velocity (cm/s)	16 ± 4	14 ± 3	0.001	0.046
Tricuspid A' peak velocity (cm/s)	13 ± 4	11 ± 4	0.002	0.034
Tricuspid E'/E	5 ± 2	5 ± 2	0.003	0.183
Tricuspid IVRT' (ms)	45 ± 7	47 ± 7	0.012	0.399

continued…

Table 6.5.1 (cont). Echocardiographic evaluation at 6 months of age.

	Controls (n=100)	IUGR (n=100)	*p*	*Adjusted P values*
Cardiac morphometry				
Left atrial area (cm^2)	3.6 ± 0.9	3.8 ± 0.7	0.092	0.006
Normalized left atrial area (cm^2/BSA)*	9.8 ± 2.3	11.3 ± 1.8	<0.001	0.004
Left sphericity index	1.92 ± 0.28	1.67 ± 0.22	<0.001	0.007
Left ventricular end-diastolic diameter (mm)	23.7 ± 2.9	23.5 ± 3.0	0.631	0.418
Normalized left ventricular end-diastolic diameter (mm/√BSA)	39.4 ± 4.7	40.5 ± 4.9	0.143	0.525
Left ventricular end-systolic diameter (mm)	15.8 ± 2.6	14.9 ± 2.8	0.029	0.032
Normalized left ventricular end-systolic diameter (mm/√BSA)	26.2 ± 4.3	25.6 ± 4.6	0.386	0.085
Left posterior wall thickness (mm)	4.6 ± 0.7	5.1 ± 0.9	0.002	0.019
Normalized left posterior wall thickness (mm/√BSA)	7.6 ± 1.2	8.7 ± 1.8	<0.001	0.027
Interventricular septum thickness (mm)	3.9 ± 0.7	4.6 ± 0.9	<0.001	<0.001
Normalized interventricular septum thickness (mm/√BSA)	6.5 ± 1.2	8.0 ± 1.7	<0.001	<0.001

IUGR, intrauterine growth restriction; MAPSE, mitral annular plane systolic excursion; S', systolic annular peak velocity; TAPSE, tricuspid annular plane systolic excursion; E, peak early transvalvular filling velocity; A, peak late transvalvular filling velocity; E', early diastole annular peak velocity; A', late diastole annular peak velocity; IVRT', isovolumetric relaxation time by tissue Doppler.

*Normalization by body surface area or its square root when appropriate. *P* values adjusted with linear regression for gender, gestational age at delivery, birth weight centile, prenatal glucocorticoid exposure, cesarean section, NICU hospitalization and body surface area.

Figure 6.5.1. Tissue Doppler S' velocities in infant controls and cases.

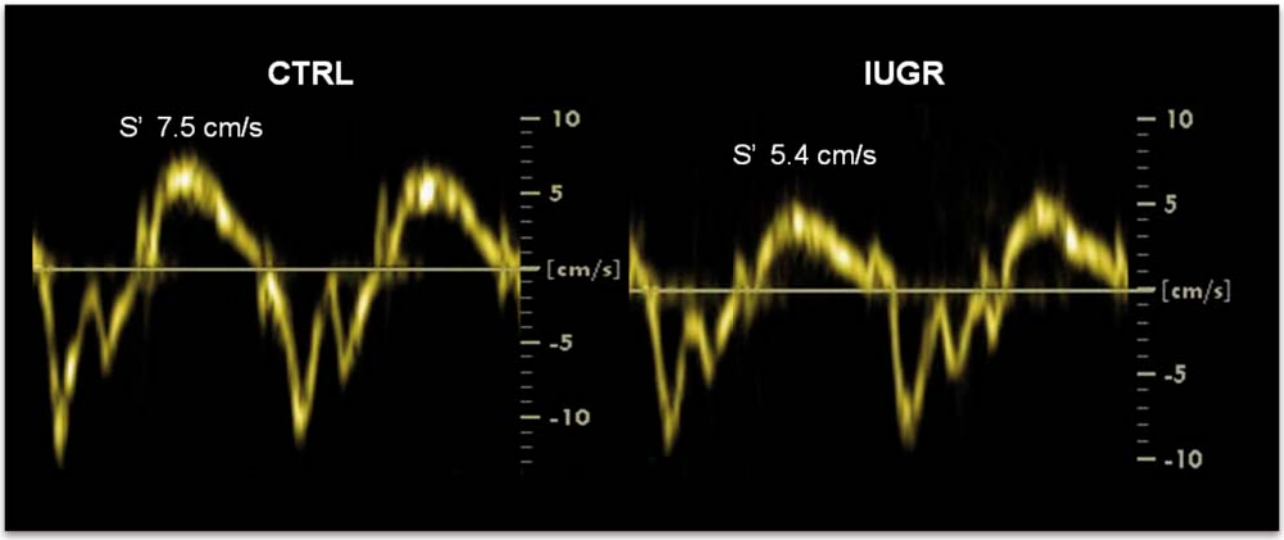

Figure 6.5.2. aIMT in infant controls and cases.

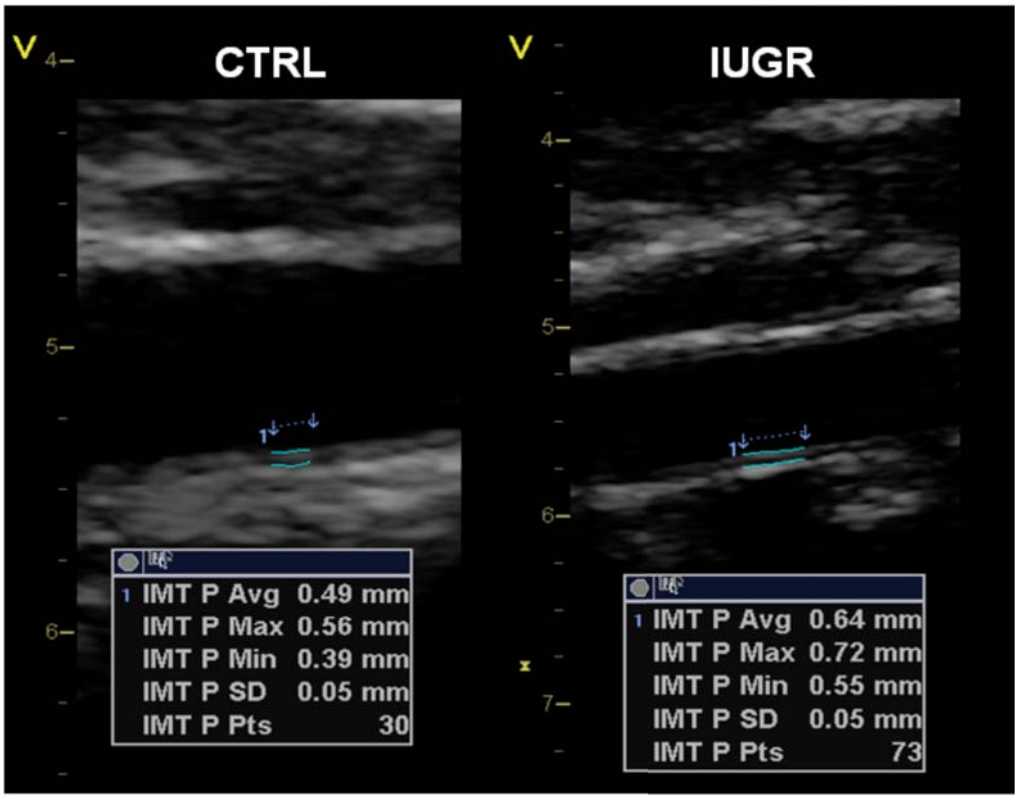

Figure 6.5.3. Left sphericity index in infant controls and cases.

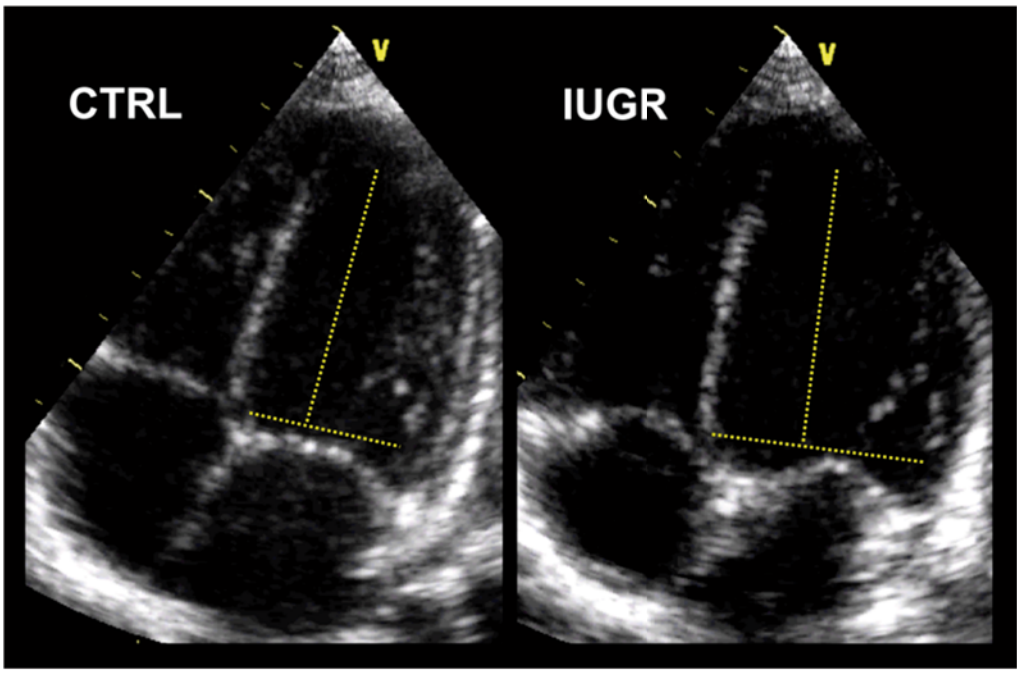

7. DISCUSSION

7. DISCUSSION

This thesis confirms previous studies showing fetal cardiac dysfunction can be documented by fetal echocardiography; it validates different methods for evaluating cardiac function in the fetus and demonstrates the predictive value of these parameters for perinatal and postnatal cardiovascular outcome.

Our **first study** demonstrates for the first time the validity of M-mode to assess longitudinal axis motion in IUGR. It further confirms previous research that IUGR fetuses have a significant decrease in longitudinal myocardial motion, as part of the fetal cardiovascular adaptation to placental insufficiency. These changes can be quantified with TDI or M-mode, but the data suggests that M-mode could be as sensitive as TDI for detecting subtle cardiac dysfunction. To our knowledge, this is the first study which evaluates longitudinal motion with M-mode in IUGR fetuses as a potential tool for describing subclinical cardiac dysfunction in this group. In this study, differences in longitudinal motion were more pronounced by M-mode in the right annulus (TAPSE). This is consistent with previous fetal studies[30, 43], and with the notion that the right ventricle could be more suited to assess longitudinal motion, owing to the longitudinal nature of its fibers as opposed to left ventricle fibers, which are mainly circumferential[50, 103, 104]. TAPSE has also shown a higher reproducibility and lower variability than other cardiovascular measurements more commonly used[105-107].

Changes observed with M-mode showed a trend towards equal performance as TDI, and these changes remain significant when adjustment by cardiac-size is performed. Changes in cardiovascular parameters were small, which would qualify as subclinical cardiac dysfunction. The clinical relevance of these changes is still unknown; however, as the concept of pre-hypertension, where small changes in blood pressure (even within normal ranges) have demonstrated to increase cardiovascular risk, we believe it is reasonable to assume that small changes in cardiac function are relevant at this small age. When the groups' data mean differences in z-scores were compared, a similar performance could be observed for M-mode measurements. This could be partially explained by a higher reproducibility achieved in the clinical setting, and lesser technical requirements, degree of expertise and ultrasound software/equipments as compared to TDI[50, 107, 108]. Thus, M-mode might provide a simpler means for measuring annular motion to assess fetal cardiac dysfunction in IUGR and possibly in general.

TDI and M-mode crude values were adjusted by cardiac size for the first time to our knowledge. When performing this adjustment, significant differences between groups for many of the parameters were lost, however a trend to lower values was maintained. Previous studies have reported TDI and M-mode measurement adjustment by gestational age or estimated fetal weight[43, 50]. The rationale of providing adjustment by heart size comes from the fact that annular displacement and velocities depend on heart size[96, 109]. As heart size is much correlated to body size, in normal conditions adjustment could be performed for either measurement. However, in IUGR there is a relative cardiomegaly[110, 111], thus we believe that cardiac size is a better parameter to perform adjustment.

In our **second study**, both TDI and 2D-derived strain analysis demonstrated to be feasible and reproducible to evaluate deformation parameters in the fetal heart. The study standardized a protocol of acquisition and off-line analysis for TDI and 2D-strain using a dummy ECG by manually indicating the onset of each cardiac cycle based on mitral valve motion. It also demonstrates that these both techniques cannot be interchanged as their correlation is relatively poor.

Evaluation of ventricular longitudinal strain and strain-rate of the fetal heart using TDI was feasible in most cases with a high intra- and inter-observer reproducibility, which is concordant with studies in adults,[37] children[38] and latest reports of TDI in fetal life[35,39-40.] Our study showed a high repeatability with tendency to better agreement for strain as compared to strain-rate which is consistent with previous data[37,38]. Additionally, there was a tendency towards better results in the right as compared to the left free wall which is concordant with previous data in annular peak velocities[5] and may be explained by the easier insonation and dominance of right ventricle during fetal life. Finally, the most innovative contribution of the present study is the introduction of a dummy ECG based on manual indication of the cardiac cycle onset based on valve motion. This enables to provide a proper and physiological onset for the calculation of strain and thus results in a better definition and standardization of the maximal value and additionally offers a natural way for the averaging of the traces from several heart beats. In our experience, this approach highly improves the performance and reduces the need for drift compensation (data not shown), a sign of better and more reliable strain (-rate) traces. Despite that it may account for an increase in the time required for the analysis since it is necessary to carefully review all cardiac cycles frame by frame, it results in much better estimates of deformation and therefore improves its performance and reliability.

Speckle tracking based 2D-strain analysis also showed good feasibility and reproducibility, which was similar to TDI in this study. Results from the present study using dummy ECG based on mitral valve motion led to high a reproducibility, similar to the more recent published data in fetuses using high frame rate and dummy ECG by M-mode[31,33,34]. As with TDI, 2D-strain results also showed a higher reliability for strain as compared to strain-rate analysis. In spite of the high reliability of both techniques per se, we have shown a relatively poor correlation between them. These results are consistent with recent reports in adulthood[42-43] demonstrating a low correlation among deformation measurements which supports the notion that TDI and 2D-strain cannot be interchanged. Similarly, strain and strain-rate values obtained from different ultrasound equipments or software may yield to variable results which cannot be directly compared[43].

Our **third study** evaluated the independent and combined contribution of fetal cardiovascular parameters to the prediction of early-onset IUGR perinatal mortality. The study suggests an algorithm illustrating the chances of perinatal death against gestational age and DV, which might help clinical decisions in the management of early-onset IUGR fetuses.

Our data confirmed previous studies showing that gestational age is the strongest predictor for perinatal mortality[10, 112, 113]. These findings are in line with studies suggesting that IUGR fetuses delivered below 26 weeks are associated with extremely high mortality rates, independently of the Doppler parameters. On the other end of the spectrum, IUGR fetuses delivered after 28 weeks gestation have a much lower mortality[10, 113], which in our population was 3%. Apart from gestational age, the results confirmed previous studies suggesting DV atrial flow as the strongest Doppler predictor for perinatal mortality in preterm IUGR [112, 114, 115]. We further demonstrate that DV is particularly informative in fetuses delivered between 26 and 28 weeks. In such cases, DV allowed to discriminate a subgroup of fetuses with a higher mortality risk. These results support the use of DV as a reason to indicate delivery at these gestational ages. On the contrary, the findings of this study support that the value of DV in predicting mortality beyond 28 weeks is marginal. Nonetheless, DV might still have a role in the prediction of morbidity and poor neurodevelopmental outcomes[43]. The present study could not demonstrate any additive value of MPI with respect to DV in the prediction of perinatal mortality. MPI failed to improve the prediction of DV by itself in the multivariate analysis despite its significant association with perinatal mortality. We could therefore not confirm our previous findings suggesting

that inclusion of MPI could marginally improve the performance of gestational age and DV[112].

The **fourth study** provides, for the first time, evidence that fetal echocardiographic parameters are strongly associated to postnatal hypertension and arterial remodeling, which are recognized cardiovascular risk factors and surrogates for early-onset cardiovascular disease. It supports that a fetal cardiovascular score is strongly associated with the presence of postnatal hypertension and arterial remodeling at 6 months of age in IUGR. Echocardiographic parameters demonstrated a far better performance than perinatal factors and fetoplacental Doppler used for establishing the severity of IUGR.

Echocardiographic measurements in fetuses were consistent with previous studies demonstrating significant differences in cardiac function under IUGR[4, 17, 28, 43, 46, 75, 77, 96, 116-118]. Likewise, increased blood pressure and aIMT had previously been reported in IUGR neonates and children[17, 28, 75, 77, 119, 120]. The present study expands previous findings; our data at 6 months of age showed consistency with that previously published in children demonstrating lower longitudinal parameters such as tissue Doppler velocities, cardiac remodeling demonstrated by a lower sphericity index, as well as increased blood pressure and aIMT (**fifth study**).

As expected, gestational age and birth weight centile showed no association with the occurrence of hypertension and arterial remodeling in childhood. Likewise, fetoplacental Doppler parameters used in fetal management because of their association with perinatal outcome, had only a weak association with postnatal cardiovascular outcome. The absence of a direct relationship between these factors, which are widely accepted severity criteria and bear a strong association with perinatal and neurological outcome[10, 19, 121] suggests that cardiovascular programming may require the presence of predisposing factors. In line with this notion, fetal echocardiographic parameters showed a strong association with hypertension and arterial remodeling. This might indicate that, irrespective of conventional perinatal criteria, there is a fraction of subjects displaying more pronounced adaptative cardiovascular changes under IUGR, and in which these changes persist postnatally. The cardiovascular score developed in this study could identify this high-risk subgroup with a sensitivity of 90%.

Our proposed score logically combines information for cardiovascular remodeling, namely the severity of the IUGR (cerebroplacental ratio), cardiac morphology (sphericity index), systolic function (TAPSE) and diastolic function (IVRT). All indices comprised by the

score can be obtained with any obstetrical ultrasound device equipped with M-mode, conventional pulsed and color Doppler, and are reproducible in fetuses[32, 50, 61]. TAPSE has been used in fetuses to describe cardiovascular dysfunction in IUGR, reflecting subclinical longitudinal dysfunction of the right ventricle[116]. Postnatally, TAPSE has been reported as a good predictor for mortality in Eisenmenger's syndrome, or to monitor postoperatory function in resychronisation therapy[105, 122]. Changes in sphericity index had been previously described in IUGR children by our group[28, 46], showing more globular hearts probably due to cavity dilation secondary to hypoxia; in this study we first report that these changes are already present *in utero*. IVRT is a known parameter for the evaluation of diastolic dysfunction due to poor myocardial relaxation, and is used commonly in fetal echocardiography[58, 61, 98].

Overall, our results show that fetal echocardiography can predict mid-term cardiovascular risk factors and support the concept of including the selected IUGR population as a high-risk group for early screening in cardiovascular guidelines[28]. From a clinical perspective, this study opens a line that may find new applications for echocardiography in fetal life. Considering that diagnosis of IUGR is established in about 5-10% of pregnancies, the findings of this study would affect thousands of children per year. In addition, recent prospective validation with long term follow-up is required to confirm the value of predictive scores based on fetal echocardiography with a clear clinical application. If these expectations are confirmed, prediction of hypertension and arterial remodeling from perinatal life would represent a public health opportunity for intervention. It is recognized that mild cardiovascular changes that remain subclinical during childhood may represent significant health issues if combined with additional behaviors or stressors during adulthood[123]. Hypertension in the child has been associated with substantial long-term health risks and considered an indication for lifestyle modifications[72]. In addition, aIMT measurement allows detection of increased cardiovascular risk as an indicator of arterial remodeling in children[75-77]. Interventions in this target group could go from blood pressure monitoring before 3 years of age, recommending lack of exposure to other risk factors (secondary smoking, obesity), surveillance of catch-up growth or administration of hypotensors[71, 78] and specially, promoting exercise and physical activity. Particularly, high intake of dietary long-chain omega-3 fatty acids is associated with lower blood pressure and may prevent progression of subclinical atherosclerosis in children born with low birth weight[124]. A recent randomized trial in a large cohort of children suggest that the inverse

association of fetal growth with arterial wall thickness in childhood can be prevented by dietary ω-3 fatty acid supplementation over the first 5 years of life[79]. Identification of high-risk groups within IUGR fetuses and other conditions described to be associated with cardiovascular programming[125] would lead to new clinical applications for echocardiography in pregnancy, and would represent a step forward in personalized fetal and pediatric cardiology. If these results are validated by other authors this research could open the door for designing targeted interventions to reduce the risks of cardiovascular disease from perinatal life.

An important strength of our project was the recruiting of a specific cohort with a complete work-up of structural and functional echocardiography in fetal life and subsequent follow-up into infancy. This allowed to prospectively examine the effects of impaired fetal growth, while controlling for postnatal confounders as much as possible. Examination at 6 months of age was decided because it is a reasonable point in time to avoid the effects of neonatal cardiovascular transition to postnatal life and potential interference with temporary blood pressure changes. While we acknowledge that longer term evaluation would provide more robust data on the long term prediction value, this would entail the need for correction of potential confounders associated with diet, exercise or socioeconomic factors. In addition, there is strong evidence on the longer term effects of IUGR in children and adolescents[71, 75, 124]. Notwithstanding these comments, we acknowledge that longer term follow up is necessary to validate the clinical value of echocardiographic scores to predict hypertension and other cardiovascular outcomes in childhood. Likewise, we acknowledge that there is no standard definition for increased cardiovascular risk at 6 months of age and that an ideal outcome for this type of study would be information of cardiovascular disease or clinical events at adult age, such as myocardial infarction, heart failure or death. Therefore, further long term follow-up of an extended cohort to validate the findings here reported is warranted.

This project has some limitations that should be acknowledged. For many of these techniques, the relatively small size of the fetal heart compared to the spatial resolution of the system may limit the evaluation of fetal cardiac function. For example, when delineating the fetal heart for 2D-strain analysis, even the smallest segment width available is usually thicker than the myocardial wall. The variable fetal position makes optimal acquisition of the different planes difficult; however someone with experience in fetal echocardiography will manage to obtain most, if not all measurements. Regarding cardiovascular function in the

infant, we acknowledge that there is no standard definition for increased cardiovascular risk at 6 months of age and that an ideal cardiovascular endpoint for this type of study would be information of cardiovascular disease or clinical events at adult age, such as myocardial infarction, heart failure or death. Therefore, a further follow-up of this cohort aiming to confirm our findings later in life is warranted.

Fetal cardiovascular parameters characterize subclinical cardiac dysfunction and cardiac remodeling prenatally, allowing prediction of postnatal hypertension and arterial remodeling better than perinatal severity parameters currently used. Our results suggest that fetal echocardiographic parameters identify a high-risk group within the IUGR fetuses, which could be targeted for early screening of blood pressure and other cardiovascular risk factors, as well as for promoting a healthy diet and physical exercise. This could aid in designing interventions for prevention of cardiovascular disease in the long run in this subset of the population.

8. CONCLUSIONS

8. CONCLUSIONS

IUGR fetuses present signs of subclinical cardiac dysfunction in comparison with normally grown fetuses, which can be characterized by prenatal functional echocardiography.

1. Functional echocardiographic techniques such as M-mode longitudinal-axis motion, TDI and 2D-derived strain parameters, are feasible and reproducible in the fetus.

2. Fetal cardiovascular parameters characterize cardiac function and morphometry prenatally, demonstrating subclinical cardiac dysfunction and cardiac remodeling in IUGR.

3. Fetal cardiovascular Doppler parameters are significantly associated with perinatal outcomes, specifically mortality, in IUGR. Gestational age at delivery is the strongest predictor of mortality in this group of fetuses before 26 and after 28 weeks with DV allowing stratification between 26-28 weeks.

4. Fetal cardiovascular parameters characterize subclinical cardiac dysfunction and cardiac remodeling prenatally, allowing prediction of postnatal hypertension and arterial remodeling better than perinatal severity parameters currently used. Fetal echocardiographic parameters identify a high-risk group within the IUGR fetuses, which could be targeted for early screening of blood pressure and other cardiovascular risk factors, as well as for promoting a healthy diet and physical exercise. This could aid in designing interventions for prevention of cardiovascular disease in the long run in this subset of the population.

9. REFERENCES

9. REFERENCES

1. Hansson GK. Inflammation, atherosclerosis, and coronary artery disease. *N Engl J Med,* 2005;352:1685-1695.
2. Murray CJ, Lopez AD. Global mortality, disability, and the contribution of risk factors: Global Burden of Disease Study. *Lancet,* 1997;349:1436-1442.
3. Berry JD, Dyer A, Cai X, Garside DB, Ning H, Thomas A, Greenland P, Van Horn L, Tracy RP, Lloyd-Jones DM. Lifetime risks of cardiovascular disease. *N Engl J Med,* 2012;366:321-329.
4. Barker DJ, Osmond C, Golding J, Kuh D, Wadsworth ME. Growth in utero, blood pressure in childhood and adult life, and mortality from cardiovascular disease. *BMJ,* 1989;298:564-567.
5. Shonkoff JP, Boyce WT, McEwen BS. Neuroscience, molecular biology, and the childhood roots of health disparities: building a new framework for health promotion and disease prevention. *JAMA,* 2009;301:2252-2259.
6. Gardosi J. New definition of small for gestational age based on fetal growth potential. *Horm Res,* 2006;65 Suppl 3:15-18.
7. Berkley E, Chauhan SP, Abuhamad A. Doppler assessment of the fetus with intrauterine growth restriction. *Am J Obstet Gynecol,* 2012;206:300-308.
8. Maulik D. Fetal growth compromise: definitions, standards, and classification. *Clin Obstet Gynecol,* 2006;49:214-218.
9. Ott WJ. Sonographic diagnosis of fetal growth restriction. *Clin Obstet Gynecol,* 2006;49:295-307.
10. Baschat AA, Cosmi E, Bilardo CM, Wolf H, Berg C, Rigano S, Germer U, Moyano D, Turan S, Hartung J, Bhide A, Muller T, Bower S, Nicolaides KH, Thilaganathan B, Gembruch U, Ferrazzi E, Hecher K, Galan HL, Harman CR. Predictors of neonatal outcome in early-onset placental dysfunction. *Obstet Gynecol,* 2007;109:253-261.
11. Eixarch E, Meler E, Iraola A, Illa M, Crispi F, Hernandez-Andrade E, Gratacos E, Figueras F. Neurodevelopmental outcome in 2-year-old infants who were small-for-gestational age term fetuses with cerebral blood flow redistribution. *Ultrasound Obstet Gynecol,* 2008;32:894-899.

12. Savchev S, Sanz-Cortes M, Cruz-Martinez R, Arranz A, Botet F, Gratacos E, Figueras F. Neurodevelopmental outcome of full-term, small-for-gestational-age infants with normal placental function. *Ultrasound Obstet Gynecol,* 2013.

13. Miller J, Turan S, Baschat AA. Fetal growth restriction. *Semin Perinatol,* 2008;32:274-280.

14. Baschat AA, Gembruch U, Harman CR. The sequence of changes in Doppler and biophysical parameters as severe fetal growth restriction worsens. *Ultrasound Obstet Gynecol,* 2001;18:571-577.

15. ACOG committee opinion. Utility of antepartum umbilical artery Doppler velocimetry in intrauterine growth restriction. Number 188, October 1997 (replaces no. 116, November 1992). Committee on Obstetric Practice. American College of Obstetricians and Gynecologists. *Int J Gynaecol Obstet,* 1997;59:269-270.

16. Figueras F, Eixarch E, Meler E, Iraola A, Figueras J, Puerto B, Gratacos E. Small-for-gestational-age fetuses with normal umbilical artery Doppler have suboptimal perinatal and neurodevelopmental outcome. *Eur J Obstet Gynecol Reprod Biol,* 2008;136:34-38.

17. Rossi P, Tauzin L, Marchand E, Boussuges A, Gaudart J, Frances Y. Respective roles of preterm birth and fetal growth restriction in blood pressure and arterial stiffness in adolescence. *J Adolesc Health,* 2011;48:520-522.

18. Savchev S, Figueras F, Cruz-Martinez R, Illa M, Botet F, Gratacos E. Estimated weight centile as a predictor of perinatal outcome in small-for-gestational-age pregnancies with normal fetal and maternal Doppler indices. *Ultrasound Obstet Gynecol,* 2012;39:299-303.

19. Cruz-Lemini M, Crispi F, Van Mieghem T, Pedraza D, Cruz-Martinez R, Acosta-Rojas R, Figueras F, Parra-Cordero M, Deprest J, Gratacos E. Risk of perinatal death in early-onset intrauterine growth restriction according to gestational age and cardiovascular Doppler indices: a multicenter study. *Fetal Diagn Ther,* 2012;32:116-122.

20. Figueras F, Gardosi J. Intrauterine growth restriction: new concepts in antenatal surveillance, diagnosis, and management. *Am J Obstet Gynecol,* 2011;204:288-300.

21. Oros D, Figueras F, Cruz-Martinez R, Meler E, Munmany M, Gratacos E. Longitudinal changes in uterine, umbilical and fetal cerebral Doppler indices in late-

onset small-for-gestational age fetuses. *Ultrasound Obstet Gynecol,* 2011;37:191-195.

22. Turan OM, Turan S, Gungor S, Berg C, Moyano D, Gembruch U, Nicolaides KH, Harman CR, Baschat AA. Progression of Doppler abnormalities in intrauterine growth restriction. *Ultrasound Obstet Gynecol,* 2008;32:160-167.

23. Bilardo CM, Wolf H, Stigter RH, Ville Y, Baez E, Visser GH, Hecher K. Relationship between monitoring parameters and perinatal outcome in severe, early intrauterine growth restriction. *Ultrasound Obstet Gynecol,* 2004;23:119-125.

24. Hecher K, Bilardo CM, Stigter RH, Ville Y, Hackeloer BJ, Kok HJ, Senat MV, Visser GH. Monitoring of fetuses with intrauterine growth restriction: a longitudinal study. *Ultrasound Obstet Gynecol,* 2001;18:564-570.

25. Cruz-Martinez R, Figueras F, Benavides-Serralde A, Crispi F, Hernandez-Andrade E, Gratacos E. Sequence of changes in myocardial performance index in relation to aortic isthmus and ductus venosus Doppler in fetuses with early-onset intrauterine growth restriction. *Ultrasound Obstet Gynecol,* 2011;38:179-184.

26. Illa M, Coloma JL, Eixarch E, Meler E, Iraola A, Gardosi J, Gratacos E, Figueras F. Growth deficit in term small-for-gestational fetuses with normal umbilical artery Doppler is associated with adverse outcome. *J Perinat Med,* 2009;37:48-52.

27. Egana-Ugrinovic G, Sanz-Cortes M, Figueras F, Bargallo N, Gratacos E. Differences in cortical development assessed by fetal MRI in late-onset intrauterine growth restriction. *Am J Obstet Gynecol,* 2013.

28. Crispi F, Bijnens B, Figueras F, Bartrons J, Eixarch E, Le Noble F, Ahmed A, Gratacos E. Fetal growth restriction results in remodeled and less efficient hearts in children. *Circulation,* 2010;121:2427-2436.

29. Chaiworapongsa T, Espinoza J, Yoshimatsu J, Kalache K, Edwin S, Blackwell S, Yoon BH, Tolosa JE, Silva M, Behnke E, Gomez R, Romero R. Subclinical myocardial injury in small-for-gestational-age neonates. *J Matern Fetal Neonatal Med,* 2002;11:385-390.

30. Comas M, Crispi F, Cruz-Martinez R, Figueras F, Gratacos E. Tissue Doppler echocardiographic markers of cardiac dysfunction in small-for-gestational age fetuses. *Am J Obstet Gynecol,* 2011;205:57 e51-56.

31. Cruz-Martinez R, Figueras F, Hernandez-Andrade E, Oros D, Gratacos E. Changes in myocardial performance index and aortic isthmus and ductus venosus Doppler in

term, small-for-gestational age fetuses with normal umbilical artery pulsatility index. *Ultrasound Obstet Gynecol,* 2011;38:400-405.

32. Baschat AA, Gembruch U. The cerebroplacental Doppler ratio revisited. *Ultrasound Obstet Gynecol,* 2003;21:124-127.

33. Baschat AA. Pathophysiology of fetal growth restriction: implications for diagnosis and surveillance. *Obstet Gynecol Surv,* 2004;59:617-627.

34. Crispi F, Hernandez-Andrade E, Pelsers MM, Plasencia W, Benavides-Serralde JA, Eixarch E, Le Noble F, Ahmed A, Glatz JF, Nicolaides KH, Gratacos E. Cardiac dysfunction and cell damage across clinical stages of severity in growth-restricted fetuses. *Am J Obstet Gynecol,* 2008;199:254 e251-258.

35. Cruz-Martinez R, Figueras F, Oros D, Padilla N, Meler E, Hernandez-Andrade E, Gratacos E. Cerebral blood perfusion and neurobehavioral performance in full-term small-for-gestational-age fetuses. *Am J Obstet Gynecol,* 2009;201:474 e471-477.

36. Fouron JC, Gosselin J, Raboisson MJ, Lamoureux J, Tison CA, Fouron C, Hudon L. The relationship between an aortic isthmus blood flow velocity index and the postnatal neurodevelopmental status of fetuses with placental circulatory insufficiency. *Am J Obstet Gynecol,* 2005;192:497-503.

37. Hatem MA, Zielinsky P, Hatem DM, Nicoloso LH, Manica JL, Piccoli AL, Zanettini J, Oliveira V, Scarpa F, Petracco R. Assessment of diastolic ventricular function in fetuses of diabetic mothers using tissue Doppler. *Cardiol Young,* 2008;18:297-302.

38. Van Mieghem T, Gucciardo L, Done E, Van Schoubroeck D, Graatsma EM, Visser GH, Verhaeghe J, Deprest J. Left ventricular cardiac function in fetuses with congenital diaphragmatic hernia and the effect of fetal endoscopic tracheal occlusion. *Ultrasound Obstet Gynecol,* 2009;34:424-429.

39. Kiserud T, Acharya G. The fetal circulation. *Prenat Diagn,* 2004;24:1049-1059.

40. Buckberg G, Hoffman JI, Mahajan A, Saleh S, Coghlan C. Cardiac mechanics revisited: the relationship of cardiac architecture to ventricular function. *Circulation,* 2008;118:2571-2587.

41. Nesbitt GC, Mankad S, Oh JK. Strain imaging in echocardiography: methods and clinical applications. *Int J Cardiovasc Imaging,* 2009;25 Suppl 1:9-22.

42. Van Mieghem T, DeKoninck P, Steenhaut P, Deprest J. Methods for prenatal assessment of fetal cardiac function. *Prenat Diagn,* 2009;29:1193-1203.

43. Comas M, Crispi F, Cruz-Martinez R, Martinez JM, Figueras F, Gratacos E. Usefulness of myocardial tissue Doppler vs conventional echocardiography in the evaluation of cardiac dysfunction in early-onset intrauterine growth restriction. *Am J Obstet Gynecol,* 2010;203:45 e41-47.

44. Larsen LU, Sloth E, Petersen OB, Pedersen TF, Sorensen K, Uldbjerg N. Systolic myocardial velocity alterations in the growth-restricted fetus with cerebroplacental redistribution. *Ultrasound Obstet Gynecol,* 2009;34:62-67.

45. Opie LH, Commerford PJ, Gersh BJ, Pfeffer MA. Controversies in ventricular remodelling. *Lancet,* 2006;367:356-367.

46. Crispi F, Figueras F, Cruz-Lemini M, Bartrons J, Bijnens B, Gratacos E. Cardiovascular programming in children born small for gestational age and relationship with prenatal signs of severity. *Am J Obstet Gynecol,* 2012;207:121 e121-129.

47. Huhta JC. Guidelines for the evaluation of heart failure in the fetus with or without hydrops. *Pediatr Cardiol,* 2004;25:274-286.

48. Rychik J, Tian Z, Bebbington M, Xu F, McCann M, Mann S, Wilson RD, Johnson MP. The twin-twin transfusion syndrome: spectrum of cardiovascular abnormality and development of a cardiovascular score to assess severity of disease. *Am J Obstet Gynecol,* 2007;197:392 e391-398.

49. Bijnens BH, Cikes M, Claus P, Sutherland GR. Velocity and deformation imaging for the assessment of myocardial dysfunction. *Eur J Echocardiogr,* 2009;10:216-226.

50. Gardiner HM, Pasquini L, Wolfenden J, Barlow A, Li W, Kulinskaya E, Henein M. Myocardial tissue Doppler and long axis function in the fetal heart. *Int J Cardiol,* 2006;113:39-47.

51. Matsui H, Germanakis I, Kulinskaya E, Gardiner HM. Temporal and spatial performance of vector velocity imaging in the human fetal heart. *Ultrasound Obstet Gynecol,* 2011;37:150-157.

52. Willruth AM, Geipel AK, Fimmers R, Gembruch UG. Assessment of right ventricular global and regional longitudinal peak systolic strain, strain rate and velocity in healthy fetuses and impact of gestational age using a novel speckle/feature-tracking based algorithm. *Ultrasound Obstet Gynecol,* 2011;37:143-149.

53. Comas M, Crispi F. Assessment of fetal cardiac function using tissue Doppler techniques. *Fetal Diagn Ther,* 2012;32:30-38.

54. Lee W, Allan L, Carvalho JS, Chaoui R, Copel J, Devore G, Hecher K, Munoz H, Nelson T, Paladini D, Yagel S. ISUOG consensus statement: what constitutes a fetal echocardiogram? *Ultrasound Obstet Gynecol,* 2008;32:239-242.

55. Cardiac screening examination of the fetus: guidelines for performing the 'basic' and 'extended basic' cardiac scan. *Ultrasound Obstet Gynecol,* 2006;27:107-113.

56. Rychik J, Ayres N, Cuneo B, Gotteiner N, Hornberger L, Spevak PJ, Van Der Veld M. American Society of Echocardiography guidelines and standards for performance of the fetal echocardiogram. *J Am Soc Echocardiogr,* 2004;17:803-810.

57. Germanakis I, Gardiner H. Assessment of fetal myocardial deformation using speckle tracking techniques. *Fetal Diagn Ther,* 2012;32:39-46.

58. Hernandez-Andrade E, Benavides-Serralde JA, Cruz-Martinez R, Welsh A, Mancilla-Ramirez J. Evaluation of conventional Doppler fetal cardiac function parameters: E/A ratios, outflow tracts, and myocardial performance index. *Fetal Diagn Ther,* 2012;32:22-29.

59. Crispi F, Gratacos E. Fetal cardiac function: technical considerations and potential research and clinical applications. *Fetal Diagn Ther,* 2012;32:47-64.

60. Godfrey ME, Messing B, Cohen SM, Valsky DV, Yagel S. Functional assessment of the fetal heart: a review. *Ultrasound Obstet Gynecol,* 2011;39:131-144.

61. Hernandez-Andrade E, Lopez-Tenorio J, Figueroa-Diesel H, Sanin-Blair J, Carreras E, Cabero L, Gratacos E. A modified myocardial performance (Tei) index based on the use of valve clicks improves reproducibility of fetal left cardiac function assessment. *Ultrasound Obstet Gynecol,* 2005;26:227-232.

62. Godfrey ME, Messing B, Valsky DV, Cohen SM, Yagel S. Fetal cardiac function: M-mode and 4D spatiotemporal image correlation. *Fetal Diagn Ther,* 2012;32:17-21.

63. Jessup M, Abraham WT, Casey DE, Feldman AM, Francis GS, Ganiats TG, Konstam MA, Mancini DM, Rahko PS, Silver MA, Stevenson LW, Yancy CW. 2009 focused update: ACCF/AHA Guidelines for the Diagnosis and Management of Heart Failure in Adults: a report of the American College of Cardiology Foundation/American Heart Association Task Force on Practice Guidelines: developed in collaboration with the International Society for Heart and Lung Transplantation. *Circulation,* 2009;119:1977-2016.

64. Carvalho JS, O'Sullivan C, Shinebourne EA, Henein MY. Right and left ventricular long-axis function in the fetus using angular M-mode. *Ultrasound Obstet Gynecol,* 2001;18:619-622.

65. Ho CY, Solomon SD. A clinician's guide to tissue Doppler imaging. *Circulation,* 2006;113:e396-398.

66. Harada K, Tsuda A, Orino T, Tanaka T, Takada G. Tissue Doppler imaging in the normal fetus. *Int J Cardiol,* 1999;71:227-234.

67. Van Mieghem T, Giusca S, DeKoninck P, Gucciardo L, Done E, Hindryckx A, D'Hooge J, Deprest J. Prospective assessment of fetal cardiac function with speckle tracking in healthy fetuses and recipient fetuses of twin-to-twin transfusion syndrome. *J Am Soc Echocardiogr,* 2010;23:301-308.

68. Lai WW, Geva T, Shirali GS, Frommelt PC, Humes RA, Brook MM, Pignatelli RH, Rychik J. Guidelines and standards for performance of a pediatric echocardiogram: a report from the Task Force of the Pediatric Council of the American Society of Echocardiography. *J Am Soc Echocardiogr,* 2006;19:1413-1430.

69. Reeves ST, Glas KE, Eltzschig H, Mathew JP, Rubenson DS, Hartman GS, Shernan SK. Guidelines for performing a comprehensive epicardial echocardiography examination: recommendations of the American Society of Echocardiography and the Society of Cardiovascular Anesthesiologists. *J Am Soc Echocardiogr,* 2007;20:427-437.

70. Notomi Y, Srinath G, Shiota T, Martin-Miklovic MG, Beachler L, Howell K, Oryszak SJ, Deserranno DG, Freed AD, Greenberg NL, Younoszai A, Thomas JD. Maturational and adaptive modulation of left ventricular torsional biomechanics: Doppler tissue imaging observation from infancy to adulthood. *Circulation,* 2006;113:2534-2541.

71. Williams CL, Hayman LL, Daniels SR, Robinson TN, Steinberger J, Paridon S, Bazzarre T. Cardiovascular health in childhood: A statement for health professionals from the Committee on Atherosclerosis, Hypertension, and Obesity in the Young (AHOY) of the Council on Cardiovascular Disease in the Young, American Heart Association. *Circulation,* 2002;106:143-160.

72. Adolescents NHBPEPWGoHBPiCa. The fourth report on the diagnosis, evaluation, and treatment of high blood pressure in children and adolescents. *Pediatrics,* 2004;114:555-576.

73. Perk J, De Backer G, Gohlke H, Graham I, Reiner Z, Verschuren M, Albus C, Benlian P, Boysen G, Cifkova R, Deaton C, Ebrahim S, Fisher M, Germano G, Hobbs R, Hoes A, Karadeniz S, Mezzani A, Prescott E, Ryden L, Scherer M, Syvanne M, Scholte op Reimer WJ, Vrints C, Wood D, Zamorano JL, Zannad F. European Guidelines on cardiovascular disease prevention in clinical practice (version 2012). The Fifth Joint Task Force of the European Society of Cardiology and Other Societies on Cardiovascular Disease Prevention in Clinical Practice (constituted by representatives of nine societies and by invited experts). Developed with the special contribution of the European Association for Cardiovascular Prevention & Rehabilitation (EACPR). *Eur Heart J,* 2012;33:1635-1701.

74. Stein JH, Korcarz CE, Hurst RT, Lonn E, Kendall CB, Mohler ER, Najjar SS, Rembold CM, Post WS. Use of carotid ultrasound to identify subclinical vascular disease and evaluate cardiovascular disease risk: a consensus statement from the American Society of Echocardiography Carotid Intima-Media Thickness Task Force. Endorsed by the Society for Vascular Medicine. *J Am Soc Echocardiogr,* 2008;21:93-111; quiz 189-190.

75. Jarvisalo MJ, Jartti L, Nanto-Salonen K, Irjala K, Ronnemaa T, Hartiala JJ, Celermajer DS, Raitakari OT. Increased aortic intima-media thickness: a marker of preclinical atherosclerosis in high-risk children. *Circulation,* 2001;104:2943-2947.

76. Dulac Y, Tauber M, Jouret B. Aortic or carotid intima-media thickness to evaluate children born small for gestational age? *Horm Res Paediatr,* 2012;77:340.

77. Skilton MR, Evans N, Griffiths KA, Harmer JA, Celermajer DS. Aortic wall thickness in newborns with intrauterine growth restriction. *Lancet,* 2005;365:1484-1486.

78. Kavey RE, Allada V, Daniels SR, Hayman LL, McCrindle BW, Newburger JW, Parekh RS, Steinberger J. Cardiovascular risk reduction in high-risk pediatric patients: a scientific statement from the American Heart Association Expert Panel on Population and Prevention Science; the Councils on Cardiovascular Disease in the Young, Epidemiology and Prevention, Nutrition, Physical Activity and Metabolism, High Blood Pressure Research, Cardiovascular Nursing, and the Kidney in Heart Disease; and the Interdisciplinary Working Group on Quality of Care and Outcomes Research: endorsed by the American Academy of Pediatrics. *Circulation,* 2006;114:2710-2738.

79. Skilton MR, Ayer JG, Harmer JA, Webb K, Leeder SR, Marks GB, Celermajer DS. Impaired fetal growth and arterial wall thickening: a randomized trial of omega-3 supplementation. *Pediatrics,* 2012;129:e698-703.

80. Figueras F, Meler E, Iraola A, Eixarch E, Coll O, Figueras J, Francis A, Gratacos E, Gardosi J. Customized birthweight standards for a Spanish population. *Eur J Obstet Gynecol Reprod Biol,* 2008;136:20-24.

81. Hadlock FP, Harrist RB, Shah YP, King DE, Park SK, Sharman RS. Estimating fetal age using multiple parameters: a prospective evaluation in a racially mixed population. *Am J Obstet Gynecol,* 1987;156:955-957.

82. Gomez O, Figueras F, Fernandez S, Bennasar M, Martinez JM, Puerto B, Gratacos E. Reference ranges for uterine artery mean pulsatility index at 11-41 weeks of gestation. *Ultrasound Obstet Gynecol,* 2008;32:128-132.

83. Arduini D, Rizzo G. Normal values of Pulsatility Index from fetal vessels: a cross-sectional study on 1556 healthy fetuses. *J Perinat Med,* 1990;18:165-172.

84. Hecher K, Campbell S, Snijders R, Nicolaides K. Reference ranges for fetal venous and atrioventricular blood flow parameters. *Ultrasound Obstet Gynecol,* 1994;4:381-390.

85. Del Rio M, Martinez JM, Figueras F, Lopez M, Palacio M, Gomez O, Coll O, Puerto B. Reference ranges for Doppler parameters of the fetal aortic isthmus during the second half of pregnancy. *Ultrasound Obstet Gynecol,* 2006;28:71-76.

86. Rizzo G, Arduini D, Romanini C. Doppler echocardiographic assessment of fetal cardiac function. *Ultrasound Obstet Gynecol,* 1992;2:434-445.

87. Ruskamp J, Fouron JC, Gosselin J, Raboisson MJ, Infante-Rivard C, Proulx F. Reference values for an index of fetal aortic isthmus blood flow during the second half of pregnancy. *Ultrasound Obstet Gynecol,* 2003;21:441-444.

88. Awadh AM, Prefumo F, Bland JM, Carvalho JS. Assessment of the intraobserver variability in the measurement of fetal cardiothoracic ratio using ellipse and diameter methods. *Ultrasound Obstet Gynecol,* 2006;28:53-56.

89. Lang RM, Bierig M, Devereux RB, Flachskampf FA, Foster E, Pellikka PA, Picard MH, Roman MJ, Seward J, Shanewise JS, Solomon SD, Spencer KT, Sutton MS, Stewart WJ. Recommendations for chamber quantification: a report from the American Society of Echocardiography's Guidelines and Standards Committee and the Chamber Quantification Writing Group, developed in conjunction with the

European Association of Echocardiography, a branch of the European Society of Cardiology. *J Am Soc Echocardiogr,* 2005;18:1440-1463.

90. Kono T, Sabbah HN, Rosman H, Alam M, Jafri S, Goldstein S. Left ventricular shape is the primary determinant of functional mitral regurgitation in heart failure. *J Am Coll Cardiol,* 1992;20:1594-1598.

91. Lowes BD, Gill EA, Abraham WT, Larrain JR, Robertson AD, Bristow MR, Gilbert EM. Effects of carvedilol on left ventricular mass, chamber geometry, and mitral regurgitation in chronic heart failure. *Am J Cardiol,* 1999;83:1201-1205.

92. Allan LD, Joseph MC, Boyd EG, Campbell S, Tynan M. M-mode echocardiography in the developing human fetus. *Br Heart J,* 1982;47:573-583.

93. Schneider C, McCrindle BW, Carvalho JS, Hornberger LK, McCarthy KP, Daubeney PE. Development of Z-scores for fetal cardiac dimensions from echocardiography. *Ultrasound Obstet Gynecol,* 2005;26:599-605.

94. Kiserud T, Ebbing C, Kessler J, Rasmussen S. Fetal cardiac output, distribution to the placenta and impact of placental compromise. *Ultrasound Obstet Gynecol,* 2006;28:126-136.

95. DeVore GR, Siassi B, Platt LD. Fetal echocardiography. IV. M-mode assessment of ventricular size and contractility during the second and third trimesters of pregnancy in the normal fetus. *Am J Obstet Gynecol,* 1984;150:981-988.

96. Comas M, Crispi F, Gomez O, Puerto B, Figueras F, Gratacos E. Gestational age- and estimated fetal weight-adjusted reference ranges for myocardial tissue Doppler indices at 24-41 weeks' gestation. *Ultrasound Obstet Gynecol,* 2011;37:57-64.

97. Reed KL, Appleton CP, Sahn DJ, Anderson CF. Human fetal tricuspid and mitral deceleration time: changes with normal pregnancy and intrauterine growth retardation. *Am J Obstet Gynecol,* 1989;161:1532-1535.

98. Cruz-Martinez R, Figueras F, Bennasar M, Garcia-Posadas R, Crispi F, Hernandez-Andrade E, Gratacos E. Normal reference ranges from 11 to 41 weeks' gestation of fetal left modified myocardial performance index by conventional Doppler with the use of stringent criteria for delimitation of the time periods. *Fetal Diagn Ther,* 2012;32:79-86.

99. Hernandez-Andrade E, Figueroa-Diesel H, Kottman C, Illanes S, Arraztoa J, Acosta-Rojas R, Gratacos E. Gestational-age-adjusted reference values for the modified

myocardial performance index for evaluation of fetal left cardiac function. *Ultrasound Obstet Gynecol,* 2007;29:321-325.

100. Robinson HP, Sweet EM, Adam AH. The accuracy of radiological estimates of gestational age using early fetal crown-rump length measurements by ultrasound as a basis for comparison. *Br J Obstet Gynaecol,* 1979;86:525-528.

101. Carrascosa A, Fernandez JM, Fernandez C, Ferrandez A, Lopez-Siguero JP, Sanchez E, Sobradillo B, Yeste D. Spanish growth studies 2008. New anthropometric standards. *Endocrinol Nutr,* 2008;55:484-506.

102. Report of the National High Blood Pressure Education Program Working Group on High Blood Pressure in Pregnancy. *Am J Obstet Gynecol,* 2000;183:S1-S22.

103. Godfrey ME, Messing B, Cohen SM, Valsky DV, Yagel S. Functional assessment of the fetal heart: a review. *Ultrasound Obstet Gynecol,* 2012;39:131-144.

104. Ho SY, Nihoyannopoulos P. Anatomy, echocardiography, and normal right ventricular dimensions. *Heart,* 2006;92 Suppl 1:i2-13.

105. Cappelli F, Cristina Porciani M, Ricceri I, Perrotta L, Ricciardi G, Pieragnoli P, Paladini G, Michelucci A, Padeletti L. Tricuspid annular plane systolic excursion evaluation improves selection of cardiac resynchronization therapy patients. *Clin Cardiol,* 2010;33:578-582.

106. Koestenberger M, Nagel B, Ravekes W, Urlesberger B, Raith W, Avian A, Halb V, Cvirn G, Fritsch P, Gamillscheg A. Systolic Right Ventricular Function in Preterm and Term Neonates: Reference Values of the Tricuspid Annular Plane Systolic Excursion (TAPSE) in 258 Patients and Calculation of Z-Score Values. *Neonatology,* 2011;100:85-92.

107. Papaioannou VE, Pneumatikos IA. *The use of Tricuspid Annular Plane Systolic Excursion and Tissue Doppler Imaging Velocities for the Estimation of Pulmonary Hypertension and Right Ventricular Function in Mechanically Ventilated Patients*. First ed: InTech; 2011.

108. Papaioannou VE, Stakos DA, Dragoumanis CK, Pneumatikos IA. Relation of tricuspid annular displacement and tissue Doppler imaging velocities with duration of weaning in mechanically ventilated patients with acute pulmonary edema. *BMC Cardiovasc Disord,* 2010;10:20.

109. Batterham A, Shave R, Oxborough D, Whyte G, George K. Longitudinal plane colour tissue-Doppler myocardial velocities and their association with left ventricular length, volume, and mass in humans. *Eur J Echocardiogr,* 2008;9:542-546.

110. Batton DG, Roberts C, Cacciarelli A. Cardiothoracic ratio in newborns with severe intrauterine growth retardation. *Clin Pediatr (Phila),* 1992;31:564-565.

111. Bozynski ME, Hanafy FH, Hernandez RJ. Association of increased cardiothoracic ratio and intrauterine growth retardation. *Am J Perinatol,* 1991;8:28-30.

112. Hernandez-Andrade E, Crispi F, Benavides-Serralde JA, Plasencia W, Diesel HF, Eixarch E, Acosta-Rojas R, Figueras F, Nicolaides K, Gratacos E. Contribution of the myocardial performance index and aortic isthmus blood flow index to predicting mortality in preterm growth-restricted fetuses. *Ultrasound Obstet Gynecol,* 2009;34:430-436.

113. Morris RK, Selman TJ, Verma M, Robson SC, Kleijnen J, Khan KS. Systematic review and meta-analysis of the test accuracy of ductus venosus Doppler to predict compromise of fetal/neonatal wellbeing in high risk pregnancies with placental insufficiency. *Eur J Obstet Gynecol Reprod Biol,* 2010;152:3-12.

114. Robertson MC, Murila F, Tong S, Baker LS, Yu VY, Wallace EM. Predicting perinatal outcome through changes in umbilical artery Doppler studies after antenatal corticosteroids in the growth-restricted fetus. *Obstet Gynecol,* 2009;113:636-640.

115. Baschat AA. Doppler application in the delivery timing of the preterm growth-restricted fetus: another step in the right direction. *Ultrasound Obstet Gynecol,* 2004;23:111-118.

116. Cruz-Lemini M, Crispi F, Valenzuela-Alcaraz B, Figueras F, Sitges M, Gomez O, Bijnens B, Gratacos E. Value of annular M-mode displacement versus tissue Doppler velocities to assess cardiac function in intrauterine growth restriction. *Ultrasound Obstet Gynecol,* 2013.

117. Hecher K, Campbell S, Doyle P, Harrington K, Nicolaides K. Assessment of fetal compromise by Doppler ultrasound investigation of the fetal circulation. Arterial, intracardiac, and venous blood flow velocity studies. *Circulation,* 1995;91:129-138.

118. Makikallio K, Vuolteenaho O, Jouppila P, Rasanen J. Ultrasonographic and biochemical markers of human fetal cardiac dysfunction in placental insufficiency. *Circulation,* 2002;105:2058-2063.

119. Chiolero A, Bovet P, Paradis G. Screening for Elevated Blood Pressure in Children and Adolescents: A Critical Appraisal. *JAMA Pediatr,* 2013:1-8.

120. Dawson JD, Sonka M, Blecha MB, Lin W, Davis PH. Risk factors associated with aortic and carotid intima-media thickness in adolescents and young adults: the Muscatine Offspring Study. *J Am Coll Cardiol,* 2009;53:2273-2279.

121. Gratacos E. The problem of predicting neurological outcome in early-onset intrauterine growth restriction. *Ultrasound Obstet Gynecol,* 2009;33:5-7.

122. Moceri P, Dimopoulos K, Liodakis E, Germanakis I, Kempny A, Diller GP, Swan L, Wort SJ, Marino PS, Gatzoulis MA, Li W. Echocardiographic predictors of outcome in eisenmenger syndrome. *Circulation,* 2012;126:1461-1468.

123. Rogers LK, Velten M. Maternal inflammation, growth retardation, and preterm birth: insights into adult cardiovascular disease. *Life Sci,* 2011;89:417-421.

124. Skilton MR, Raitakari OT, Celermajer DS. High Intake of Dietary Long-Chain omega-3 Fatty Acids Is Associated With Lower Blood Pressure in Children Born With Low Birth Weight: NHANES 2003-2008. *Hypertension,* 2013;61:972-976.

125. Valenzuela-Alcaraz B, Crispi F, Bijnens B, Cruz-Lemini M, Creus M, Sitges M, Bartrons J, Civico S, Balasch J, Gratacos E. Assisted Reproductive Technologies are Associated with Cardiovascular Remodeling in Utero that Persists Postnatally. *Circulation,* 2013.